Proceedings of

Two Day National Conference

on

Materials and their Applications: A Broad Perspective

9th-10th January 2020

at

Thorale Bajirao Peshwe Sabhagruha, Thane

Organized by

Vidya Prasarak Mandal's

B.N. Bandodkar College of Science, Thane

- FIST 'O' Level Grant (2013-14)
- Best College Awarded by University of Mumbai (2009-10)
- Re-Accredited by NAAC with "A" Grade
- Celebrated Golden Jubilee (2019)

In Collaboration with

Department of Physics

The Institute of Science, Mumbai

- DST-FIST Supported Department
- NAAC Re-Accredited 'A' Grade
- Celebrating Centenary Year (1920-2020)

Proceedings of

Two Day National Conference

on

Materials and their Applications: A Broad Perspective

9th-10th January 2020

at

Thorale Bajirao Peshwe Sabhagruha, Thane

Organized by

Vidya Prasarak Mandal's

B.N. Bandodkar College of Science, Thane

● FIST 'O' Level Grant (2013-14) ● Best College Awarded by University of Mumbai (2009-10)
● Re-Accredated by NAAC with "A" Grade ● Celebrated Golden Jubilee (2019)

In Collaboration with

Department of Physics

The Institute of Science, Mumbai

● DST-FIST Supported Department ● NAAC re-accredited 'A' Grade
● Celebrating Centenary Year (1920-2020)

Patron

Dr. V. V. Bedekar
Chairman
Vidya Prasarak Mandal, Thane

Dr. Jairam Khobragade
Director
The Institute of Science, Mumbai

Convener

Prof. S. Venkatraman Prof. Ajay Chaudhari

Organizing Secretary

Prof. B. K. Mandlekar Dr. Pravin S. More

Organizing Committee

Prof. S. G. Bapat (Co-Convener)

Dr. S. B. Kulkarni (Co-Convener)

Prof. (Mrs.) S. S. Meshram (Treasurer)

National Advisory Committee

Prof. Pushan Ayyub, TIFR Mumbai.

Prof. R. Nagrajan, Emeritus Professor, UM-DAE CBS, Mumbai.

Prof. N. Venkatramani, I.I.T., Mumbai.

Prof. P. M. Shirge, I.I.T., Indore.

Prof. C. S. Gopinath, N. C. L. Pune.

Dr. M. N. Nyayate, Emeritus Professor, UM-DAE CBS, Mumbai.

Dr. S. K. Omanwar, SGBAU, Amravati.

Prof. R. J. Sengwa, J.N.V. University, Jodhpur.

Prof. U. P. Verma, Jiwaji University, Gwalior.

Prof. A. C. Kumbharkhane, S. R. T. M. University, Nanded.

Dr. Rajeev Joshi, Central University of Karnataka.

Dr. P. M. Dongre, University of Mumbai.

Dr. Mrs. M. K. Pejaver, Director, Advanced Study Centre, VPM, Thane

Technical Committee

Mrs. Savita Dange
DR. (Mrs.) U. B. Gokhe
Prof. A. S. Dani
Prof. G. S. Tawde
Prof. H. H. Tadwalkar
Prof. (Mrs.) S. S. Meshram
Prof. A. A. Koli
Prof. N. V. Nandi
Prof. S. S. Pawar

Local Organising Committee

Dr. D. R. Ambavadekar
Dr. S. D. Rathod
Dr. (Mrs.) V. M. Manjaramkar
Dr. V. M. Jamdhade
Dr. (Mrs.) R. Y. Mandhare
Dr. (Mrs.) J. M. Pawar
Dr. Nigvendra Sharma
Dr. K. R. Jagdeo
Dr. (Mrs.) M. Saha
Dr. (Mrs.) P. N. Kurve
Dr. (Mrs.) A. S. Goswami-Giri
Dr. S. S. Kahandal
Dr. (Mrs.) K. B. Muley
Dr. U. C. Kumavat
Dr. Milind Jog

ISBN : 978-81-923628-7-8

Published by:
Department of Physics
VPM's B.N.Bandodkar College of Science"
Jnanadweepa", Chendani Bunder Road,
Thane (W) 400601, Maharashtra,
India.Tel: 25336507
www.vpmthane.org

Printed at
Perfect Prints
22, Jyoti Industrial Estate,
Nooribaba Darga Road,
Thane 400601Tel: 25341291 / 25413546
Email: perfectprints@gmail com

Citation: *Proceedings of National Conference on Materials and Their Applications: A Broad Prospective (NCMA-2020)*. Edited by Prof. S. G. Bapat, Dr. S. B. Kulkarni, Prof. (Mrs.) S. S. Meshram, Mrs. Savita Dange, Prof. (Mrs.) S. S. Meshram, DR. (Mrs.) U. B. Gokhe, Prof. A. A. Koli, Prof. A. S. Dani, Prof. N. V. Nandi, Prof. G. S. Tawde, Prof. S. S. Pawar, Prof. H. H. Tadwalkar Published by Dept. of Physics, V.P.M.'s B. N. Bandodkar College of Science, Thane 400601; January, 2020.

Chairman's Message

Vidya Prasarak Mandal has been organizing conferences at national as well as international levels on various themes associated with current world scenario. This helps the students and teachers of the campus to have glimpse of all the subjects of various streams and to get updated with the subjects of their own interest.

This year VPM's B. N. Bandodkar College of Science, Thane has organized a conference on 9th and 10th of January 2020. The theme of the conference is advanced material research and their applications for helping mankind towards fulfillment of many needs. This conference intends to facilitate the scientific discussion among the researchers, promote new collaborations, provide a friendly platform to share the scientific knowledge, and prioritize the future efforts that are needed to revolutionize the field of materials science.

I express my earnest thanks to the Institute of Science, Kalina for the collaboration extended toward the conference. I am delighted in presenting this volume of proceeding on "Materials and their Applications: A Broad Perspective". I sincerely hope that that the conference will go long way in opening many avenues and opportunities in the field.

I extend my heartfelt warm welcome to all the expert faculty members and participants.

I wish this conference all the success.

Dr. Vijay Bedekar
Chairman
Vidya Prasarak Mandal, Thane

Principal's Message

Every year, the month of January is the time when a National or an International Conference is organised by our college. It gives me great pleasure to welcome you all in this "National Conference on Materials and Their Applications -2020" jointly organised by VPM's B. N. Bandodkar College of Science, Thane and Institute of Science, Madam Cama Road, Mumbai. Two preparatory workshops related to this conference were held on July 2019 and November 2019. The purpose of this conference is to understand latest materials and their wide range of applications in various fields.

I appreciate the efforts of all teaching and non-teaching staff of both VPM's B. N. Bandodkar College of Science, Thane and Institute of Science, Mumbai. I also express my deep sense of gratitude to our management Vidya Prasarak Mandal for their continuous suuport and encouragement. I wish the Conference Grand success.

Prof. S. Venkatraman
I/c Principal
B. N. Bandodkar College of Science
Thane

Director's Message

It is indeed a matter of great pleasure that ***"Two Days National Conference on Materials and their Applications : A Broad Perspective"*** *is being jointly organized by the B. N. Bandodkar College of Science and institute of Science Mumbai, on 9th and 10th January 2020. This event is a noble endeavour to streamline and enrich the thought process of all the Researchers. The theme of the conference is quite contemporary considering the changing scientific environment world over. The participants have a rare opportunity to pay attention and contribute the views of one of the greatest visionary, Indian nuclear physicist and illustrious personality of modern India, Padma Vibhushan, Padma Bhushan, Padma Shri* ***Dr. Anil Kakodkar*** *The organization of Convention provides ample opportunities to share the wisdom, generate views as to how to meet the today's challenges.*

I, extend my heartiest wishes to B. N. Bandodkar College of Science and The Institute of Science, Mumbai for a grand success of ***Two Days National Conference*** *.*

Dr. Jayram Khobragade
Director,
Institute of Science,
15 Madam Cama Road,
Mumbai 400 032.

Welcome Message from the Conveners

Hello and welcome to Mumbai and to the National Conference on Materials and Their Appications : A Broad Perspective (NCMA-2020). It is out great pleasure to serve as Convener for the NCMA-2020 jointly organized by B. N. Bandodkar College of Science. Thane and The Institute of Science, Mumbai. Materials represent a very promising role to develop novel economic and environmentally friendly industrial processes. The field of materials science is rapidly growing and several new discoveries calls for renewed mention of involved researchers. This gathering under NCMA-2020 aims to stimulate the scientific discussion between the researchers, promote new collaborations and provide a friendly platform to share the scientific knowledge. The topics to be covered in the conference are very comprehensive which include : Materials for energy applications, Materials for Catalysis and Environment, Smart and Functional Materials, Biomaterials and Synthesis and Characterization of Materials. The Subject matter of topics will cover fundamental physics and chemistry, modeling and computations, experimental techniques and industrial applications. The multidisciplinary nature of many topics should provide insights into the emerging frontiers in materials science. The conference will feature several keynote/plenary/invited speakers who are internationally recognized experts in their discipline of research. The conference will provide an excellent forum for exchange of ideas, scientific interactions and potential for collaboration. I trust you will have a very productive time at the conference. We look forward to meeting you all in Mumbai under NCMA-2020 ! Thus, welcome and enjoy the conference!

Prof. Ajay Chaudhari
Prof. and Head
Dept. of Physics
The Institute of Science,
Mumbai

Prof. S. Venkatraman
I/c Principal
B. N. Bandodkar College of Science
Thane

Organizing Secretary's Message

On be half of the organizing committee, I would like to welcome all the delegates to the Two Day National Conference on Materials and their Applications: A Broad Perspective, organised by Department of Physics, VPM's B.N.Bandodkar College of Science,Thane, Maharashtra on 9th and 10th January, 2020.

Universe is full of different materials.New age technology has developed materials from superconductors to supercapacitors. This conference will elaborate a part of the Universe of materials and it's applications.This conference is a genuine reflection of scientific, academic, and social contribution to the development of materials and it's applications.It will be a collective effort where various institutes, researchers, academicians and students will share their work on a common platform.

Special thanks to Institute of Science, Mumbai for collaborating with us.I would like to thank our sponsors for their contribution.I would like to thank Vidya Prasarak Mandal for its kind support.I extend warm welcome to our distinguished guests and delegates for contributing in National Conference on Materials and their Applications : A Broad Perspective.

Prof. B. K. Mandlekar
Organizing Secretary, NCMA-2020
B. N. Bandodkar College of Science
Thane

From the Editorial Desk

The interdisciplinary field of materials science, also commonly termed materials sciences and engineering is the design and discovery of new materials.

Many of most pressing scientific problems humans currently face due to limits of the materials that are available and how they are used. Thus, breakthroughs in materials science are likely to affect the future of technology significantly.

The two-day National Conference on "Materials and Their applications: A broad perspectives", is an effort to motivate inherent research talent in material sciences. This is reflected from the work shared by the participants in the form of abstracts as well as full length papers.

We as an editorial team are pleased to present the proceedings of the conference and we are happy to express that we have received a satisfactory response from researchers in the field of material sciences.

In this proceeding we have tried our best to publish full length papers received within the speculated time limit. We have also included the abstracts which are supposed to be presented in the conference either in oral or poster form. We are grateful and also congratulate the speakers and authors for making this proceeding resourceful.

Editorial Team

Contents

Nanoscience and Nanotechnology for harvesting Solar Energy

C. S. Gopinath

National Chemical Laboratory, Dr. Homi Bhabha Road, Pune 411 008.

After the industrial revolution, information revolution, currently Nano Revolution is in progress. There is lot of progress is happening silently on several fronts of nanoscience and converting them into nanotechnology is also occurring at some speed. Climate changes compel the present (and future) generations to produce energy in a sustainable manner, so that addition of carbon dioxide to the atmosphere can be slowly reduced. Indeed, energy would be future currency. Nanoscience and nanotechnology can contribute to harvest solar energy (as well as wind energy and other renewable energy sources) in a big way. Indeed, more focused work is necessary on this front. A broad introduction of nanomaterials to be provided, followed by the employment of nanomaterials for solar energy harvesting through water splitting.

ISBN : 978-81-923628-7-8

Metal Oxide Materials for Multifunctional Applications

Parasharam M. Shirage
Discipline of Metallurgy Engineering and Materials Science,
Indian Institute of Technology Indore-452553.
E-mail: pmshirage@iiti.ac.in

Functional metal oxide hybrid nanostructures combine the favourable properties of the constituent materials for achieving multifunctionality. Functional metal oxide nanostructures and nano-hybrids have attracted significant attention for diverse applications, *i.e*. energy storage, mechanical energy harvesting, chemical sensing and other applications. The present talk is concerned with the engineering of the properties of the functional metal oxide nanostructures and nanocomposite prepared by the facile wet chemical method, hydrothermal and thermal decomposition method for supercapacitor, nanogenerators, gas sensing, and room temperature magnetic applications. With the development of the modern economy, faster and higher energy storage systems are essential for several applications. Supercapacitors are the best candidates for providing the necessary high power and long durability needed for new energy devices for uninterrupted power supply. WO_x, MnO_2, Co_3O_4 nanostructures are identified as promising materials for energy storage purposes [1-3]. Further, *r*GO-Ag/PVDF nanocomposite was used to realize a mechanical energy harvesting device that could light LEDs, charge capacitors and harvest bio-mechanical energy [4]. The ability to monitor indoor air quality is realized by studying the gas and humidity sensing properties of Sr- and Ni- doped ZnO nanostructures. The as fabricated chemical sensors showed good sensitivity, selectivity and stability towards H_2O, CO, CO_2, etc. [5, 6]. The size and shape-controlled $CoFe_2O_4$ nanoparticles were explored for room temperature magnetic applications. The excellent magnetic properties indicated the capabilities of $CoFe_2O_4$ NPs in permanent magnets for current technological applications [7].

Acknowledgement: PMS thanks to Advanced Functional Materials Research Group for their hard work and fruitful work. Professor Pradeep Mathur, Director, IITI, for providing excellent research facility and environment.

References :

[1] L. Sinha, P.M. Shirage, *J. Electrochem. Soc.*, 2019, 166, A3496-A3503.

[2] L. Sinha, S. Pakhira, P. Bhojane, S. Mali, C. K. Hong, P. M. Shirage, *ACS Sustain. Chem. Eng.*, 2018, 6, 13248-13261.

[3] P. Bhojane, L. Sinha, R. S. Devan, P. M. Shirage, *Nanoscale*, 2018, 10, 1779–1787.

[4] M. Pusty, L. Sinha, P.M. Shirage, New J. Chem., 2019, 43, 284-294.

[5] P.M. Shirage, A.K. Rana, Y. Kumar, S. Sen, S.G. Leonardi, G. Neri, RSC Adv., 2016, 6, 82733-82742.

[6] A. Sharma, Y. Kumar, K. Mazumder, A.K. Rana, P. M. Shirage, New J. Chem., 2018, 42, 8445-8457

[7] Y. Kumar, A. Sharma, Md. A. Ahmed, S. S. Mali, C. K. Hong, P. M. Shirage, New J. Chem., 2018, 42, 15793-15802.

Nano-phase Luminescent Materials for Sustainable Development

S. K. Omanwar

UGC-BSR Faculty Fellow & Former Sr. Professor, Department of Physics,
Sant Gadge Baba Amravati University, Amravati-444602 India
E-Mail: omanwar@rediffmail.com , omanwar@sgbau.ac.in

It is now high time to promote research in the innovative materials, devices, and technologies for sustainable development. India is obviously making the effort in the direction and in recent years government is making attempt to promote by funding for innovative technologies, functional materials and systems.

A big amount of efforts are witnessed in recent years for motivation of ideals and inherent talent in pure sciences and that too for research and development areas. Nowadays talented students are showing interest in this area and this will be the big investment for the bright future of the country.

Luminescence is an interdisciplinary field of research. Developing Luminescent Materials becomes now a backbone of all such devices that are playing very important role in diverse field of applications such as lighting, display, radiation dosimetry, solar PV conversion, diagnostic, phototherapy, guided drug delivery, sensing/actuation devices, etc.

The presentation includes advances in luminescent materials for beneficial applications to the society in future.

- Efficient solar energy utilization for photovoltaic conversion using QC-phosphor materials,
- Developing radiation dosimetry sensor materials for safety aspects that are import substitute,
- Innovative materials for future phototherapy devices which are not only portable but programmable also with regard to power and selection of wavelength
- Innovative biomaterials for various application
- Innovative techniques of electro-spin processing for the better performance and making devices to work in adverse situation
- New media for carbon quantum dots for medical and advance applications at low cost.

The theme of talk would be the witnessed findings which will encourage the new generations to accept the challenges under present scenario of work culture with reference to India and suggestions for its remedy for betterment of future of the country.

ISBN : 978-81-923628-7-8

Studies on Bilayer Thin Film Magnetoelectric Composites

Prof. N. Venkatramani

Over the past five years, we have been working with multiferroic magnetoelectric composite thin films grown using the pulsed laser deposition technique. We deposit spinel ferrites as the ferrimagnetic material and niobate/ titanate type of ferroelectrics in thin film form. These 2-2 structures work quite well as a magnetoelectric composite. We have realised a magnetoelectric response of over one volt/cm.Oe in these composite thin film systems at room temperature. I will present our recent work with some of the current results, whilst highlighting the systems and the characteristics we have studied in the laboratory

ISBN : 978-81-923628-7-8

"Material research at SAMEER, Mumbai"

Alok Verma

1. MBE for AlGaAs and GaN based devices (Laser and Detector)
2. Optical device fabrication, testing and packaging ($LiNbO_3$, BK7 glass and Si)
3. Photonics Packaging

ISBN : 978-81-923628-7-8

Formation of Functional Oxides and Their Use in Energy Generation and Storage

Deepa Khushalani
Materials Chemistry Group, TIFR

Our current research in the materials chemistry group at TIFR involves templating mediated synthetic routes to form novel architectured inorganic materials. To elaborate the work entails synthesis, characterization and application of a variety of oxides such that (1) the morphology, phase, and size are carefully manipulated and, (2) the ensuing materials are then applied in areas involving heterogeneous photocatalysis, fluorescent biosensors, photoanodes of solar cells and in energy storage devices (such as batteries and supercapacitors). We also work on structures that are biocompatible and can be used in drug delivery applications. We employ simple chemical routes to prepare a wide variety of functional materials, and the talk will highlight two particular projects currently ongoing. One involves use of vanadates as functional materials that serve as anodes in supercapacitor applications and the other project will highlight our current efforts in working with new family of organic-inorganic hybrid halide structures: $CH_3NH_3PbI_3$ that serve as impressive light absorbers when coupled with a variety of photoanodes in heterojunction solar cells.

ISBN : 978-81-923628-7-8

Spintronic Materials and Devices - A New Avenue

Rajeev Shesha Joshi
Department of Physics, Central University of Karnataka,
Kalaburagi – 585367

Spintronics is a blooming area of active research which has contributed significantly to the development of new conceptual devices with tremendous potential of innovation ahead, both in terms of fundamental science and technology. Here, one exploits the spin degree of freedom of the electrons along with its charge. So, spintronics combines standard electronics with spin dependent effects[1,2]. In standard electronics one manipulates the electrons by using their charge to store or process information. In spintronics one manipulates electrons by using their spin along with their charge to process or store information. Hence one can expect a new generation of materials and related devices with completely different functionality[3].

In the talk I will try to explain the basic concepts of Spintronics and the materials presently used in the field, at a popular level. Further I will try to put forth the idea of Magnetic Anisotropy enhanced materials and spin polarized materials with the example of alloys and oxides. I will try to elaborate our work in the area of magnetic wire based devices. I will explain the efforts using NiFe based Nano wires[4]. The micromagnetic simulation results and the related experimental outputs will be presented[5]. I will conclude with the glimpse of recent developments and future scope in the area of Spintronic materials.

References:

1. Chambers, S.A., Mater. Today 2002, 2, 34.
2. Wolf, S.A.; Awschalom, D.D.; Buhrman, R.A.; Daughton, J.M.; von Molnar, S.; Roukes, M.L.; Chtchelkanova, A.Y.; Treger, D.M., Science, 2001, 294, 1488.
3. Parkin, S.; Jiang, X. ; Kaiser, C.; Panchula, A.; Roche, K.; Samant, M., Proc. IEEE 2003, 91, 661.
4. Venkateswarlu, D.; P. V. Mohanan, Rajeev S. Joshi, and P. S. Anil Kumar, IEEE Transactions On Magnetics, 48-11(2012) 1-4
5. Rajeev S. Joshi, Venkateswarlu, D.; A. Prabhakar, Venkat, G and P. S. Anil Kumar, IEEE Transactions On Magnetics (Communicated Manuscript.)

 ISBN : 978-81-923628-7-8

Review of Terahertz (THz) Spectroscopy and THz Studies of Metamaterials

S. S. Prabhu[1]

[1] Department of Condensed Matter Physics and Material Science, Tata Institute of Fundamental Research, Homi Bhabha Road, Mumbai 400005 India.
E-mail: prabhu@tifr.res.in

We demonstrate many novel photo-conductive antenna (PCA) designs, capable of emitting Terahertz radiation with high average power. Some of the designs show enhanced bandwidth of the emitted THz radiation pulse. For Example, one such device consists of Au electrodes on a semi-insulating GaAs substrate. A Photonic Crystal like plasmonic nano-structure array is embedded in the substrate between the two electrodes. This array shows plasmonic enhancement of the 800 nm IR light near the nano-structures enhancing THz radiation emission. Secondly, the nano-structures act as defect sites which enables fast carrier capture, enhancing THz bandwidths. At the same time, the terminal currents are highly reduced implying robustness of the device to high applied bias voltages[1].

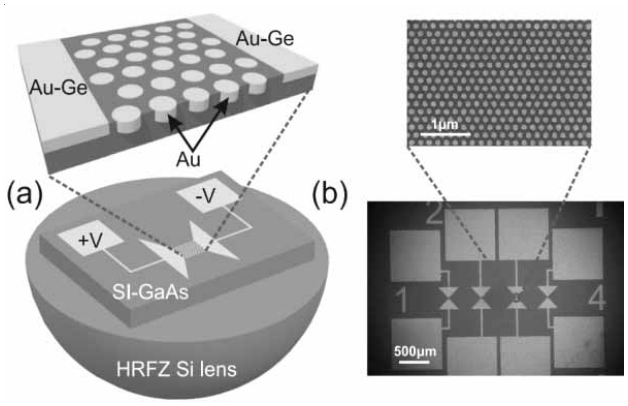

Fig. 1: (a) Schematic of the device is shown with (b) SEM photograph of the device.

THz spectroscopy is useful in material studies as well. Resonant transmission of electromagnetic radiation through an array of rectangular apertures occurs when electric field vectors of the incident wave are perpendicular to the long axis of the aperture. We study several designs of Metmaterials. Here we will mention about periodic array of asymmetric aperture and demonstrate that introducing a taper along long axis can yield transmission for both orthogonal polarizations[2]. We present several studies of different Metamaterial designs and describe some interesting results obtained using external perturbations on these Metamaterial substrates.

References:

1. A. Bhattacharya; D. Ghindani and S. S. Prabhu, "Enhanced terahertz emission bandwidth from photoconductive antenna by manipulating carrier dynamics of semiconducting substrate with embedded plasmonic metasurface," *Optics Express*, 27, 30272 (2019).

2. Arnab Pattanayak, Goutam Rana, Ravikumar Jain, Arkabrata Bhattacharya, Siddhartha P. Duttagupta, Prasanna S. Gandhi, Venu Gopal Achanta, and S. S. Prabhu "Near-unity THz transmission through asymmetric aperture array with polarization controlled resonant peaks and Q-factors", *Accepted in Journal of Applied Physics 2020.*

ISBN : 978-81-923628-7-8

Advanced Magnetic Materials and their Applications

K. G. Suresh
Department of Physics, IIT Bombay, India

Magnetic materials constitute one of the most important classes of applied materials in modern day science and technology. They also find applications in many walks of life and this has happened due to the sustained efforts in understanding the underlying physics and the development of novel materials. There are several phenomena exhibited by magnetic materials and many of these are being exploited for applications. Some of these materials are even multifunctional. In addition, several classes of novel classes of materials such as "quantum materials" etc. have been identified. In this lecture, I will give a detained discussion on the relation between the structure and these physical properties with necessary introduction to various phenomena involved. I will also present some of the most potential materials identified in the recent past and also their special features with regard to applications.

ISBN : 978-81-923628-7-8

Moringa Leaves: Synthesis of Biomaterial and Its Application

Anita S. Goswami-Giri*, Jagdish B.Kudav, Anjali A.Yadav, Pooja J. Singh and Sumit R. Singh

Department of Chemistry, B. N. Bandodkar College of Science, Thane (MS) - 400601.

Corresponding Author- anitagoswami@yahoo.com

Abstract: A miracle tree; moringa is rich in nutrients and minerals. Due to its high active constituents it exhibits therapeutic application. Hence, leaves were selected for the preparation of biomaterial/ soap which acts as antibacterial. To get rid of moisture content from moringa leaves different drying methods was used and analyzed by spectrophotometrically. The resulting material can commercialize.

Keywords: *Cosmetic; phytochemicals; herbal formulation; bioactive material*

1] Introduction

Moringa oleifera (Moringaceae) is fast-growing, deciduous plant tree[1]. The diversity of wild types of *Moringa* was observed largely on wastes land in India. Arial parts of it are edible and used for the treatment of various disease and disorders. Moringa plant is rich in polyphenols, antioxidants, and minerals etc. Its oil has remarkable beautifying value, and has been reported in folk medicine. The oil uses to relive pain, in fungal infections, constipation, prostate function, bladder function, moisturizer for hair and skin conditioner etc. [2, 3]. Due to its versatile application, and rich in nutrients, has been used for the treatment for malnutrition. Therefore, it is called as 'Miracle tree' and 'God's Gift to Man'. It's leaves, stem and seed powders are used as detoxifying agent and also for commercial purpose. Moringa seed oil will leave volunteers/applicant feeling soft and hydrated reported by the body shop [4]. Though the seed are used for oil, drumsticks are using as vegetables and preparation of soup in daily routine; for soap preparation, researchers are paid attention towards the drumstick seed for its sap and ester values and preparation of soap bar. Leaves were used for the liquid soap. Traditionally, soaps are prepared by using animal fat and lye by using saponification [5]. In sinister season, leaves as drowning fingers clutching on land. Hence, current research paid attention towards herbal formulation of soap from fresh leaves of moringa. After spectroscopic analysis of moringa leaves by exploring it to various drying methods and its change characteristics taking into consideration soap was prepared.

2] Material and Methods

Plants material: Leaves of *Moringa oleifera* Lam. were collected from local area of Thane, Maharashtra India. The fresh leaves of Moringa oleifera Lam. were separated and washed thoroughly with distilled water, equal part of leaves dried in Microwave oven dried (MD), Sunlight dried (SD) and also Air dried (AD) and powdered separately. To get rid of moisture and fungal growth, all dried powder stored in plastic sealed bags until used.

Methods:

2.1] Preparation of extract

Leaves powder (10gm) MD, SD and AD blended with different solvent such as water, acetone, ethanol, pet ether, chloroform, methanol, hexane under magnetic stirring at RT from. Aliquots were collected after intervals of 30 minutes for spectroscopic analysis and for its rf values. The analysis was compared with fresh leaves.

2.2] Thin layer chromatography and spectroscopic analysis

Rf values calculated by solvent system pet ether. UV analysis was carried out in Shimadzu's double beam spectrophotmeter-1800 and FTIR of all samples carried out on Thermofischer scientific Nicolet iS5 .

2.3] Extraction of oil

Ten gram powdered of Air dried, oven dried, sunlight dried and extract of fresh leaves were used for oil extraction separately. The oil was extracted using soxhlet apparatus and using oil extractor with green solvent. After comparison of oil in both methods, and its characterization, extractor - oil was used for further formulation of soap bar. Characterization of oil was carried out in term of sap values, ester values.

2.4] Preparation of soap by press cold method:

Fresh leaves of moringa (50gm) washed with distilled water, pulped it followed by warming, the filtrate was used for the synthesis of soap. The base of soap is prepared with NaOH and glycerine along with coconut oil. The base is added into moringa leaves pulp. To observe fragrance to bar camphor and natural aroma base liquid were added, boiled and poured soap mixture into mold evenly. The mold containing soap mixture kept for 1 to 2 hrs. in the deep freezer. After attaining the cold temperature by the mixture, it started solidifying.

The second set of base was prepared by replacing coconut oil with moringa leaves oil for its therapeutic used.

2.5] Soap bar is tested against pH, in hard water and in soft water

Prepared soaps were washed with hard water and soft water tested for its scum. The soap was tested against pH paper.

3] Result and Discussion:

After collecting moringa leaves were washed well and dried in three different methods such as Sun dried, Air dried and microwave dried. All methods dried powders were extracted using different solvent such as Acetone, alcohol, Methanol ,Pet ether, Chloroform, n-Hexane and compared it with fresh leaves with aqua extract. The extraction of all sample were carried out with magnetic stirrer to derive out the desired natural product/Biomaterial for further application. The extractions were monitored by time and TLC. Rf values of each aliquots were compared. Negligible change was observed in Rf value using less polar solvent. Rf values of 30' shown in table 1. The all samples spectrums were measured which is shown in table 2.

Table 1 Change in Retention values of moringa leaves powder in various Drying methods and in different solvent. The values exhibited in table for 30 min aliquots since there is no notable change in Rf values observed. Microwave and sundried powder was extracted in green solvent.

Solvent	Fresh leaves	Air dried	Sun dried	Microwave dried
Water	0.89	0.89	0.97	0.94
Acetone	0.88	0.55,0.67,0.74,0.89	—	—
Alcohol	0.89	0.59,0.68,0.76, 0.89	—	—
Petether	0.95	0.89	—	—
Chloroform	0.89	0.49,0.56,0.65,0.73,0.85	—	—
n-Hexane	0.44,0.83	0.44,0.61,0.67,0.74	—	—

Table 2 UV spectra of moringa leaves in different dying methods

Sr. No.	Solvent system	Fresh leaves (wet) λ (nm)	Microwave λ(nm)	Air dried λ(nm)	Sunlight λ(nm)
1.	Distilled Water	240,260, 285, 381	287, 416	287, 416	248, 284, 420
2.	Acetone	404 ,429	289 , 416	432	420
3.	Ethanol	435	287, 428	290	235, 422
4.	Pet Ether	257, 267, 298, 360	247, 260,286, 425	267, 290, 390	257, 267, 298, 422
5.	Chloroform	257, 267, 298, 360	287,416, 460	240, 287, 298, 388	257, 267, 298, 435
6.	Methanol	387	287,416	416	257, 267, 298, 360
7.	n-Hexane	257, 267, 298, 360	287 , 416	278, 402, 360	257, 267, 298, 360

 ISBN : 978-81-923628-7-8

According to figure 1, FTIR spectra a, b and c, the phenolic compounds may contribute directly to antioxidative effect. The presence of 3-OH group as well as hydroxyl groups is related to the superoxide scavenging activity of flavonoids which is observed in fresh leaves extract as well as in microwave dried powder extract. Thus, the free radical scavenging ability of *Moringa leaves* may provide health benefits to humans by protection against oxidative stress. Hence, its oil and soap is synthesized. Natural antioxidants such as tocopherols and pigments like carotenoids, flavonoids are responsible for the antioxidant property and antimicrobial property [1]. Furthermore, phenolic compounds have phenolic hydroxyl groups dissociated to negatively charged phenolates. Dissociated phenolics form hydrogen and ionic bonds with various proteins, which lead to a interrupt of their structures and in consequence to a change in their bioactivity [7] that confirms the extract may utilize for the preparation of soap.

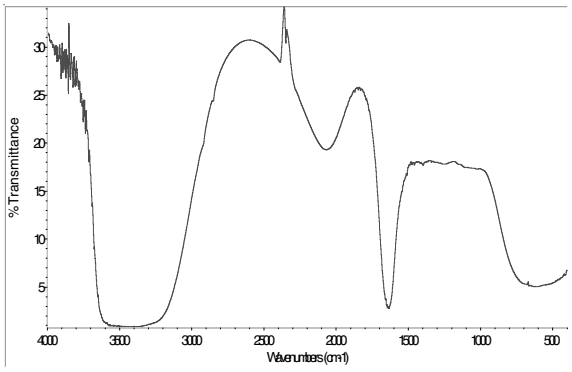

a)Fresh moringa leaves aqua extract -3691cm-1(O-H stretching), 3600cm-1(O-H stretching), 2348cm-1(O=C=O stretching), 1634cm-1(-C=C- Monosubstituted), 795cm-1(C=C bending , alkene-trisubstituted)

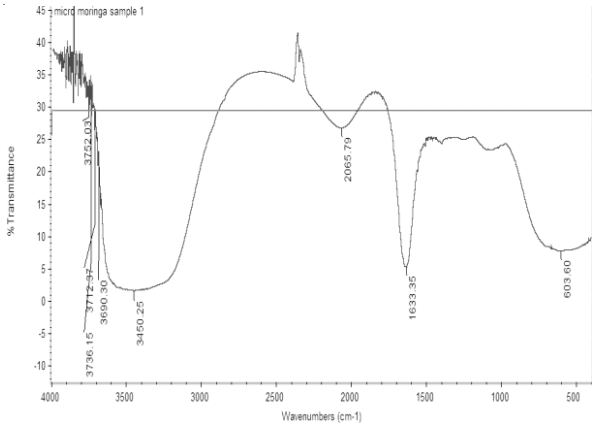

b)Microwave dried moringa leaves powder -3751cm-1 (O-H stretching), 3712cm-1 (free OH frequency), 3736cm-1(O-H stretching),3690cm-1(O-H stretching), 3450cm-1(N-H stretching aliphatic primary amine), 2065cm-1 (C=C=N stretching ketenimine),1633cm-1 (-C=C- stretching),

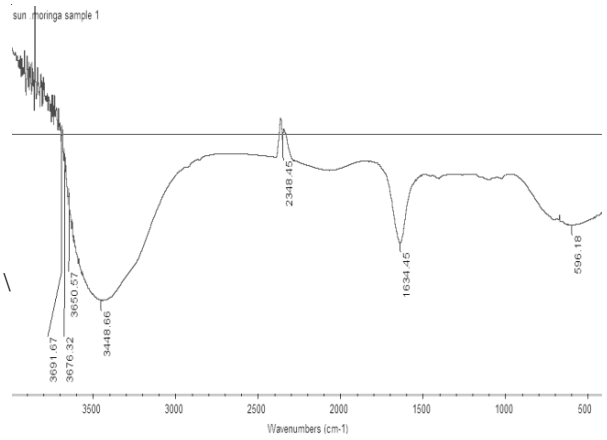

c)Sundried dried moringa leaves powder -3690cm-1(O-H stretching),3676cm-1(O-H stretching), 3448cm-1(N-H stretching; aliphatic primary amine), 2348cm-1(O=C=O stretching),,1634 cm-1(-C=C- stretching Monosubstituted),596 cm-1(alkyl halide)

Increase in demand due to world population pressure moringa leaves oil may meets the need of fuel, food and energy. Moringa leaves oil was extracted with extractor required 30 minutes while with soxhklet apparatus required 2hrs. to 14 hrs. Oil with aqueous medium is exhibited stickiness with good quality. 10gms of fresh leaves procured 10 cm3 of oil while others are gives more quantity but with medium characteristics. Hence, present study moringa leaves oil was selected for preparation of soap and was compared with the use of coconut oil soap.

Characterization of oil is shown below figure 2 and table 3. Acid value of oil affects the transesterification of oils. Higher the acid value has more soap during transesterification. The similar observation was reported by Rose et,al 2017 [8]. The moisture content in the soap is corrected as per the environmental conditions. All oils are having different colour the ester and sap values are shown in figure 2. The oil extracted with aqua media was used for the synthesis of soap bar.

Figure 2 Moringa leaves oil extracted by Oil extractor with Acetone , Alcohol, Methanol ,Pet ether, Chloroform, n-Hexane and with aqua extract.

Table 3 Oil observed in hexane, methanol, acetone, chloroform and distilled water.

Oils from leaves (10gm) with	Quantity (cm3)	Colour	Density	Viscosity milipoise	Boiling point ^{0}C	Rf values	Acid values Mg	Ester values mg	Sap value mg	Iodine values Per gm of oil	CARVONE Quantity in oil	
											Volume cm3	Rf values
Aqueous media	04	Clear Pale yellow	Stickiness	247.08	178	0.29	2.4-3.7	38.7	198	128	2	0.21

The use of plant extracts in the synthesis of herbal soap is a very attractive approach in the field of green synthesis. To benefit from the potential synergy between the biological activities of the *Moringa oleifera* leaves extract and fat/lye. Basic requirement for the preparation of soap is fat hence moringa leaves is tested for its sap values and ester values. Soap makes skin healthy and helps bring back balance to natural skin color and tone. It also cleanses and detoxifies the skin by exhibiting the antibacterial activity. The prepared soap stem are shown in figure 3.

Soap mixture

Soap molds

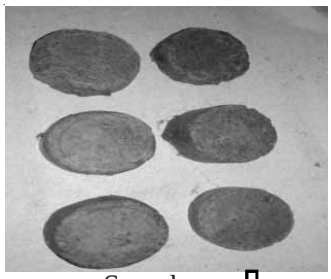

Soap bar

Testing of soap bar

Testing of soap with soft water

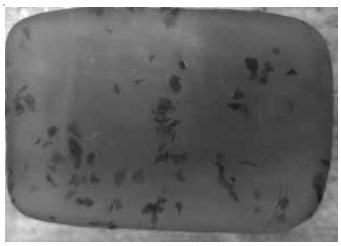

Glycerol soap

Figure 3 Step for the preparation of moringa leaves soap by cold press method

ISBN : 978-81-923628-7-8

Soaps react with hard water and form insoluble precipitate known as soap film or scum when the moringa leaves soap used for hand washed the scum is not observed. When it was tested with soft water, the foam of soap was observed though the soap pH is 6.8(figure 3). Still it is needed to check against various surfactants.

When cold and hot/conventional process compared the change in colour was observed in soap. Hot process involves alkali, lime to make caustic soda with leaching process followed by boiling, the produced fat for the fabrication of soap. Saponification reaction is exothermic[9]. The fatty acid salts are less soluble in salt water than they are in fresh water and so they will precipitate from the solution.

Quality Assurance

All content used in synthesis of moringa leaves soap is healthy such as coconut oil, moringa oil glycerin, water, NaOH for saponication and maintain soaps pH is 6.8. When soap is tested against the washing hand it cleans the hand. The soap, tested with hard and soft water separately with each condition exhibits, the moringa fatty acid salts will float to the top while the glycerol stays in solution. Moringa leaves extract (50cm3) procured 60gm of soap bar. The bar exhibits effective cleaning and possible used of washing. High iodine produced hard soap bar. The moringa leaves is rich in photochemical such as flavonoids, phenolics and terpenes that formulate antimicrobial agent.

4] Conclusion

The prepared herbal biomaterial is cost effective, natural and also user friendly. The fat, sap and iodine values of moringa leaves sustain the ability of soap preparation.

5] Acknowledgement

Greatly acknowledge to the management VPM'S B N Bandodkar College of Science,Thane(w)-1

6] Reference

[1] Horseradish tree (2015). Encyclopædia Britannica. 04-25.

[2] Julia P.Coppin, H. Rodolfo, Juliani Qingli, Wu James, E.Simon; (2015).Chapter 79-"Variations in polyphenols and lipid soluble vitamins in Moringa oleifera" Processing and Impact on Active Components in Food, 655-663.

[3] Hasanah Mohd,Ghazali Abdulkarim, Sabo Mohammed,(2011). Chapter 93 – "Moringa (Moringa oleifera) Seed Oil: Composition, Nutritional Aspects, and Health Attributes" Nuts and Seeds in Health and Disease Prevention, 787-793.

[4] https://www.thebodyshop.in/moringa-soap.html

[5] Belen Torondel, David Opare, Bjorn Brandberg , Sandy Cairncross , (2014). "Efficacy of Moringa oleifera leaf powder as a hand- washing product: A crossover controlled study among healthy volunteers" BMC Complementary and Alternative Medicine, 14(1):57 DOI: 10.1186/1472-6882-14-57.

[6] Anna Baldisserotto, Piergiacomo Busa, Matteo Radice, Valeria Dissette, Ilaria Lampronti, Roberto Gambari, Stefana Manfredini, Silvia Vertuani (2018). "Moringa oleifera Leaf Extracts as Multifunctional Ingredients for "Natural and Organic" Sunscreens and Photoprotective Preparations" Molecules. Mar; 23(3): 664.

[7] S. Dehshahri, M. Wink, S. Afsharypuor, G. Asghari, and A. Mohagheghzadeh "Antioxidant activity of methanolic leaf extract of Moringa peregrina (Forssk.)" Fiori. Res Pharm Sci. 2012, 7(2):111–118

[8] G. Rekha, Dr. A. Leema Rose (2017). "Physicochemical properties of moringa oleifera seed oil." International Journal of Advanced Engineering $_{\text{Research}}$ and Technology, 5 (10), 709-714.

[9] A.A. Warra, L.G. Hassan, S.Y. Gunu and S.A. Jega, (2010)."Cold-Process Synthesis and Properties of Soaps Prepared From Different Triacylglycerol Sources" Nigerian Journal of Basic and Applied Science (2010), 18(2): 315-321.

NO_2gas Sensing Properties of ZnO Thin Film Prepared by Sol-gel Method

K. V. Madhale[a], B.N.Jamadar[b], A. R. Nimbalkar[c*], N. B. Patil[d] and S. B. Kulkarni[e]

[a] Department of Physics, Walchand college of Engineering, Sangli.
[b] Department of Physics, Walchand college of Engineering, Sangli.
[c] Department of Physics, DKASC College, Ichalkaranj.
[d] Sharad Institute of Technology, Polytechnic, Yadrav, Ichalkaranji
[e] Department of Physics, The Institute of Science, Mumbai.
*Corresponding Author : amolakshay28@gmail.com

Abstract : Nitrogen dioxide (NO_2) sensing properties of ZnO thin film synthesized by simple Sol-gel spin coating method are studied. The structural, optical and gas sensing properties of the thin film is studied byusing X-ray diffraction (XRD), field emission scanning electron microscopy (FESEM), UV-Visible spectroscopy (UV-VIS). X-ray diffraction and scanning electron microscopy showed that the ZnO thin films have hexagonal wurtzite crystal structure. The optical band gap of deposited film is found to be 3.18 eV. The ZnO thin film shows the highest gas response to NO_2 at 200 °C operating temperature. Maximum response up to 2.30 is achieved towards 10 ppm NO_2 at 200 °C operating temperature. ZnO films are highly selective towards NO_2 in comparison with other gases like H_2S, Cl_2 and LPG.

Keywords*: ZnO thin film, NO_2 gas, XRD, Gas sensor.*

1. Introduction

Zinc oxide is a multifunctional material in II-VI semiconductor group and having a broad energy band gap (3.37eV), large exciton binding energy of 60 meV at room temperature and high thermal, mechanical stability at room temperature make it attractive for potential use in different fields like sensors, electrical, piezoelectric devices etc.[1-3].

Gas sensors have been used for the detection of toxic environmental pollutant gasses such as NO, NO_2, and CO, etc. and for the prevention of hazardous gas leaks, which comes from the many industrial processes. There are numbers of types of gas sensors that have been used to detect various toxic gasses: catalytic gas sensors, infrared gas sensors, semiconductor gas sensors, etc. However, gas sensors based on metal-oxides that are playing a vital role in the detection of toxic pollutants. The two types of metal oxide material gas sensors that have been used are p-type such as nickel oxide and cobalt oxide or n-type such as tin dioxide, titanium oxide, iron oxide and zinc oxide. ZnO was leading material in gas sensing because a large variety of nanostructures in form of nanoparticles, nanowires, nanobelts, nanorods or nanotetrapods have been synthesized i.e., with morphologies ideal for gas sensing [4-7].In this study, ZnO thin film was synthesized by the sol–gel spin coating technique and investigate structural, optical, and gas sensing properties.

2. Experimental details

ZnO thin films were synthesized by the sol–gel method, zinc acetate ($(CH_3.COO)_2$ $Zn.2H_2O$) with 99.5% purity (Thomas Baker) as a source of zinc oxide and RG grade ethanol was used. Zinc acetate (0.2M) was added to 40 ml of ethanol and stirred at 60°C for 60min., leading to the formation of a clear and homogeneous solution. The solution was deposited on to a glass substrate by a single wafer spin processor (APEX Instruments, Model spin NXG-P1). After setting the substrate on the substrate holder of the spin coater, the prepared solution (~0.2 ml) was dropped and spin-coated at 2000 rpm for 30 seconds in an air and dried on a hot plate at 100 °C for 5 min, the above procedure repeated 5 times. The as-prepared film was annealed at 400°C for 60 min in an ambient air to obtain nanocrystalline ZnO film.

The structural properties of the films were investigated by X-ray diffraction (XRD) (Bruker D2 phaser) using filtered Cu Kα radiation (1.54056Å). Morphological study of the films was carried out using field emission scanning electron microscopy (FESEM, JEOL 2300, Japan). The optical absorption spectra of ZnO thin films were obtained using UV-Vis Spectrophotometer-1800 (Shimadzu) in the 300–800 nm-wavelength range. NO_2 sensing measurements were measured at 200°C, the change in resistance was monitored continuously and recorded using Keithley (6514) electrometer incorporated into a PC during the measurements.

 ISBN : 978-81-923628-7-8

3. Results and discussion

3.1. Structural studies

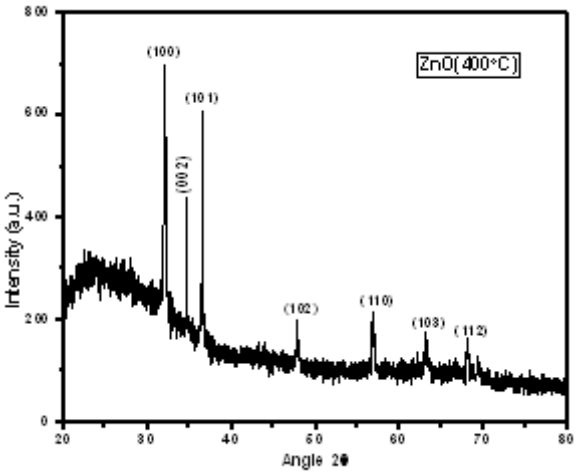

Fig.1. XRD pattern of a ZnO thin film annealed at 400°C for 60 min**.**

Fig.1 shows the X-ray diffraction spectra and FESEM image of ZnO thin film annealed at temperature 400 °C for 60 min and the result shows that the ZnO material grows hexagonal wurtzite crystal structure. The X-ray pattern of the film matches with the JCPDS card no. 79-0205 and it shows main significant peaks viz. (1 0 0), (0 0 2), (1 0 1), (1 0 2), (1 1 0), (1 0 3) and (1 1 2). The average value of grain size of ZnO was determined using Scherrer formula and the average grain size was found to be 70 nm [6]. The lattice constants calculated from the present data are a = 3.2316 Å and c = 5.1839 Å. The various parameters calculated using XRD study represented in Table 1.

Table 1. The various parameters calculated using XRD.

Sr. No.	Relative Intensity (%)	FWHM	d(Obs.)(Å)	d(Std.)(Å)	hkl plane	Lattice Strain
1	100	0.1181	2.79833	2.81761	(100)	0.0018
2	53.02	0.1181	2.59191	2.60755	(002)	0.0017
3	94.01	0.1378	2.46299	2.47894	(101)	0.0018

3.2. Optical study

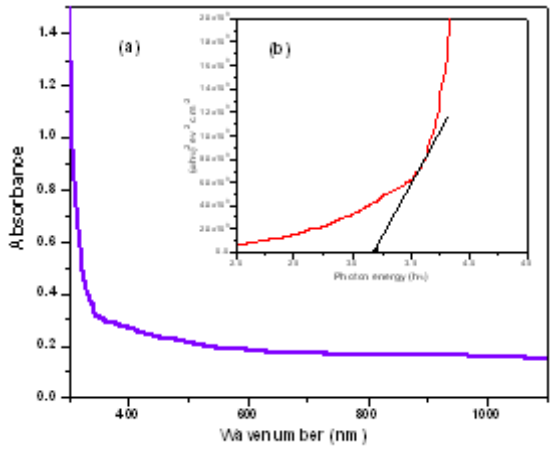

Fig.2. (a) The absorbance spectra of ZnO thin film at room temperature inset (b) the graph of (áh ˆ)^2 versus hˆ plots.

The optical absorbance spectra of ZnO thin film in the wavelength region of 300–11000 nm are shown in Fig. 2. The optical absorption at absorption edge illustrates the transmission from the valence band to conduction band and the absorption in the visible region because of some localized energy states in the bandgap [8]. It is seen that the ZnO thin film have less absorption in the visible region. The bandgap energy is calculated using the Tauc relationship as follows:

$$\alpha h\nu = A(h\nu - E_g)^n$$

Where 'α' is the absorption coefficient,'h' is Plancks constant,'ν' is the photon frequency, 'A' is a constant, E_g is the optical band gap, and n = 1/2 for direct semiconductor [9]. The inset of Fig. 2 shows the plot of $(ah\nu)^2$versus *hí* for the ZnO thin film. The value of direct band gap (E_g) of the ZnO film is found to be 3.15eV.

3.3. Gas sensing performance

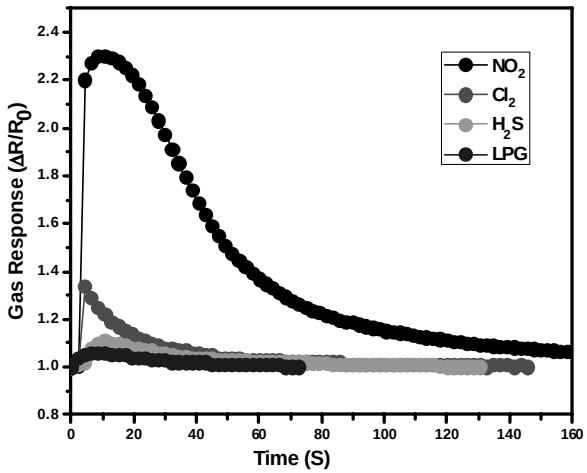

Fig.3. Gas response versus time graphs for ZnO thin film.

The as-prepared ZnO thin film was tested to different gasses such as LPG, H_2S, Cl_2 and NO_2 at 200°C for 10 ppm gas concentrations. Fig.3. shows the sensor response = ÄR/R_0 versus time, (where ÄR is the change in resistance and R_0 is the value of baseline) for ZnO thin film at 200°C. It shows maximum response up to 2.30 is achieved towards 10 ppm NO_2 in presence of other gasses [10-11].

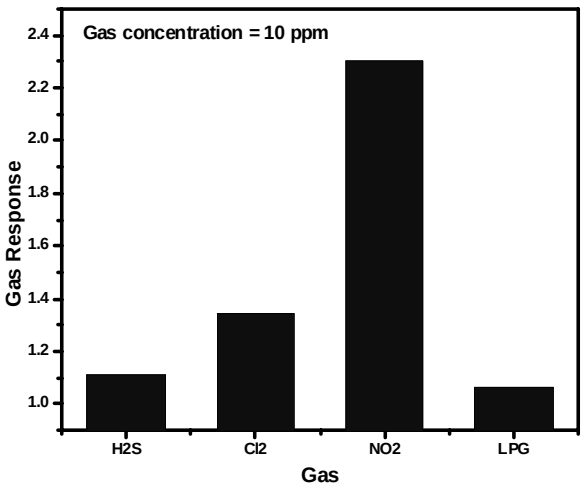

Fig.4. Selectivity study of ZnO thin film.

The selectivity study of ZnO thin film carried out at 200°C and at fixed 10 ppm towards different gases viz. nitrogen dioxide (NO_2), chlorine (Cl_2),hydrogen sulfide (H_2S)and LPG. Selectivity study shows the ZnO thin film was fairly sensitive and higher response towards NO_2 gas as compared to other test gases because of the higher reactivity of NO_2 and sensing layer of a sensor and also higher electron affinity (2.28 eV) of NO_2 in comparison with preadsorbed oxygen (0.43 eV) and various test gases [12]. Selectivity coefficient (K) of a target gas with respect to interfering gas is calculated using the following equation and represented in Table 2.

$$K = |S_a/S_b|$$

Where S_a is the responses of a sensor film towards NO_2 gas and S_b is the responses of a sensor film towards interfering gas. ZnO thin film sensor shows maximum gas response towards NO_2 (2.3) as compared to other gases at 200°C operating temperature and more selective towards NO_2 than other gases.

Gases	H_2S	Cl_2	LPG
Selectivity coefficient (K)	2.07	1.71	2.16

4. Conclusions

ZnO thin film has been successfully synthesized by sol-gel spin coating technique. ZnO material grows hexagonal wurtzite crystal structure. The optical band gap of the film is 3.15 eV. The ZnO thin film is selective and sensitive towards NO_2 gas against the other interfering gasses for 10 ppm fixed concentrations.

References

[1] V. B. Patil, S. G. Pawar, S. L. Patil, S. B. Krupanidhi,J Mater Sci: Mater Electron (2009).

[2] A. Muthuvinayagam, Boben Thomas, P. Dennis Christy, R. Jerald Vijay, T. Manovah David, and P. Sagayaraj, Archives of Applied Science Research, 3 (2011)(4):256-264.

[3] C.S. Prajapati, P.P. Sahay, Applied Surface Science 258 (2012) 2823– 2828.

[4] K. Arshak, I. Gaidan, Materials Science and Engineering B 118 (2005) 44–49.

[5] M.C. Carotta , A. Cervi, V. di Natale, S. Gherardi, A. Giberti, V. Guidi, D. Puzzovio, B. Vendemiati, G. Martinelli, M. Sacerdoti, D. Calestani, A. Zappettini, M. Zha, L. Zanotti, Sensors and Actuators B 137 (2009) (164–169).

 ISBN : 978-81-923628-7-8

[6] S. L. Patil, S. G. Pawar, A. T. Mane, M. A. Chougule, V. B. Patil, J Mater Sci: Mater Electron (2010) 21:1332–1336.

[7] Sergiu T. Shishiyanu, Teodor S. Shishiyanu, Oleg I. Lupan, Sensors and Actuators B 107 (2005) 379–386.

[8] C. S. Prajapati, P. P. Sahay, Applied Surface Science 258 (2012) 2823–2828.

[9] Amit Kumar Chawla, Davinder Kaur, Ramesh Chandra, Optical Materials 29 (2007) 995–998.

[10] S. Öztürk, N. Kýlýnç, N. Taþaltin, Z.Z. Öztürk, Thin Solid Films 520 (2011) 932–938.

[11] S.D. Shinde, G.E. Patil, D.D. Kajale, V.B. Gaikwad, G.H. Jain, Journal of Alloys and Compounds 528 (2012) 109–114.

[12] V. V. Ganbavle, S. I. Inamdar, G. L. Agawane, J. H. Kim, K. Y. Rajpure, Chemical Engineering Journal 286 (2016) 36–47.

Synthesis and Study of Carbon Quantum Dots Using Facile Oven Assisted Carbonization Method

Samiksha Pandey[a], Soni Yadav[b] and V. Raikwar[c]

[a, b, c] R. J. College, Ghatkopar, Mumbai-400086.

Abstract: Carbon quantum dots which are generally small carbon nanoparticles (less than 10 nm in size) with various unique properties, have found wide use in many fields during the last few years. In this work, we describe the recent progress in the field of CQDs, focusing on their synthesis method, luminescent mechanism, and applications in biomedicine, optronics, and catalysis and sensor issue. We have used extracts of fruits like coconut, apple and papaya which are commonly found in markets as precursors. We have developed a fast, environmental friendly and low cost oven -assisted carbonization method for synthesis of highly fluorescent carbon dots. The properties of carbon dots were investigated by UV visible spectroscopy, photoluminescence spectroscopy and scanning electron microscopy. The CQDs have found application in different areas such as biomedicine, photocatalysis, photosensor, solar energy conversion, light emitting diodes etc.

Keywords: *Carbon quantum dots, fruit extracts, carbonization*

1. Introduction

Carbon quantum dots (CQDs) have received global attention as fluorophores due to easy methods of synthesis and properties such as small size, good photo stability, excellent biocompatibility, tunable photoluminescence (PL), and chemical stability. The CQDs are small nanoparticles made of carbon which include different surface passivation by functionalization or modification. The CQDs can be crystalline or amorphous. The carbon hybridization in CQDs is sp^2 while in some cases; sp^3 hybridization has also been reported. Carbon quantum dots are quasizero dimensional carbon nanoparticles with an average particle less than 10 nm with some form of surface passivation. In 2004, they accidentally discovered during the purification of single walled carbon nanotubes. This discovery fascinated towards extensive studies to exploit the fluorescence properties of these carbon quantum dots. The carbon is commonly a black material, and usually considered to have a low solubility in water and weak fluorescence. The wide attention has been focused on carbon quantum dots because of their good solubility and strong luminescence for which they are termed as carbon nano lights. The CDs have oxygen/nitrogen-containing functional groups or polymeric aggregations. Mainly, the CDs include graphene quantum dots (GQDs), polymer dots (PDs) and carbon quantum dots (CQDs). Oxygen-containing functional groups (hydroxyl and carboxyl) are mostly present on the CQDs surface that result in their water solubility.

2. Experimental

Many methods have been proposed to prepare CQDs during the last decade which can be classified intoTop-down and Bottom-upapproaches and they can be modified during post-treatment.In chemical ablation method the strong oxidizing acids carbonize small organic molecules to carbonaceous materials, which can be further cut into small sheets by controlled oxidation [1,2].This method may suffer from harsh conditions and drastic processes. Electrochemical soaking is a powerful method to prepare CQDs using variousbulk carbon materials as precursors [3,4]. However, there are only a few reports about electrochemically carbonizing small molecules to CQDs. Laser ablation of a carbon target in the presence of water vapour with argon as a carrier gas at 900 °C and 75 k Pa was studied [5, 6, 7, 8]. Microwave irradiation of organic compounds is a rapid method to synthesize CQDs [9,10,11,12,13,14]. The resultant CQDs are highly biocompatible and have great potential for biomedical applications.Hydrothermal carbonization (HTC) [15] is a lowcost, environmentally friendly, and nontoxic route to produce novel carbon-based materials from various precursors [16].However it requires a long time to prepare a material. CQDs were prepared via HTC from many precursors such as glucose [17], citric acid [16], chitosan [18], banana

 ISBN : 978-81-923628-7-8

juice [19], protein [20] and orange juice [21].Liu et al. reported a one-step synthesis of amino-functionalized fluorescent CQDs by hydrothermal carbonization of chitosan at180 °C for 12 hours [22]. Note that the amino-functionalized fluorescent CQDs can be used directly as novel bioimaging agents.

All these methods are either time consuming or require sophisticated facilities or environment. We have developed a facile, time efficient and low cost method for synthesizing carbon quantum dots using fruit extracts like papaya, apple and coconut. The extracts of fruits were taken as precursors in a beaker. It was kept in an oven for carbonization. The heating time varies for different precursors. After sufficient heating the black coloured dried mass was allowed to cool in a dry air. The as prepared sample was then crushed by mortar and pestle to convert into fine black powder. Further, the powder was dissolved into water and the solution was filtered using 0.25 ìm membrane filter. This aqueous solution was used for further characterization. The carbon dots were characterized by UV visible spectroscopy, Photoluminescence spectroscopy (PL) and field emission scanning electron microscopy (FESEM).

1. Results and discussion

3.1 Optical absorption:

CQDs typically show obvious optical absorption in the UV region (260–320 nm), with a tail extending to the visible range. For example, CQDs produced from the electrochemical oxidation of multiwalled carbon nanotubes (MWCNTs) show an absorption band at 270 nm, with a narrow full width at half maximum (FWHM) of 50 nm. In addition, recent studies have shown that the absorbance of CQDs can be red-shifted after specific surface modification. [23]. In this work, the testing was done on Shimadzu UV-1800 UV spectrophotometer. The spectra were recorded between wavelength range of 200 to 800 nm. Fig.1shows the absorption graphs of CQDs made from papaya, apple and coconut extracts. The graphs clearly show the CQDs are good absorber of UV light.

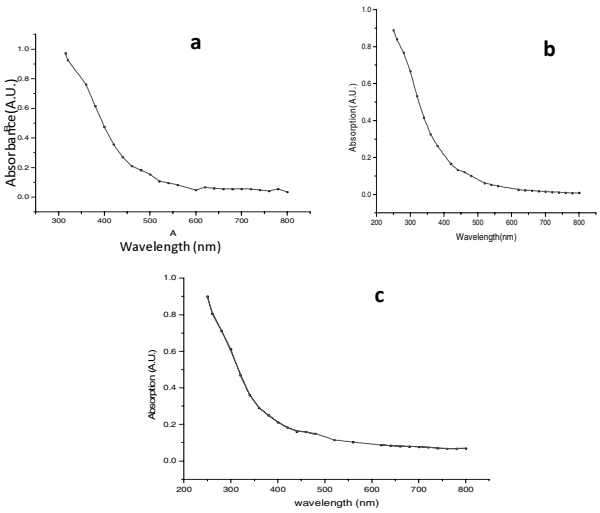

Fig 1: UV-Visible spectra of CQDs prepared by using (a) apple, (b) Papaya and (c) coconut extract

Photoluminescence (PL) property :

PL emission follows the Stokes type emission; namely, the PL emission wavelength is longer than the excitation wavelength. There have been many literature reports on the observation of PL emissions in CQDs. A large number of studies discussed the relationship between the PL emission and the excitation-wavelength of the CQDs. Sun et al. reported that fluorescent CQDs modified with polyethylene glycol (PEG1500N) display obvious λ_{ex}-dependent emission. This phenomenon was also confirmed subsequently by Bourlinos and co-workers, in which CQDs fabricated via one-step thermal treatment of 4-aminoantipyrine show λ_{ex}-dependent PL emission from 525 to 660 nm with excitation wavelength from 425 to 625 nm. However, CQDs hydrothermally synthesized from urea and separated via silica column chromatography show only one peak in the PL excitation spectrum,

Fig.2 shows the excitation and emission spectra for CQDs made by different precursors. It shows that the as prepared samples absorb UV light of wavelength (365 nm) and emit bright sky blue colour of wavelength 485 nm.

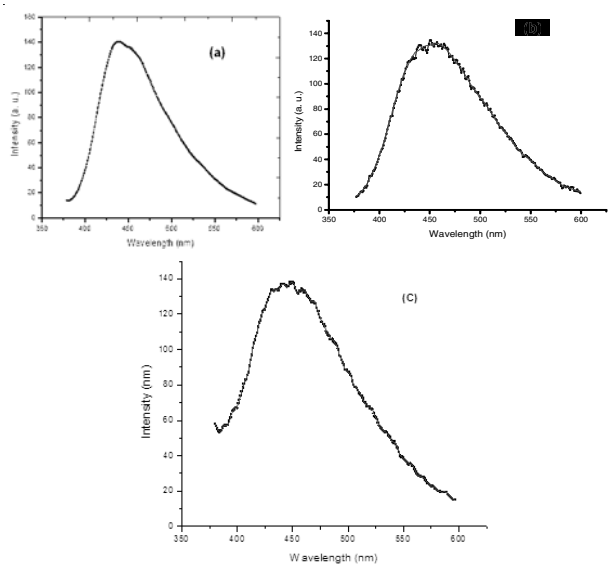

Fig 2: Emission spectra of CQDs prepared by using (a) apple, (b) Papaya and (c) coconut extract

3.1 Field emission scanning electron microscopy (FESEM)

Fig 3 shows the FESEM images of CQDs using different precursors. All the images shows Nanosized spherical particles.

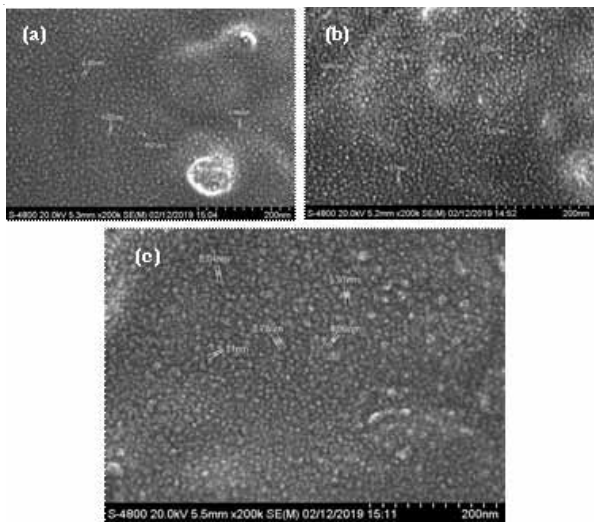

Fig 3: FESEM images of CQDs prepared by using (a) apple, (b) Papaya and (c) coconut extract

4. Conclusion

The carbon quantum dots were prepared using facile one pot oven assisted synthesis method. The precursors were procured from papaya, apple and coconut fruit extracts. The prepared CQDs were dissolved in double distilled water and shows bright sky blue emission under UV light of 365 nm. The FESEM images confirm the nanosized spherical particles having sizes less between 3 to 10 nm. The photoluminescence spectra shows that the reported material can be used by bioimaging and optical devices.

References :

1 S. Ray, A. Saha, N. R. Jana and R. Sarkar(2009)"Fluorescent Carbon Nanoparticles: Synthesis, characterization, and Bioimaging Application" J. Phys. Chem. C113:18546-1855.

2 L. Shen, L. Zhang, M. Chen, X. Chen and J. Wang(2013)"The production of pH-sensitive photoluminescent carbon nanoparticles by the carbonization of polyethylenimine and their use for bioimaging"Carbon55: 343-349.

3 J. Zhou, C. Booker, R. Li, X. Zhou, T.-K. Sham, X. Sun and Z. Ding(2007)"An Electrochemical Avenue to Blue Luminescent Nanocrystals from Multiwalled Carbon Nanotubes (MWCNTs)"J. Am. Chem. Soc.129(4): 744-745.

4 H. Li, X. He, Z. Kang, H. Huang, Y. Liu, J. Liu, S. Lian, C. H. A. Tsang, X. Yang and S. T. Lee(2010) "Water-soluble fluorescent carbon quantum dots and photocatalyst design" Angew. Chem. Int. Ed. 49(26):4430-4.

5 S.-L. Hu, K.-Y. Niu, J. Sun, J. Yang, N.-Q. Zhao and X.-W. Du, (2009)"One-step synthesis of fluorescent carbon nanoparticles by laser irradiation"J. MaterChem. 19: 484-488.

6 2 Y.-P. Sun, B. Zhou, Y. Lin, W. Wang, K. S. Fernando, P. Pathak, M. J. Meziani, B. A. Harruff, X. Wang and H. Wang, (2006) "Quantum-Sized Carbon Dots for Bright and Colorful Photoluminescence'' J Am. Chem. Soc.128: 7756-7757.

7 L. Cao, X. Wang, M. J. Meziani, F. Lu, H. Wang, P. G. Luo, Y. Lin, B. A. Harruff, L. M. Veca and D. Murray (2007)"Carbon dots for Multiphoton Bioimaging" J. Am.Chem. Soc.129: 11318-11319.

8 S.-L. Hu, K.-Y. Niu, J. Sun, J. Yang, N.-Q. Zhao and X.-W. Du, (2009) "One-step synthesis of fluorescent carbon nanoparticles by laser irradiation"J. Mater Chem.19: 484-488.

 ISBN : 978-81-923628-7-8

9 H. Zhu, X. Wang, Y. Li, Z. Wang, F. Yang and X. Yang (2009) "Microwave synthesis of fluorescent carbon nanoparticles with electrochemiluminescence properties" Chem Commun.34:5118-5120.

10 X. Zhai, P. Zhang, C. Liu, T. Bai, W. Li, L. Dai and W. Liu (2012) "Highly luminescent carbon nanodots by microwave-assisted pyrolysis" Chem. Commun.48: 7955-7957.

11 Y. Liu, N. Xiao, N. Gong, H. Wang, X. Shi, W. Gu and L. Ye (2014) "One-step microwave-assisted polyol synthesis of green luminescent carbon dots as optical nanoprobes" Carbon 68: 258-264.

12 A. Jaiswal, S. S. Ghosh and A. Chattopadhyay (2012) "One step synthesis of C-dots by microwave mediated caramelization of poly (ethylene glycol)" Chem. Commun., 48: 407-409.

13 Y. Liu, N. Xiao, N. Gong, H. Wang, X. Shi, W. Gu and L. Ye, (2014) "Microwave-assisted polyol synthesis of gadolinium-doped green luminescent carbon dots as a bimodal nanoprobe"Carbon68: 258-264.

14 Y. Liu, N. Xiao, N. Gong, H. Wang, X. Shi, W. Gu and L. Ye(2012) "Highly luminescent carbon nanodots by microwave-assisted pyrol" Chem. Commun. 48: 7955-7957.

15 B. Hu, K. Wang, L. Wu, S. H. Yu, M. Antonietti and M. M. Titirici(2010) "Engineering carbon materials from the hydrothermal carbonization process of biomass" Adv. Mater22(7): 813-28.

16 S. Zhu, Q. Meng, L. Wang, J. Zhang, Y. Song, H. Jin, K. Zhang, H. Sun, H. Wang and B. Yang, Angew(2013) "Highly photoluminescent carbon dots for multicolor patterning, sensors, and bioimaging" Chem., Int. Ed.125: 4045-4049.

17 Z.-C. Yang, M. Wang, A. M. Yong, S. Y. Wong, X.-H. Zhang, H. Tan, A. Y. Chang, X. Li and J. Wang (2011) "Intrinsically fluorescent carbon dots with tunable emission derived from hydrothermal treatment of glucose in the presence of monopotassium phosphate" Chem. Commun.47: 11615-11617.

18 Y. Yang, J. Cui, M. Zheng, C. Hu, S. Tan, Y. Xiao, Q. Yang and Y. Liu(2012)"One-step synthesis of amino-functionalized fluorescent carbon nanoparticles by hydrothermal carbonization of chitosan" Chem. Commun. 48: 380-382.

19 B. De and N. Karak (2013) "A green and facile approach for the synthesis of water soluble fluorescent carbon dots from banana juice" RSC Adv3: 8286-8290.

20 Z. Zhang, J. Hao, J. Zhang, B. Zhang and J. Tang,(2012)) "Protein as the source for synthesizing fluorescent carbon dots by a one-pot hydrothermal route" RSC Adv. 2: 8599-8601.

21 S. Sahu, B. Behera, T. K. Maiti and S. Mohapatra(2012) "Simple one-step synthesis of highly luminescent carbon dots from orange juice: Application as excellent bio-imaging agents" Chem. Commun. 48: 8835-8837.

22 Y. Yang, J. Cui, M. Zheng, C. Hu, S. Tan, Y. Xiao, Q. Yang and Y. Liu(2012) "One-step synthesis of amino-functionalized fluorescent carbon nanoparticles by hydrothermal carbonization of chitosan" Chem. Commun. 48: 380-382.

23 S. Mitra, S. Chandra, S. H. Pathan, N. Sikdar, P. Pramanik and A. Goswami(2013) "Room temperature and solvothermal green synthesis of self passivated carbon quantum dots" RSC Adv.3: 3189-3193.

Molecular Interaction Studies in Binary Liquid Mixtures of Allyl Amine (AA) and 2-Methoxy Ethanol (2ME) from Ultrasonic Studies and IR Spectroscopy

Sangita S. Meshram[a], Bhalchandra K. Mandlekar[b], Umakant B. Tumberphale[c] and Prashant G. Gawli[d]

[a] Dept of Physics, B.N. Bandodkar Science College, Thane-431605, Maharashtra. India.
[b] Dept of Physics, B.N. Bandodkar Science College, Thane-431605, Maharashtra. India.
[c] Dept of Physics, N.E.S. Science College, Nanded-431605, Maharashtra. India
[d] Head of Department of Physics, B.S. College, Basmath, Dist. Hingoli – 431512, Maharashtra. India.

Abstract : Ultrasonic studies is a potential tool in evaluating intermolecular interactions and nonlinear properties in binary liquid mixtures. Ultrasonic Velocity for binary mixture Allyl amine (AA)and 2-Methoxy Ethanol (2ME) have been measured for 2MHz ultrasonic frequency at 303 K. Various theoretical approaches for sound Simple Mixing Rule (U_{SMR}),Rao (U_{Rao}) ,Impedance Relation (U_{IR}), Vandeel ($U_{Vandeel}$) and Nomatto ($U_{Nomatto}$) have been applied to obtain the theory of best fit for the system for the temperature taken for investigation. Conformational analysis of the formation of hydrogen bond between Allyl amine (AA)and 2-Methoxy Ethanol (2ME) is supported by the FT-IR .The present investigation is aimed at experimental determination of ultrasonic velocity and its comparison with different theories and molecular interactions.

Keywords*: Ultrasonic velocity; Molecular interactions ; Simple Mixing Rule; Impedance Relation*

Introduction:

The rapid development of ultrasonic techniques opened up wide field of research and technical applications in Physics, Chemistry, biology medicine and industry. The present investigation is aimed at experimental determination of ultrasonic velocity and its comparison with different theories and molecular interactions. This study leads to understand molecular interactions in binary liquid mixtures using FTIR too. Alcohols are industrially and scientifically important organic compounds and their physical and chemical properties are largely determined by the –OH group. Alcohols are strongly associated in solution because of dipole-dipole interaction and hydrogen bonding Methoxy ethanol is used mainly as solvent for many different purposes such as varnishes, dyes, and resins**[1]** Amines are among the most valuable classes of compounds in chemistry, amine present natural products, particularly alkaloids and widely used as pharmaceuticals, agrochemicals and lubricants**.[2]** Cream or pills made from Allyl amine is used as antifungal medicine for the treatment of skin and scull ringworm. Amine is used to make antibiotic, diuretic and sedative medicine .The ultrasonic velocity of pure liquids and their binary mixtures has been measured by using a fixed frequency ultrasonic interferometer (M-83 model) supplied by Mittal Enterprises, New Delhi, at a fixed frequency of 2MHz with an accuracy of ±0.2%.

Material And Methods:

In the present study allyl amine and 2-Methoxy Ethanol is of AR grade were procured from Across, Qualigen, Merck and S.D. fine chemical, Mumbai respectively and used without further purification. Samples of solution with different mole fractions of Allyl amine in 2-Methoxy Ethanol were prepared. The density (ρ), viscosity (η) and ultrasonic velocity (U) of pure components and their mixtures were measured using pycknometer, Ostwald's viscometer and ultrasonic frequency interferometer model No. M-83.

The theoretical values of sound speeds are evaluated using the following empirical and semi-empirical relations such as Nomoto's relation, Vandeal ideal mixing relation and Impedance Dependence Relation.

Nomotos relation (NOM) :

An empirical formula was established by Nomoto for sound velocity in binary liquid mixtures based on the assumption of the linearity of molar sound velocity namely,

$$R=x_1R_1+x_2R_2 \qquad (1)$$

where *x* is the mole fraction and the molar sound velocity for molecular liquids is defined as

$$R=(m/r)\,(U^{\frac{1}{3}}) =V \qquad (2)$$

 ISBN : 978-81-923628-7-8

and the additive molar volume (V) is given by

$V=x_1V_1+x_2V_2$ (3)

whcre suffix 1 and 2 refer to the components of the mixture. Hence the empirical formula for sound speed in binary liquid mixtures given by Nomoto can be written as [3] [4] [5] [6]

$$U^{Nomatto} = \left[\frac{x_1R_1+x_2R_2}{x_1V_1+x_2V_2}\right]^3$$

Impedance dependence relation (IDR) :

The acoustic impedance is a product of sound speed and density of liquid and is given by the relation

$Z = U.$ (5)

where *U* and *p* are sound speed and density of the medium, respectively.According to Kinsler and Frey [7] has greater significance as a parameter describing a medium and intermolecular interactions as compared to U and p individually. The condition of linearity of the acoustic impedance with composition is written as

$Z_{Exp} = x_1z_1+x_2z_2$ (6)

It also satisfies the additive acoustic impedance and thus the sound speed in the mixture is given by Impedance dependence relation [8] [9]

$$5H_{5<5E} = \sum \frac{X_i Z_i}{X_i \rho_i}$$ (7)

Where, Zi is Acoustic Impedance.

On the basis of ideal mixing of adiabatic compressibility [10] Van Dael obtained ideal mixing relation for ultrasonic velocity

$$\frac{1}{U^2} = (M_1X_1 + M_2X_2)\left(\frac{X_1}{M_1U_1^2}+\frac{X_2}{M_2U_2^2}\right)$$ (8)

Where, U = Ideal mixing Ultrasonic Velocity in liquid mixture. U1 & U2 are ultrasonic

velocities in species and X1 and X2 are mole fractions of the species.

Rao's specific sound velocity[11] relation is

$$5H_{5E5N5\backslash} = (\sum X_i r_i \rho_i)^3$$ (9)

Where, $= \frac{U_i^{\frac{1}{3}}}{\rho_i}$

According to the **simple mixing Relation,**

$$U_{SMR}=(U_1X_1 + U_2X_2)$$ (10)

The values of density (ñ), ultrasonic velocity (U), acoustic impedance (Z), effective mass

(Meff), density, along with the values calculated by using the Nomoto relation, Van Dael ideal mixing relation, Impedance relation, Rao's specific velocity relation Simple mixing relation, of the binary liquid mixture of AA+ 2-Methoxy Ethanol obtained at room temperature are listed in table (1).

Table 1.

Mole Fraction X_1	Mole Fraction X_2	Density ρ (kg/ m^3	Ultrasonic Velocity U(m/sec)	M_{eff}	Acoustic impedance Z 10^6 kg / m^2 sec	U_{SMR}	U_{Rao}	U_{IR}	$U_{Vandeel}$	$U_{Nomatto}$
0	1	959.1	1653.32	76.10	1.5857	1653.32	1653.32	1653.29	1653.32	1653.32
0.1317	0.8683	940.3	1328.89	73.64	1.2496	1604.56	1331.28	1328.88	1557.90	1602.35
0.2578	0.7422	915.7	1333.33	71.20	1.2208	1555.93	1333.33	1333.19	1487.99	1553.81
0-3847	0.6153	885.4	1471.10	68.79	1.3025	1507.99	1471.10	1471.10	1430.98	1505.33
0.5103	0.4897	846.4	1466.66	66.40	1.2414	1460.54	1466.66	1466.66	1385.29	1357.68
0.6346	0.3654	830.2	1302.22	64.04	1.0811	1413.59	1302.22	1302.22	1348.43	1410.89
0.7576	0.2424	803.8	1297.76	61.70	1.0431	1367.12	1297.76	1297.76	1318.63	1364.95
0.8794	0.1206	789.7	1431.11	59.38	1.1302	1321.11	1431.11	1431.11	1294.64	1319.83
1	0	761.0	1275.55	57.09	0.9707	1275.55	1275.55	1275.56	1275.55	1275.55

Table-2

Experimental velocities and percentage Deviation are listed for the System AA+2-ME

Mole Fraction X_1	Ultrasonic Velocity U Experimental (m/sec)	$\%U_{S.M.R}$ (m/sec)	$\%\ U_{Rao}$ (m/sec)	$\%\ U_{IR}$ (m/sec)	$\%U_{Vandeel}$ (m/sec)	$\%\ U_{Nomatto}$ (m/sec)
0	1653.32	0	0	0	0	0
0.1317	1328.89	-20.74	-0.18	0	-17.23	-20.58
0.2578	1333.33	-16.70	0	0.10	-11.60	-16.54
0-3847	1471.10	-2.51	0	0	5.83	-2.33
0.5103	1466.66	0.41	0	0	5.55	0.61
0.6346	1302.22	-8.55	0	0	-3.55	-8.35
0.7576	1297.76	-5.34	0	0	-1.61	-5.18
0.8794	1431.11	7.69	0	0	9.54	7.78
1	1275.55	0	0	0	0	0

Result and Discussion:

Fig 1.

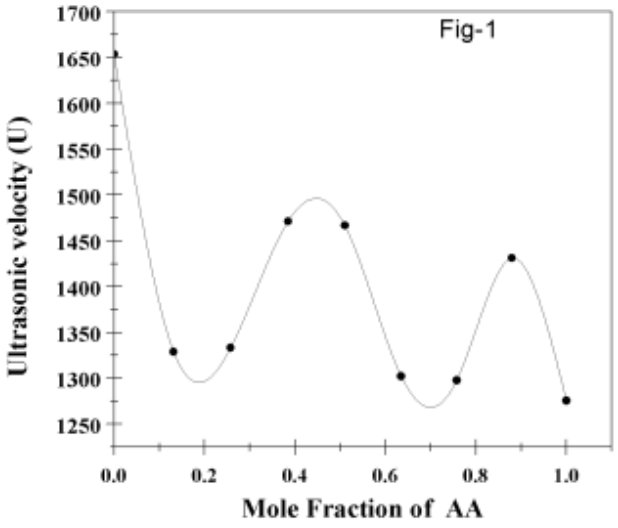

Fig 2.

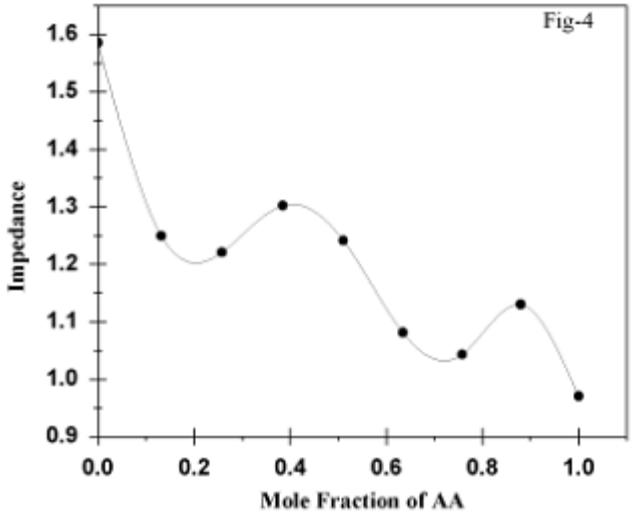

The density values is minimum for lower composition and maximum for higher composition of Allyl amine. But the ultrasonic velocity values vary nonlinearly due to molecular to molecular dissociation, with various compositions. The increase or decrease in these parameters with various compositions shows the existence of strong interactions between the components of molecules in the binary mixtures. This indicates the Dipole-dipole interaction or hydrogen bonded complex formation between unlike molecules The maximum deviation from the linearity, where change in the slope is maximum indicating the complex formation.**[12]** In present system the formation of the

 ISBN : 978-81-923628-7-8

complex is at 0.3847 and 0.8794 mole fraction of AA or the minima between the two maxima. The complex formation in present case is at 0.5103**.[13]** On mixing two liquids, the interactions between the molecules of the two liquids takes place because of the presence of various types of forces such as dispersion forces, charge transfer, hydrogen bonding, dipole-dipole and diploe-induced dipole interactions. Thus, the observed deviation of theoretical values shows that the molecular interaction is taking place between the unlike molecules in the liquid mixtures. Thus, the linearity of molar sound velocity and additivity of molar volumes, as suggested by Van Dael and Impedance relation, in deriving the empirical relations have been truly observed in the aforementioned binary liquid mixturesFrom table 1 it is observed that in the binary system of AA+ 2-Methoxy Ethanol, there is a good agreement between the experimental and theoretical values.

Table 2 shows higher deviations in some intermediate concentration range suggest the existence of strong tendency for the association between the component molecules, where hydrogen bonding may be formed [14]

The predictive abilities of various ultrasonic theories depend upon the strength interaction prevailing in a system; these theories generally fail to predict accurately the ultrasonic velocities where strong interactions supposed to exist and the average absolute percentage relative deviation is small in systems where the interactions are less or nil [15] (S. Nithiyanantham, 2017)..[16]

FTIR- Figure-3

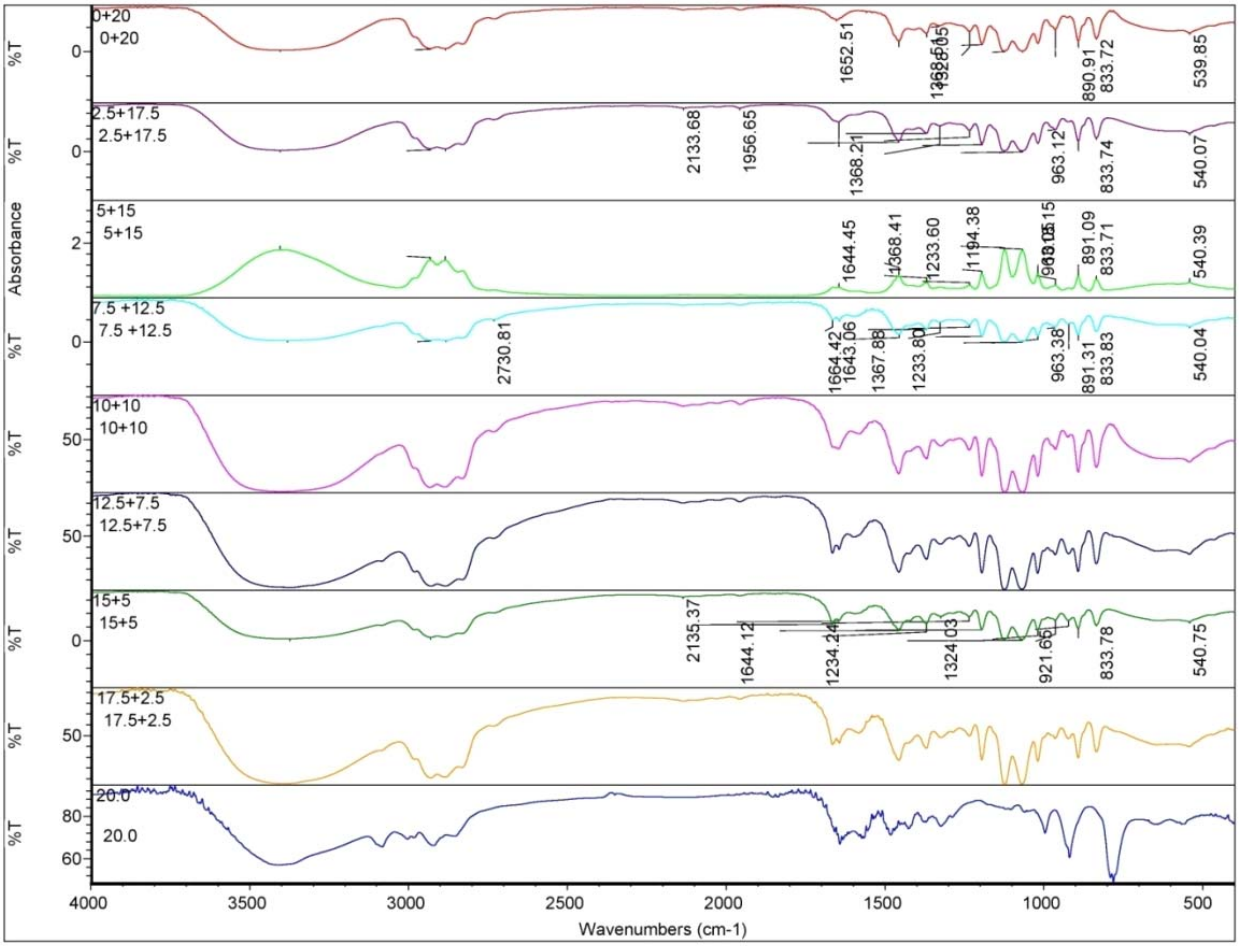

The spectroscopic study of solute-solvent interaction is important to understand the structure and dynamics of the pure and mixed liquids. In the present investigation, infrared spectra of the AA+2-ME and its mixtures have been taken at room temperature. **[17].**The spectrum clearly indicates multiple functionality, occurring mutual interaction .The Fourier-transform infrared spectroscopy (FTIR) analysis of AA+2-ME proved the presence of amines, **alcohols, Nitro compounds,carboxylic acids,esters,ethers and** hydroxy group. Lump at 2730.81cm^{-1} gradually disappeared.No significant change in the hydroxy group bands with concentration is a strong indication of intramolecular (internal) hydrogen bonding. [18]

Conclusion:

1. The acoustical parameters in the AA+2-ME system suggests the molecular interactions in the unlike molecules of the system.
2. Complex formation happens to be at two mole fraction.
3. Multiple functionality, suggest mutual interaction.
4. Out of five theories and relations discussed above the, van Deal ideal mixing relation, Rao's specific velocity and Impedance relation provided good results.
5. Strong indication of intramolecular (internal) hydrogen bonding.

Acknowledgment:

Authors are greatly acknowledged to VPM's B.N.Bandodkar college of Science.

References:

[1] B.G. Nemaniwar, S.S. Mokle, P.L. Kadam, "Effect of temperature on the dielectric relaxation time of binary mixture of 2-chloroaniline and 2-ethoxy ethanol in 1-4 dioxane solution losing microwave absorption data," Pakistan Journal of Chemistry, Vol. 3, No. 2, pp. 1-6, 2013]

[2] Guillena, G., Ramon, D. J. & Yus, M. Hydrogen autotransfer in the Nalkylation of amines and related compounds using alcohols and amines as electrophiles. Chem. Rev. 110, 1611–1641 (2010)]

[3] O Nomoto *J. Phys. Soc. Jpn.* 13 1528 (1958)

[4] O Nomoto *J. Phys. Soc. Jpn.* 11 1146 (1956).

[5] O. Nomoto, Journal of the Physical Society of Japan, vol. 4, p. 280, 1949

[6] O. Nomoto, "Empirical Formula for Sound Velocity in Liquid Mixtures," Journal of the Physical Society of Japan, vol. 13, pp. 1528–1532, 1958

[7] L E Kinsler and A R Frey in Fundamentals o f Acoustics New york: Wiley) (1962)

[8] M Kalidoss and R Srinavasamoorthy J. Pure Appl. Ultrason 94 (1997)

[9] S. Baluja and R. H. Parsania, "Studies on acoustical properties of diclofanac sodium methanol-water system at 30%C," Asian Journal of Chemistry, vol. 9, no. 1, pp. 149–152, 1997.

[10] W. van Dael and E . Vangeel, in Proceedings of the International Conference on Calorimetry and Thermodynamics, p. 555, Warsaw, Poland, 1955

[11] K. Rayapa Reddy, D. Bala Karuna Kumar, C. Rambabu, and G. Srinivasa Rao, "Theoretical evaluation of ultrasonic velocities in binary liquid mixtures of N-Methyl-2-pyrrolidone at different temperatures with Some cyclic compounds," E-Journal of Chemistry, vol. 9, no. 2, pp. 553–562, 2012.

[12] Tumberphale U.B. Thesis, 2013."Molecular Interaction Studies in Binary Liquid Mixtures from Dielectric Data at Microwave Frequency".

[13] Deogaonkar V.S (1977). Dielectric studies of binary mixtures of alkoxy Ethanols and aniline at 9.85 GHz microwave frequency. Indian Journal of Pure and Applied Physics 15 98.

[14] G.V.Rama,Rao,A.Viswanatha Sarma,J.Shiva Rama Krishna, C.Ramababu (2005)],Theoretical evolution of ultrasonic velocities in binary liquid mixtures of o-chlorophenol at different temperatures. Indian journal of pure and applied physics, Volume 33, 345-354

[15] S. Nithiyanantham , Thiru. A. Govindasamy (2017) Ultrasonic Velocity Models in Liquids (Nano-Fluids) Rev. Theor. Sci. 2017, Vol. 5, No. 1 2327-1515/2017/5/001/006 doi:10.1166/rits.

 ISBN : 978-81-923628-7-8

[16] Zareena Begum, P. B. Sandhya Sri, and C. Rambabu Theoretical Evaluation of Ultrasonic Velocities in Binary Liquid Mixtures of Anisaldehyde with Some Alcoxyethanols at Different Temperatures International Scholarly Research Network ISRN Physical Chemistry Volume 2012, Article ID 943429, 12 pages doi:10.5402/2012/94342

[17] A.Anis Fathima spectroscopic studies on molecular interactions in binary liquid mixtures a.anis fathima madurai kamaraj university May 2008 synopsis of the thesis submitted to madurai kamaraj university in partial fulfilment of the requirements for the degree of doctor of philosophy in physics.

[18] John Coates Coates Consulting, Newtown, USA INTERPRETATION OF INFRARED SPECTRA, A PRACTICAL APPROACH Encyclopedia of Analytical Chemistry R.A. Meyers (Ed.) Copyright Ó John Wiley & Sons Ltd,1-23

Synthesis and Fluorescence Properties of Eu^{3+} to Eu^{2+} in $BaAl_2Si_2O_8$ Phosphor under Charcoal Atmosphere

U. B. Gokhe[1*], K. A. Koparkar[2] and S. K. Omanwar[2]

[1]Department of Physics, B N Bandodkar college of science, Thane (MS) 400601, India
[2]Department of Physics, SGB Amravati University, Amravati (MS) 444101, India

Abstract : The series of Eu^{3+}/Eu^{2+} doped $Ba_{(1-x)}Al_2Si_2O_8$(x=Eu=0.01, 0.02, 0.03, 0.04 and 0.05 mole) phosphors were prepared by traditional solid state reaction method. The crystalline phase of $BaAl_2Si_2O_8$ host was verified by X-ray diffraction (XRD) analysis. Moreover, scanning electron microscopy (SEM) and EDAX was investigated for morphological and for content present in the as-prepared sample. On the SEM analysis, the average particle size was in the range of 2-10 µm. The photoluminescence (PL) excitation (lem = 615 nm) and emission (lex = 395 nm) of $Ba_{(1-x)}Al_2Si_2O_8:_xEu^{3+}$ were investigated. The optimum PL intensity was observed at 615 nm ($^5D_0 \rightarrow {}^7F_2$). The concentration quenching was observed at 0.03 mole concentration of Eu^{3+} ions in $BaAl_2Si_2O_8$. However, The PL excitation (lem = 428 nm) and emission (lex = 325 nm) of $Ba_{(1-x)}Al_2Si_2O_8:_xEu^{2+}$ were investigated. The optimum PL intensity was observed at 428 nm ($4f^65d^1 \rightarrow 4f^7$). The CIE color coordinates (*x=0.648, y=0.343*) clearly indicated that the phosphor $Ba_{0.97}Al_2Si_2O_8:_{0.03}Eu^{3+}$can be used as a potential candidate for deep red light emitting diodes under near-UV (n-UV) excitation. Also the CIE color coordinates of $Ba_{0.95}Al_2Si_2O_8:_{0.05}Eu^{2+}$ phosphor (*x=0.159, y=0.107*) is in blue region.

Keywords: *$BaAl_2Si_2O_8$:Eu;solid state reaction; XRD; n-UV LEDs.*

1. Introduction

In the recent years, trivalent rare earth-doped silicate based phosphor is an important class in the field of luminescence for solid state lightning and display technology, etc due to their excellent chemical and physical properties with high luminescence intensity under UV radiation [1-3]. Also silicate phosphors are almost completely snowy-white in body color and consequently their light absorption is low, and lamp efficacy is very high [4, 5]. Moreover, the silicates based phosphors are more susceptible to the thermal degradation of luminescent properties with structural changes than the other phosphors [6-9].

The $BaAl_2Si_2O_8$ host, in which Ba^{2+} and Sr^{2+} cations may occupy a single nine-fold coordinated site, whereas Ca^{2+} cations lie at four two-fold crystallographically independent sites exhibiting either a six-fold or a seven-fold coordination. Low-temperature synthesis of pure $BaAl_2Si_2O_8$ glass–ceramic powder by citrate process was reported by Hsin-Lung Lin *et al.*[10]. These types of frameworks consist of a 3D network of AlO_4 and SiO_4 tetrahedral bound by vertices, with alkaline-earth Ba^{2+}, Sr^{2+}, Ca^{2+} cations housed in channels along the crystallographic axes. In this structure each aluminium cation is surrounded by four silicon atoms and vice versa [11].

Clabau et al. reported luminescence properties of Eu^{2+} activated $MAl_2Si_2O_8$ (M=Ca, Sr, Ba) phosphors, which show stable phases prepared by solid state reaction [12]. Fluorescence and phosphorescence properties of the low temperature forms of the $MAl_2Si_2O_8:Eu^{2+}$ (M = Ca, Sr and Ba) compounds was reported by clabau and Zhang et al.reduced from Eu^{3+} to Eu^{2+} in

$MAl_2Si_2O_8$(M= Ca, Sr and Ba) in air condition by Cuimiao [12, 13]. Recently, $Ba_2MgSi_2Al_xO_7$ host used for white light emitting diodes by doping Eu^{2+}, Mn^{2+} [14, 15].

After that, Ye et al. in 2009 studied the effect of Sr^{2+} doping on structure and luminescence properties of $BaAl_2Si_2O_8:Eu^{2+}$ phosphor [16] and Ma et al. studied trap depth and Dy^{3+} luminescence in $BaAl_2Si_2O_8$ phosphor [17]. Rare earth (Eu^{2+}, Ce^{3+}) activated $BaAl_2Si_2O_8$ blue emitting phosphor was reported by V.B. Pawade et al.[18]. pure hexagonal and monoclinic Sm^{2+}/Sm^{3+}codoped $BaAl_2Si_2O_8$ phase using a simple sol–gel technique was reported by Lia et al. and studied photoluminescence properties [19].

In this paper, we have focused on synthesis of Eu^{3+} to Eu^{2+} in $BaAl_2Si_2O_8$ by conventional solid state reaction method under charcoal atmosphere and studied the phase, morphology and photoluminescence

 ISBN : 978-81-923628-7-8

characteristics of red to blue emitting $BaAl_2Si_2O_8:Eu^{3+}/Eu^{2+}$ emittingphosphor via carbon reduction atmosphere.

2. Experimental

2.1 Methods and materials

The series of $Ba_{(1-x)}Al_2Si_2O_8:xEu^{3+}/Eu^{2+}$ (x=0.01, 0.02, 0.03, 0.04 and 0.05 mole) phosphors were synthesized through traditional solid state reaction method. High purity $BaCO_3$(99.9%), Al_2O_3 (99.9%, AR), SiO_2(99.9%) and Eu_2O_3(99.9%, AR), were used as starting materials. Small amount of H_3BO_3 was adopted as a flux. Stoichiometric amount of starting materials and small quantity of acetone was used for mixed in ball milling for 2 h thoroughly. The mixture was first calcined at 1250°C for 4 h and then kept in charcoal (carbon) reducing atmosphere created by activated charcoal powder at 1000°C for 3 h. The phosphor was allowed to cool slowly to room temperature by natural cooling.

2.2 Characterizations

The Crystal structure of the final product was determined by the conventional x-ray diffraction method. (XRD, XPERT PRO, Cu Ká, 40 kV). Energy dispersive x-ray analysis (EDAX) was done to analyze the chemical components of the phosphor. The morphology and the size of the obtained sample were observed with Scanning Electron microscopy, Quanta 200 with EDS (SEM). The excitation and emission spectra were measured by a Hitachi F-7000 fluorescence spectrofluurometer equipped with a 150W Xe lamp. All the experiments were performed at room temperature.

3. Results and discussion

3.1 XRD analysis

The crystalline phase of the $BaAl_2Si_2O_8$prepared by solid state method was confirmed by XRD pattern as shown in Fig. 1. The XRD pattern for $BaAl_2Si_2O_8$ agreed well with the standard data from ICSD file (01-077-0185). Also the XRD show that the formed material is completely crystalline and was in single phase, where $a = b = 5.293$ and $c = 7.7900$ Å. The $BaAl_2Si_2O_8$ has hexagonal crystal structure with space group is *P6/mmm (191).*

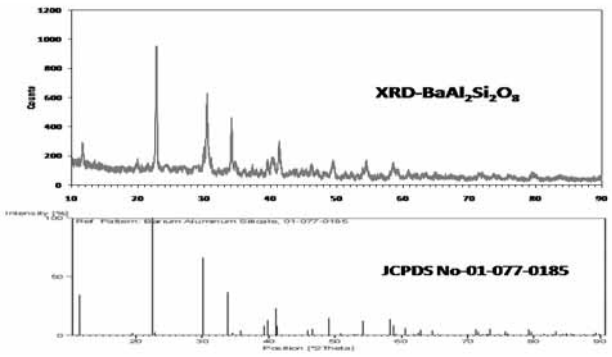

Fig. 1. XRD pattern of $BaAl_2Si_2O_8$ synthesized by solid state method.

3.2 *Morphological analysis*

The morphology of $BaAl_2Si_2O_8$:1%Eu^{2+}synthesized by solid state reaction is display in Fig. 2. SEM micrograph indicates the morphology of the phosphor. The size and shapes are not uniform. The size of the particles was observed in the range of 2-10 µm. The phosphor exhibited irregular morphology with no uniform obvious agglomeration.

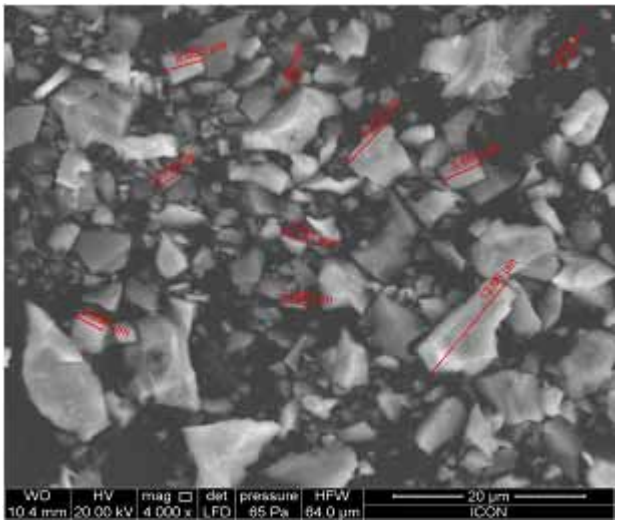

Fig.2. SEM images of $BaAl_2Si_2O_8$ host material.

Fig. 3 indicates the EDAX of the as prepared sample. It is observed at magnification of 4000 and for 30 seconds of live period. The peaks in figure shows energy lines Kα 0.523eV) corresponding to oxygen, Kα (1.486eV) corresponding to Aluminium, Kα (1.740eV) corresponding to Silicon and Mα (0.779eV) as well as Lα (4.465eV) corresponding to Barium atoms. This indicates the chemical composition of the sample $BaAl_2Si_2O_8$.

ISBN : 978-81-923628-7-8

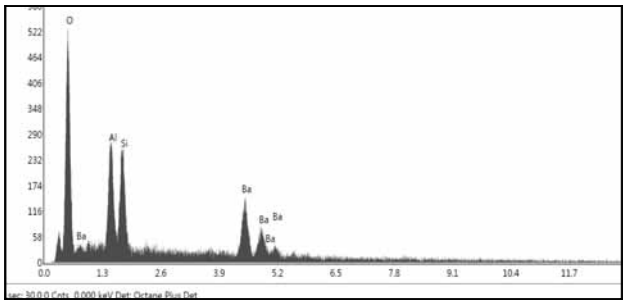

Fig.3. EDAX images of $BaAl_2Si_2O_8$ host material.

3.3 Photoluminescence study

3.3.1 PL study of $BaAl_2Si_2O_8:Eu^{3+}$ phosphors

The PL excitation spectrum of $Ba_{(1-x)}Al_2Si_2O_8:xEu^{3+}$ (x=0.01, 0.02, 0.03, 0.04 and 0.05 mole) phosphors monitoring at 615 nm emission corresponding to the ($^5D_0 \rightarrow ^7F_2$) transition is presented in Fig. 4. It can be seen that the excitation spectrum consists of two parts: one is the broad band from 200 to 350 nm and another is sharp lines from 350 to 410 nm. The intense broad band from 250 and 323 nm is assigned to the charge transfer (CT) band of $Eu^{3+} \rightarrow O^{2-}$. The broad bands in the UV region may contain the charge transfer excitation of Eu^{3+} ions and the energy transfer transition from silicate groups to Eu^{3+} ions. In most of the literature, the contribution of the two components cannot be distinguished due to spectral overlap [20]. The CT band corresponds to the electronic transition from the 2p orbital of O^{2-} to the 4f orbital of Eu^{3+}, and it is related closely to the covalency between O^{2-} and Eu^{3+} as well as coordination environment around Eu^{3+} ions. A series of sharp excitation bands present between 350 and 410 nm are associated with the typical intra-4f transitions of the Eu^{3+} ions centered at 363, 382 and 395 nm, which were attributed to the $^7F_0 \rightarrow ^5D_4$, $^7F_0 \rightarrow ^5L_7$ and $^7F_0 \rightarrow ^5L_6$ respectively. The strongest excitation peak at 395 nm contribute to the $^7F_0 ! ^5L_7$ transition in the UV region, so the $BaAl_2Si_2O_8:Eu^{3+}$ phosphor is thus suitable to be used for near-UV exciting red phosphor for white light emitting devices.

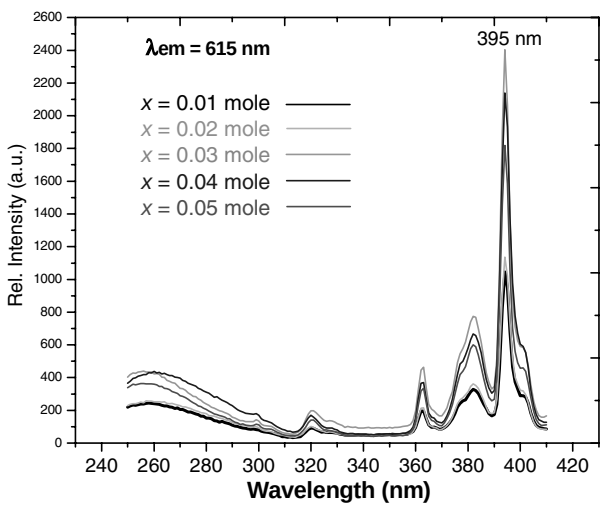

Fig.4. PL excitation spectra of $Ba_{(1-x)}Al_2Si_2O_8:xEu^{3+}$ (x=0.01, 0.02, 0.03, 0.04 and 0.05 mole) phosphors (λem = 615 nm).

The doping concentration of luminescent centers is an important factor influencing the phosphor performance. Therefore, it is necessary to confirm the optimum doping concentration. The emission spectra of $BaAl_2Si_2O_8:Eu^{3+}$ phosphors with different Eu^{3+} concentrations at 395 nm excitation are shown in Fig.5. It is observed that the emission spectra consisting of lines in the orange and red spectral range. The main peaks at 584 and 592 nm corresponding $^5D_0 \rightarrow ^7F_1$ transition and peak at 615 nmcorresponding to $^5D_0 \rightarrow ^7F_2$ transition. The transition $^5D_0 \rightarrow ^7F_1$ satisfies the selection rule of $\Delta J = \pm 1$ where, J is the angular momentum. Magnetic dipole transition obeys the selection rule of $\Delta J=0$ and $\pm 1$and electric dipole transitions only obey the selection rule of $\Delta J' \leq 6$ where J or J'=0when $\Delta J=2, 3, 6$ [21]. From Fig. 5 it is observed that the emission spectrum not only has the most intense red peaks at 615 nm due to the electric dipole transition $^5D_0 \rightarrow ^7F_2$ which indicates that Eu^{3+} occupies a site lacking inversion symmetry, but also has other powerful peaks in the range of 570–700 nm, of which involve available peaks at 584 and 592 nm ascribed to the magnetic dipole transitions, as an internal standard to gain some idea as to the relative transition strengths of the other transitions of Eu^{3+} [22].

 ISBN : 978-81-923628-7-8

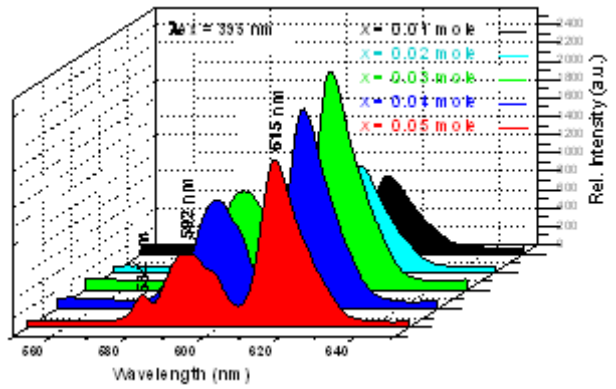

Fig.5. PL spectra of $Ba_{(1-x)}Al_2Si_2O_8$:xEu^{3+} (x=0.01, 0.02, 0.03, 0.04 and 0.05 mole) phosphors (λex = 395 nm).

Moreover, it can be seen that (Fig. 5) no distinct diversifications of the emission spectra shapes and positions occurred when the concentration of Eu^{3+} varied in a wide range. The intensity of all of the emission are enhanced significantly with the increase in Eu^{3+} concentration, and gradually decreases as the doping concentration becomes higher than *x*= 0.03 mole. That was because of an indication of nonradiative energy transfer between Eu^{3+} ions. This may occur owing to exchange interaction, radiation reabsorption, or multipole- multipole interaction. In the present case, radiation reabsorption due to spectral overlap alone cannot be fully responsible for nonradiative energy transfer among the Eu^{3+} ions. Hence, the process of energy transfer should be electric multipole-multipole interaction. The probability of energy transfer between the Eu^{3+} ions is distance-dependent, as the concentration of Eu^{3+} ions increases to some extent, the distance between the Eu^{3+} ions becomes smaller, and mutual action between the Eu^{3+} ions increases the loss of energy [23]. So, the Eu^{3+} ions concentration is the main factor to influence the emission peak intensity. The concentration quenching is due to energy transfer from one activator (donor) to another until the energy sink (acceptor) in the lattice is reached. Hence, the energy transfer will strongly depend on the distance (*R*c) between the Eu^{3+} ions, which can be obtained using the following equation [24].

$$R_C \approx 2\left[\frac{3V}{4\pi X_C Z}\right]^{1/3} \qquad (1)$$

Where *X*c is the critical concentration, *Z* is the number of cation sites in the $BaAl_2Si_2O_8$ unit cell [*Z*=12 in $BaAl_2Si_2O_8$], and *V* is the volume of the unit cell (*V*=0.189 nm^3 in this case). The critical concentration is estimated to be about *x*=0.03 mole, where the measured emission intensity begins to decrease. The critical distance (*R*c) between the donor and acceptor can be calculated from the critical concentration, for which the nonradiative transfer rate equals the internal decay rate (radiative rate). Blasse [25] assumed that, for the critical concentration, the average shortest distance between the nearest activator ions is equal to the critical distance. By taking the experimental and analytic values of *V*, *Z* and *X*c (0.189 nm^3, 1, 0.03, respectively), the critical distance *R*c is estimated by Equation (1) is equal to 2.292 nm in this host. Since Rc is not less than 0.5 nm exchange interaction is not responsible for non-radiative energy transfer process from one Eu^{3+} ion to another Eu^{3+} ion. The mechanism of radiation reabsorption is the primary method only if the fluorescence spectra of the excitation and emission have obvious overlap.

3.3.2 PL study of $BaAl_2Si_2O_8$:Eu^{2+} phosphor

The PL excitation spectrum of $Ba_{(1-x)}Al_2Si_2O_8$:xEu^{2+}(x= 0.02, 0.03, 0.04 and 0.05) phosphors monitoring at 428 nm emission corresponding to the ($4f^65d^1 \rightarrow 4f^7$) transitions of Eu^{2+} ions is presented in Fig. 5.

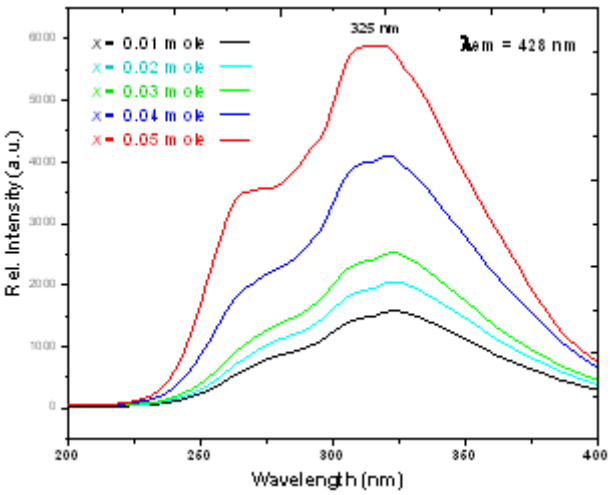

Fig.6. PL excitation spectra of $Ba_{(1-x)}Al_2Si_2O_8$:xEu^{2+} (x= 0.01, 0.02, 0.03, 0.04 and 0.05 mole) phosphors (λem = 428 nm).

PL excitation spectra of $BaAl_2Si_2O_8:Eu^{2+}$ phosphors consist of wide broad band which has two centers peaking at 262 and 325nm, respectively. These bands correspond to the electric dipole transition from the ground state to the 5d crystal field level.

The PL emission spectrum of Eu^{2+} doped $BaAl_2Si_2O_8$ phosphor excited at 325 nm is depicted in Fig. 7. In $BaAl_2Si_2O_8$ host Ba^{2+} has two sites with CN=9. Also, Ba^{2+} site in nine-coordination has two symmetry sites C_3 and C_1. Both sites have nine-coordination and the sites are similar in average bonds size as d(Ba-O)=2.286 and 0.287 nm. However, Ba^{2+} with smaller symmetry site also has shorter Ba-O distance (0.268 nm) [26] corresponding to average bonds distance of Eu^{2+}-O (0.268) nm. Therefore, Ba^{2+} may prefer to occupy the 6c site, because ionic radii of cations are Ba^{2+}=0.134 nm, Al^{3+}=0.051 nm and Eu^{2+}=0.121 nm. Thus, Eu^{2+} may prefer to occupy Ba^{2+} sites and form the blue emission centres.

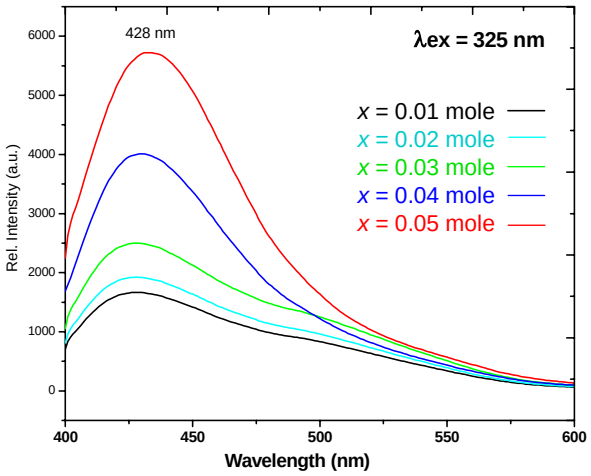

Fig.7 PL spectra of $Ba_{(1-x)}Al_2Si_2O_8:xEu^{2+}$ (x=0.01, 0.02, 0.03, 0.04 and 0.05 mole) phosphors (λex = 325 nm).

3.3.3 Color coordinates

The Commission International de'Eclairage (CIE) chromaticity coordination of the $Ba_{0.97}Al_2Si_2O_8:_{0.03}Eu^{3+}$ and $Ba_{0.95}Al_2Si_2O_8:_{0.05}Eu^{3+}$ phosphors are shown in Fig. 7.The color chromaticity coordinates of $Ba_{0.97}Al_2Si_2O_8:_{0.03}Eu^{3+}$ and $Ba_{0.95}Al_2Si_2O_8:_{0.05}Eu^{2+}$ phosphors are (*x=0.648, y=0.343*) and (*x=0.159, y=0.107*), which corresponds to red and blue emission respectively. These CIE color chromaticity coordinate are very closer to the standard NTSC (National Television System Committee) color chromaticity coordinates (*x = 0.67, y = 0.33*) and (*x = 0.14, y = 0.08*) for red and blue region respectively [27].

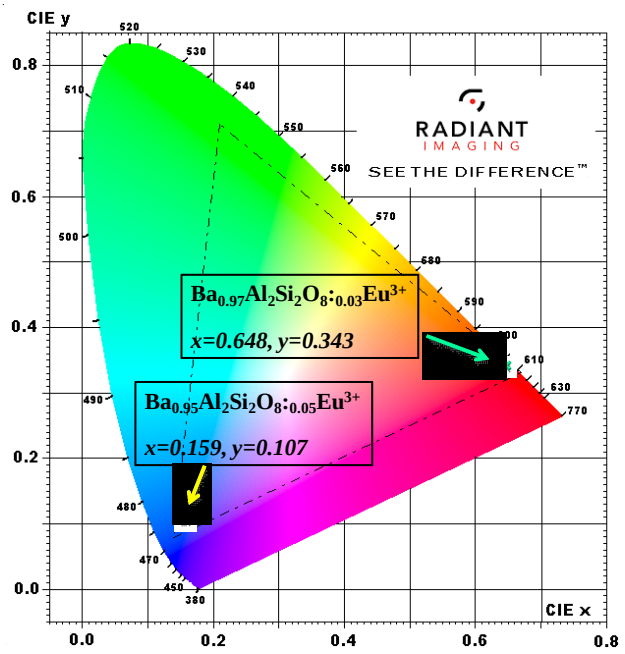

Fig.7. CIE color coordinates of $Ba_{0.97}Al_2Si_2O_8:_{0.03}Eu^{2+}$ (λex = 395 nm) and $Ba_{0.95}Al_2Si_2O_8:_{0.05}Eu^{2+}$ (λex = 325 nm) phosphor.

4. Conclusions

$Ba_{(1-x)}Al_2Si_2O_8:_xEu^{3+}/_xEu^{2+}$ phosphors were successfully synthesized by traditional solid state reaction method with particle size in the range of 2-10 µm. The EDAX analysis was done to find chemical composition of $BaAl_2Si_2O_8$. The exact phase formation of $BaAl_2Si_2O_8$ was verified by XRD analysis. PL study indicated that the phosphor exhibited deep red color emission (615 nm) under n-UV (395 nm) excitation. The $Ba_{(1-x)}Al_2Si_2O_8:_xEu^{3+}$ phosphors could be effectively excited by n-UV, which is very well matched the wavelength of n-UV chip. The concentration quenching of Eu^{3+} was found to be at 3 mole. Due reduction in carbon atmosphere, the Eu^{3+} was converted to Eu^{2+} which is responsible for blue emission. The $Ba_{(1-x)}Al_2Si_2O_8:_xEu^{2+}$ phosphors shows blue light (428 nm) emission under the excitation of 325 nm. The CIE color chromaticity coordinates of $Ba_{0.97}Al_2Si_2O_8:_{0.03}Eu^{3+}$ and $Ba_{0.95}Al_2Si_2O_8:_{0.05}Eu^{2+}$ phosphors are (*x=0.648, y=0.343*) and (*x=0.159, y=0.107*), which corresponds to red and blue emission

 ISBN : 978-81-923628-7-8

respectively. These CIE color chromaticity coordinate are very closer to the standard NTSC color chromaticity coordinates ($x = 0.67, y = 0.33$) and ($x = 0.14, y = 0.08$) for red and blue region respectively. These phosphors are promising candidate for red and blue emitting light phosphor.

References

[1] I.P. Sahu, D.P. Bisen, N. Brahme, R.K. Tamrakar, J. Radiat. Res. Appl. Sci. 8, 104 (2015).

[2] J.J. Joos, J. Botterman, P.F. Smet, Journal of Solid State Lighting 1, 6 (2014).

[3] J. McKittrick, M.E. Hannah, A. Piquette, J.K. Han, J.I. Choi, M. Anc, M. Galvez, H. Lugauer, J.B. Talbot, K.C. Mishra, ECS J. Solid State Sci. Technol. 2, R3119 (2013).

[4] P. Wen, Rare earth / alkaline earth metal magnesium silicate RE / alkaline earth metal salt aluminosilicate Amorphous silica Spherical phosphor, Dalian University of Technology (2009).

[5] http://www.lamptech.co.uk/Documents/M14E%20Silicate.htm

[6] J.S. Kim, O. H. Kwon, J. W. Jang, S. H. Lee, S.J. Han, J. H. Lee, Y. S. Cho, L-T Stable, Low-Temperature Remote Silicate Phosphor Thick Films Printed on a Glass Substrate, ACS Comb. Sci. 17, 234 (2015).

[7] W. M. Yen, S. Shionoya, H. Yamamoto, Practical Applications of Phosphors, CRC Press, 19-(2006).

[8] Y. Tian, Journal of Solid State Lighting 11, 1 (2014).

[9] D. P. Dutta, A. K. Tyagi, Solid State Phenomena 155, 113 (2009).

[10] H-L Lin, R.K. Chiang, W.T. Li, J. Non-Cryst. Solids 351, 3044 (2005).

[11] X. Rocquefelte , F. Clabau, M. Paris, P. Deniard, T.M. Le, S. Jobic, M.H. Whangbo, Inorg. Chem. 46, 5456 (2007).

[12] F. Clabau , A. Garcia, P. Bonville, D. Gonbeau , M. T. Le, P. Deniard, S. Jobic, J. Solid State Chem.181, 1456 (2008).

[13] C. Zhang, J. Yang, C. Lin, C. Li, J. Lin, J. Solid State Chem. 182, 1673 (2009).

[14] S. Ye, Z. S. Liu, X. T. Wang, J. G. Wang, L. X. Wang, X. P. Jing, J. Lumin. 129, 50 (2009).

[15] C.Y. Shen , Y. Yang, S.Z. Jin, H.J. Feng, Optik, 121, 29 (2010).

[16] M. Ma, D. Zhu, C. Zhao, T. Han, S. Cao, M. Tu, Opt. Commun. 285, 665 (2012).

[17] V.B. Pawade, S.J. Dhoble, J. Lumin. 145, 626 (2014).

[18] V.B. Pawade, N.S. Dhoble, S.J. Dhoble, J. Rare Earths 32, 593 (2014).

[19] L. Lia, X. Liua, H.M. Noh, B.K. Moon, B.C. Choi, J.H. Jeong, Ceram. Int. 41, 9722 (2015).

[20] P. Saradhi , U.V. Varadaraju, Chem. Mater.18, 5267 (2006).

[21] X.H. Xu, Y.H. Wang, W. Zeng, Y. Gong, J. Electrochem. Soc.158, J305 (2011).

[22] J. Dhanaraj, R. Jagannathan, T.R.N. Kutty, C.H. Lu, J. Phys. Chem. B105, 11098 (2001).

[23] Y. Tian, X.H. Qi, X.W. Wu, R.N. Hua, B J. Chen, J. phys. Chem. C113, 10767 (2009).

[24] G. Blasse .Philips Res. Rep. 24, 131 (1969).

[25] G. Blasse , B.C. Grabmarier, Luminescent Materials. Berlin: Springer-Verlag, 96 (1994).

[26] R.D. Shanon, ActaCryst. A 32, 751 (1976).

[27] K. A. Koparkar, N. S. Bajaj, S. K. Omanwar, Opt. Mater. 39, 74 (2015).

Synthesis and Characterization of Manganese Cobaltite as Electrode Material for Supercapacitor Application

Snehal Kadam[a], Pavan Khadekar[a], Harshita Shenoy[a], Ganesh Nagarvani[a], Jayshri Patil[a], Nidhi Tiwari, Abhishek Kakade[a], Rahul Ingole[a,b] and Shrinivas B. Kulkarni[a*]

[a] Materials Research Laboratory, Department of Physics, The Institute of Science, Mumbai-400032, Maharashtra
[b] Department of Physics, Shrimant Babasaheb Deshmukh Mahavidyalaya, Atapadi, Dist-Sangli-415301, Maharashtara
*Corresponding Author: sbk_physics@gmail.com

Abstract : In the present work, Manganese Cobaltite ($MnCo_2O_4$) electrode material was successfully synthesized by simple, low cost hydrothermal method on Stainless steel substrate. The structural, morphological and surface area characterizations of synthesized electrode material were carried out using XRD and SEM techniques. The electrochemical properties of synthesized electrode were analyzed by using cyclic voltammetry, galvonostatic charge discharge and electrochemical impedance spectroscopy in 1M KOH aqueous electrolyte. The Manganese Cobaltite electrode shows maximum specific capacitance which is 24l F/g at scan rate 5 mV/sec. The result shows that hydrothermally synthesized Manganese Cobaltite on stainless steel is the promising electrode material and would be most appropriate for supercapacitor application.

Keywords: *Manganese Cobaltite; Hydrothermal method; Stainless steel; Supercapacitor.*

1. Introduction:

Supercapacitor or ultracapacitor is an advanced energy storage device drawing more attention of researchers across the globe because of its high power density and cycling stability which is applicable in portable electronics, automobile vehicle, stationary power stations and backup power supplies etc [1, 2]. On the basis of charge storage mechanism supercapacitors are classified into two types i) Electrical Double Layer Capacitor (EDLC) which includes Graphene ,activated carbon etc [3]. ii) Pseudocapacitor which includes transition metal oxides [4-6] and Polymers [7]. Among the various transition metal oxides MnO_2 and Co_3O_4 are the most studied electrode materials because of its interesting properties such as high theoretical capacitance, low cost, environment friendly. Every electrode material has its own merits and demerits. MnO_2 is most promising electrode material because of its low cost, environment friendliness and high specific capacitance but supercapacitive properties of MnO_2 is still hampered by its poor electrical conductivity and material dissolution during electrochemical cycling, which leads to a severe specific capacitance drop as the scan rate increase [8] .Co_3O_4 is second most studied metal oxide because of its high theoretical capacitance (3560 Fg^{-1}), excellent pseudocapacitive properties etc. but it suffers from low electrochemical reversibility [9]. The shortcomings like poor cycle life, low electric conductivity & low energy density of these electrode materials are the main challenges of ES.

To overcome these challenges, there are tremendous efforts have been carriedout focusing on the development of new and cost-effective electrodes and electrolyte materials as well as electrode configuration to improve the capacitance, the energy density of electrode material. In order to further improve the pseudocapacitive performance of plain metal oxide, addition of other transition metal oxides has been attempted [10]. Binary transition metal oxide like $MnCo_2O_4$ is one of the low cost materials which posses multiple oxidation states compared to other transition metal oxides [11]. But metal oxides like MnO_2 and Co_3O_4 has fixed oxidation states. $MnCo_2O_4$ has properties of both Mn and Co as Co has higher oxidation potential and Mn has ability to transfer electron more and bring higher capacity [12]. Separately, MnO_2 is poor electrical conductor and Co_3O_4 has low energy density. But combining these two we may overcome these defects.

In view of above discussion we have synthesized $MnCo_2O_4$ electrode material by simple, cost effective hydrothermal method. Synthesized $MnCo_2O_4$ electrode shows excellent capacitive performance in terms of specific capacitance (SC), power capability and cycling stability, which is promising for supercapacitor applications.

 ISBN : 978-81-923628-7-8

2. Experimental:

2.1 Preparation of materials

All the reagents were AR grade and used without further purification. The Stainless Steel (SS) substrates with dimension 1cm × 5cm were used as substrate to deposite the electrode material. Prior to hydrothermal process SS substrates were polished with polish paper, followed by ultrasonic cleaning using acetone and dried at room temperature. In typical synthesis procedure 0.001M $MnCl_2$. $4H_2O$, 0.002 M $Co(Cl_2).6H_2O$ and 0.01M CH_4N_2O were dissolved in 40 ml double distilled water and this solution is stirred using magnetic stirrer for 0.5 hour to get clear and homogenous solution. After that this solution was transferred in Teflon liner having capacity of 40 ml solution and piece of SS substrates (1cm*5cm) was kept into Teflon liner. This Teflon liner was kept in hot air oven at 120ºC for 6 hrs. After cooling down to the room temperature naturally, the sample was taken out, rinsed with ethanol and distilled water for several times. After that prepared electrodes were annealed at 300° C for 2 hrs to form an oxide. Prepared electrodes were used for further structural morphological and electrochemical studies.

2.2 Characterization of the materials

The structural properties electrode materials were studied by using RIKAGU MINIFLEX (CuKá radiation) X-Ray diffractometer with 2è varies from 20°-80°. The morphological properties of the synthesized electrode materials were examined carried out with SEM technique by using JEOL JSM-300 instrument.

2.3 Electrochemical measurements

The supercapacitive properties of the electrode material such as cyclic Voltammetry, Galvonostatic charge-discharge and electrochemical impedance spectroscopy were studied using CHI (660 C) electrochemical workstation in three electrode system in 1M KOH as electrolyte.

3. Results and Discussion

3.1. X-ray diffraction Studies (XRD)

Fig. 1 shows the XRD spectra of $MnCo_2O_4$ electrode material. Peaks marked with SS are standard diffraction peaks of stainless steel substrate. The diffraction peaks can be well index with the spinel structure of $MnCo_2O_4$ (JCPDS card no. 23-1237) [13].

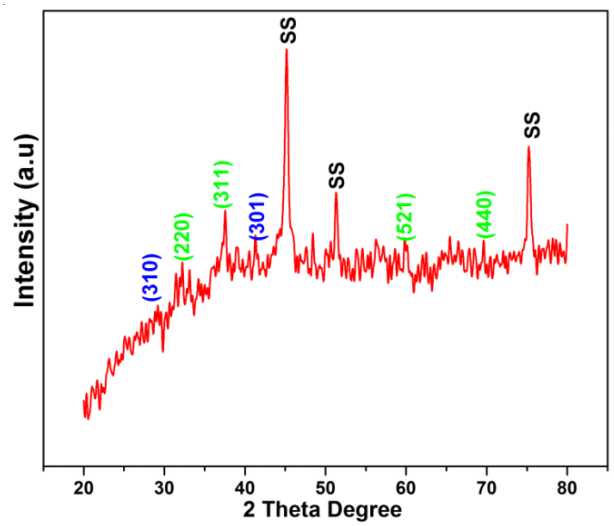

3.2 Scanning Electron Microscopy Studies (SEM)

The SEM study is one of the most significant techniques to understand surface morphology of the obtained product and provides the associated information on particles size, shape, and morphology. **Fig.2** shows SEM images at different magnification of $MnCo_2O_4$ electrode. It is evident from the SEM micrographs that hydrothermally synthesized $MnCo_2O_4$ electrode material exhibits uniformly formed and well distributed structures of nanospheres. It can been seen from Fig.2 that the $MnCo_2O_4$ nanospheres consists of various particles with an average diameter of 760nm. SEM micrographs also reveal presence of small separation between adjacent particles, which imparts a porous structure to the $MnCo_2O_4$ electrode material and thus improves the energy storage capacity of the electrode material [14-15].

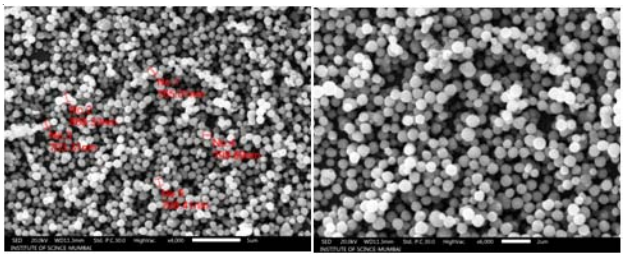

Fig.2 SEM Micrographs of $MnCo_2O_4$ electrode at different maginifications.

3.3. Supercapacitive Properties:

3.3.1 Cyclic Voltammetry:

Fig. 3 shows cyclic voltammograms of electrodes within the potential range -0.2 to 0.45 V vs SCE at different scan rate ranging from 5mV/sec to100 mV/sec. The CV show presence of redox peaks indicates the pseudocapacitive nature of electrode material [16]. With increasing scan rate oxidation peak shift towards the positive potential, and reduction peak shift towards negative potential. The redox peaks are visible even at higher scan rate which reveals the good rate capability of the electrode material.

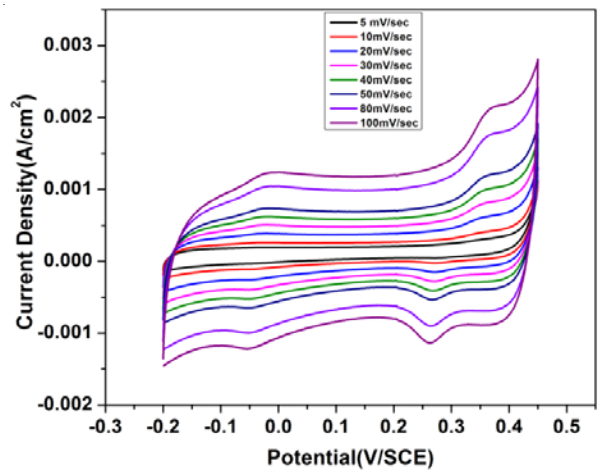

Fig.3 Combined CV of $MnCo_2O_4$ electrode at different scan rates.

3.3.2. Effect of Scan Rate

Fig.4 shows effect of scan rate on specific capacitance of $MnCo_2O_4$ electrode. At lower scan rates, electrolyte ions fully accessed in the inner matrix of electrode material leading to complete insertion reaction which results low peak currents but large amount of charge is stored. The $MnCo_2O_4$ electrode material exhibits maximum specific capacitance 241 F/g at scan rate 5mV/sec and minimum specific capacitance 143 F/g at scan rate 100 mV/sec. At higher scan rates, electrolyte ions only reached the outer surface layer of the electrode material and cannot utilize the interior surface of the electrode material. So that, the effective interaction between ions and the electrode is significantly reduced this reduces the specific capacitance of active material [17].The values of specific capacitance were calculated by using eq^n.**1** as reported elsewhere.

$$Specific\ Capacitance = \frac{C}{W} \quad F/g \qquad (1)$$

where,

C-Capacitance & W-mass of the active electrode material.

C-capacitance of the electrode material & W-mass of active material

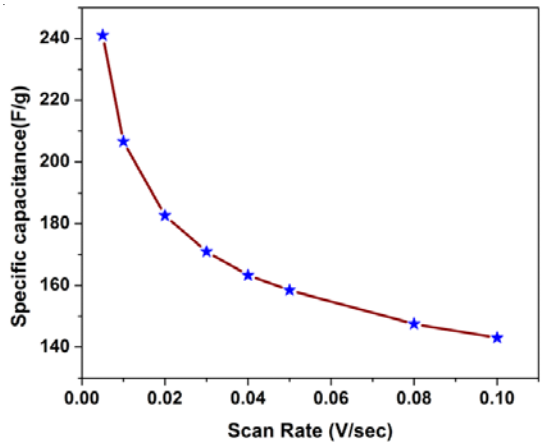

Fig.4 Effect of Scan rate on specific capacitance $MnCo_2O_4$ electrode material.

3.3.3. Galvonostatic Charge –discharge

Fig.5 show the galvonostatic charge-discharge studies at different current densities from 1 mA/cm^2 to 5 mA/cm^2 of electrodes respectively. The graph shows linear variation of the electrode material. The values of specific capacitance and efficiency were calculated from the eq^n 2-3 respectively [18]. The $MnCo_2O_4$ electrode shows 97 % efficiency as well as higher specific capacitance is 111.36 F/g at current density 1 mA/cm^2.

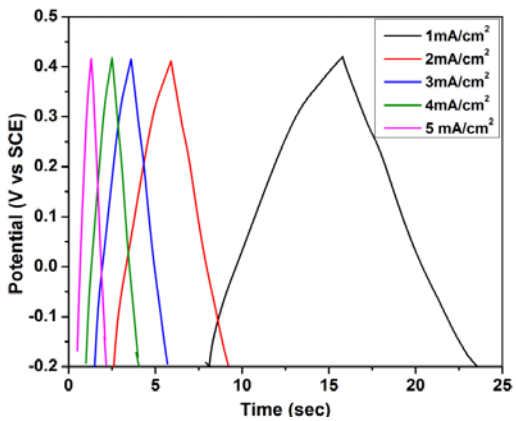

Fig.5 Galvonostatic charge-discharge studies of $MnCo_2O_4$ electrode material.

 ISBN : 978-81-923628-7-8

Specific Capacitance (SC) = $\frac{Id \times td}{V \times W}$ F/g (2)

Efficiency $_{(\ )}$ = $\frac{td}{tc} \times 100$ % (3)

Where

V- Potential window, Id-Discharge Current, Td-Discharge Time, Tc-Charging time.

Conclusions

In conclusion, nanosphere like $MnCo_2O_4$ electrode material was successfully synthesized using hydrothermal method. The SEM micrographs show nanosphere like morphology. Cyclic voltammetry studies give the maximum specific capacitance which is 241 F/g at scan rate 5mV/sec. The high performance of electrode material interms of specific capacitance, good rate capability and enhanced cycle life due to the synergy of nanosphere like morphology of $MnCo_2O_4$ electrode that not only provides a good support to stabilize MnO_2 but also facilitate the fast ion mobility and electron transfer. The $MnCo_2O_4$ electrode will be useful as efficient electrode material for energy storage application.

Aknowledgement

One of the author Miss Snehal L. Kadam thankful to CSIR for providing CSIR-SRF award no:09/877(100)2K18.

References

[1] M. Gopalakrishnan, G. Srikesh, A. Mohan, V. Arivazhagan.(2017) "*In-situ* synthesis of Co_3O_4/graphite nanocomposite for high- performance supercapacitor electrode applications."Applied Surface Sciences 403: 578–583.

[2] Editorial.(2015) "Electrochemical supercapacitors for energy storage and delivery: Advanced materials, technologies and applications."Applied Energy 153:1–2.

[3] C. Xiang, M. Li, M. Zhi, A. Manivannan, N. Wu.(2013) "A reduced graphene oxide/Co_3O_4 composite for supercapacitor electrode." Journal of Power Sources 226:65-70.

[4] M. Kuang, T.T. Li, H. Chen, S.M. Zhang, L.L. Zhang, Y.X. Zhang.(2015) "Hierarchical Cu_2O/CuO/Co_3O_4 core-shell nanowires:synthesis and electrochemical properties." Nanotechnology 26:304002.

[5] J. Xu, K. Hou, Z. Ju, C. Ma, W. Wang, C. Wang, J. Cao, Z. Chena.(2017) "Synthesis and Electrochemical Properties of Carbon Dots/Manganese Dioxide (CQDs/MnO_2) Nanoflowers for Supercapacitor Applications." Journal of Electrochemical Society 164: A430-A437.

[6] Y. Zhang, J. Wang , H. Wei, J. Hao, J. Mu, P. Cao, J.Wang, S. Zhao.(2016) "Hydrothermal synthesis of hierarchical mesoporous NiO nanourchins and their supercapacitor application." Material Letters 162: 67–70.

[7] D.S. Dhawale, D.P. Dubal, V.S. Jamadade, R.R. Salunkhe, C.D. Lokhande.(2010) "Fuzzy nanofibrous network of polyaniline electrode for supercapacitor application." Synthetic Metals, 160:519–522.

[8] M. Huang, Y. Zhang, F. Li, L. Zhang, Z. Wen, Q. Liu.(2014) "Facile synthesis of hierarchical Co_3O_4@MnO_2 coreeshell arrays on Ni foam for asymmetric supercapacitors." Journal of Power Sources 252:98-106.

[9] W.Guo, L. Hou, B. Hou, Y.Guo. (2017) "Thermally oxidized synthesis of hierarchical Co_3O_4@MnO_2 nanosheet arrays on nickel foam with enhanced supercapacitor performance." Journal of Alloys and Compounds 708: 524-530.

[10] F. Liao, X. Han.(2019) "Hydrothermal synthesis of mesoporous $MnCo_2O_4$/$CoCo_2O_4$ ellopsoid-like microstructure for high performance electrochemical supercapacitors." *Ceramics International* **6**:7244-7252.

[11] M. Li, W. Yang, J. Li, M. Feng, W. Li, H.Li and Y. Yu.(2018)"Porous layered stacked $MnCo_2O_4$ cubes with enhanced electrochemical capacitive performance." *Nanoscale*, 10: 2218.

[12] K. Shrestha, S. Kandul, G. Rajeshkhann, M. Srivastava, N. Kim and J. Lee.(2018) "An advanced sandwich-type architecture of $MnCo_2O_4$@N–C@MnO_2 as an efficient electrode material for a high-energy density hybrid asymmetric solid-state supercapacitor." *Journal* of Materials Chemistry A 6: 24509.

[13] X. Zheng, Y. Ye, Q. Yang, B.Geng and X. Zhang. (2016), "Hierarchical structures composed of $MnCo_2O_4$@MnO_2 core–shell nanowire arrays with enhanced supercapacitor properties, Dalton Transactions, 45:572-578.

[14] S. Zhou, X. Luo, L. Chen, C.Xu, D. Yan.(2018) "$MnCo_2O_4$ nanospheres for improved lithium storage performance." Ceramics International, 44:17858-17863.

[15] L. Zou, J. Cheng, Y. Jiang, Y. Gong, B.Chi, J. Pu and L. Jian.(2016) "Spinel $MnCo_2O_4$ nanospheres as an effective cathode electrocatalyst for rechargeable lithium–oxygen batteries." RSC Advances, 6:31248.

[16] S. Sahoo, K.Naik and C. Rout.(2015) "Electrodeposition of spinel $MnCo_2O_4$ nanosheets for supercapacitor applications." Nanotechnology 26:455401.

[17] P. M. Padwal, S. L. Kadam, S.M. Mane, S. B. Kulkarni.(2016) "Enhanced specific capacitance and supercapacitive properties of polyaniline–iron oxide (PANI–Fe_2O_3) composite electrode material, Journal of Materials Science 51:10499.

[18] S. L. Kadam; S.M. Mane; P.M.Tirmali; S. B. Kulkarni.(2018) "Electrochemical Synthesis of Flower like Mn-Co Mixed Metal Oxides as Electrode Material for Supercapacitor Application." Current Applied Physics 18: 397-404.

 ISBN : 978-81-923628-7-8

Plastic Peril on Species Diversity and Fish Catch: A Zone-wise Comparative Assessment between Ulhas River Estuary and Thane Creek

Sudesh Rathod*

Department of Zoology, VPM's B. N. Bandodkar College of Science, Thane, Maharashtra, India
Email: sudeshdrathod@gmail.com

Abstract : The anthropogenic activities prevalent in the Ulhas River estuary and the Thane creek were accentuated to correlate with their zone wise plastic pollution with that of existent artisanal fisheries status. The observation revealed that there is rise in plastic peril with increased anthropogenic activities which caused depletion in the fisheries of the ambient water bodies to non-profitable level. This consequently decreased the fishing activities. At 80% Bray-Curtis similarity resemblance in PCO showed that UZ-II, UZ-III and TZ-III were similar at 87.7% ordination in fish species abundance whereas UZ-III and TZ-III were similar at 89% ordination in biomass. The pattern of fish catches were in accordance with zone-wise deterioration level due to the impact of plastic peril which revealed direct correlation to that of dwindling status of the fisheries of the ambient water bodies.

Keywords : *Plastic pollution, Ulhas River estuary, Thane creek, anthropogenic activities, fisheries status, abundance, diversity, biomass, catches, PCO ordination, Bray-Curtis Similarity Matrix.*

Introduction

Thane City is a connecting land-mass amongst the sub-urban Thane, urban Mumbai and Vashi (New Mumbai) located in the Maharashtra State of India. Mumbai-Thane-Vashi complex could be considered as one of the most populous 'megacity' comprised of more than 10 billion population and stands as 4th most populous city in the world. The Thane city is well known for its high residential clusters, fostering the requisite man-power to the corporate systems of Mumbai and Navi Mumbai, owing to which hitherto, a considerable portion of forest and non-residential land has been mutated to suit the residential developments. Besides, the 'Thane-Belapur industrial belt' has been recognized as largest industrial cluster in the Asia (Zingde and Govindan, 2001) along with numerous industries located at Kalyan-Dombivli, Thane City proper and Bhiwandi (Qamrul, 1980) areas of the Thane district. The Thane City is therefore subjected to a high anthropogenic stress, lest, it exceeds the carrying capacity of the prevailing urban ecosystem.

The Ulhas River estuary and the Thane creek are the major inward waters located in the vicinity of the Thane City. The Ulhas River estuary (URE) commences from S-E near Dombivli regions upstream between latitude19°14'43"N and longitude 16°06'59"E; meanders for about 40 km before it joins the Arabian Sea towards N-W at Vasai (Bassein) creek situated between the latitude 18° 45'to19° 19', N and longitude

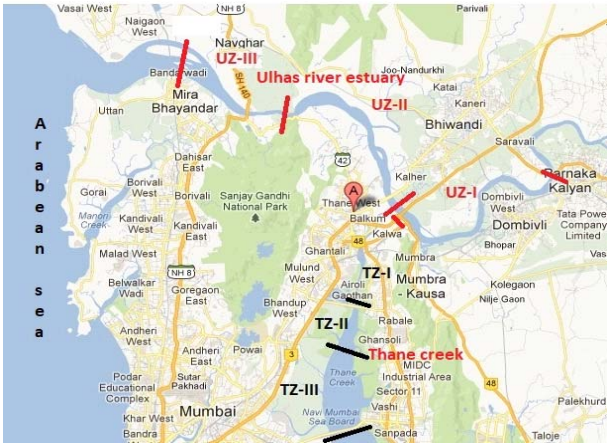

Fig 1: Map Showing study zones of URE and TC

73°21'to72° 45', E on the world map. The Thane creek (TC) runs downstream from Balkum to the Mankhurd-Vashi bridge towards the east side of the Thane City. The mouth of the creek opens towards its S-W approach to Mumbai harbor bay in the Arabian Sea between Latitude 19° 01'N and Longitude72° 58'E and heads northwards for about 26 km to join the URE at Balkum towards N-W between latitude 19° 13'N and longitude 73° 00'E on world map. Thane Creek has lesser influence of fresh water as it connects to URE with a narrow connection at upstream with feeble fresh water influx from URE during monsoon thus remaining as *euhaline* for the major part of the year. However, it is highly influenced by storm waters from

ISBN : 978-81-923628-7-8

in monsoon and urban activities (industrial, domestic, civil and cultural activities) from Thane City proper.

The two dynamic aquatic environments viz. URE and TC situated in the vicinity of the Mumbai-Thane complex are the major water bodies supporting the local fisher folks for their livelihood from many decades (Rathod, 2002). Both the ambient water bodies are known historically for their various records of lucrative fisheries (Mutsaddi, 1964; Qamrul, 1980; Tandel, 1984; Pejaver, 1984). These have turned down to be non-productive in the recent years due to the pollution pressure exerted by industrial and urban activities (Rathod, 2005).

Plastic Menace: Presently with the increased use of plastic is disposed in huge amount near shores. About 80% of the material is plastic which is non-degradable and provokes smothering. Entangling and drowning of biota (birds, mammals) may happen and inflict physical injury to animals (turtles) or even an obstruction of digestive system after ingestion of plastic objects. Once in the food-web, plastics release toxic substances. Containers or all sorts (bottles, boxes) will host alien species and help in the transportation of invasive species (Abu El-Magd and Hermas, 2010). These ultimately get into the coastal waters and pollute them and also get carried to open oceans. Besides, large gyres (vortexes) in the oceans trap floating plastic debris. The North Pacific Gyre for example has collected the so-called "Great Pacific Garbage Patch" that is now estimated at 100 times the size of Texas. Many of these long-lasting pieces wind up in the stomachs of marine birds and animals. This results in obstruction of digestive pathways which leads to reduced appetite or even starvation.

URE and TC are also highly impacted due to solid wastes, most of them were found to be of non-biodegradable type (Rathod, 2005 & 2016; Singare, 2012). Recently, the use of plastic with regard to packaging and handling of the goods has amplified several folds. The extensive uses of plastic in urbanized areas like Thane City pose high hazards to the aquatic environment in the vicinity. However, there is no appropriate disposal system available to manage the huge plastic garbage generated daily in the city, till date. The domestic plastic waste is casually discarded along with degradable garbage and is dumped without sorting on the solid waste disposal land-fills. This plastic waste is ultimately carried along with the land run-off to the waters of URE and TC during the monsoon. Several kinds of non-biodegradable elements viz. carry bags, milk and oil bags, plastic bottles, poly-feel fibres, polystyrene, foot wares, automobile tyres and tubes were observed along URE and TC during the present study. Moreover, it is of common scenario that the disposals of plastic in the ambient water bodies are customary practices or some ritual activities. The plastic disposal are often increased during the rituals practices like Idol immersion; 'nirmalya' immersion; 'naralipournima' immersion; and 'asthi-visarjan' frequented in the ambient waters in the vicinity of Thane city. Ironically, it is customary to dispose the remains of these worships or rituals in plastic bags along URE and TC. TC is a semi-isolated water body with narrow channel as compared to URE. Whereas URE not only possesses a wider channel but also is benefited by riverine fresh water flow from upper stretches.

Fishing activities were high until 1996 when Vashi-Mankhurd Bridge was constructed on harbor railway line which narrowed the orifice of the creek (Rathod, 2016). Probably the narrowing of orifice caused hindrance to the water currents during tidal movements (Sandilyan & Kathiresan, 2012; Joshi & Kale, 2013). As a result the creek water was unable to be flushed completely hence retaining plastic within creek for long and allowing it to accumulate. It was reported by fishermen that nets were inoperable in plastic laden water in entire TZ-I and TZ-II. It was reported that the plastic can affect the feeding sites of the fish (Sandilyan & Kathiresan, 2012; Joshi & Kale, 2013). Also catches were reduced to non-profitable level in the subsequent years after 1996. Consequently, it was observed that the fishing attempts were negligible in these zones (Rathod, 2016).

Materials and methods

Each study area was divided into three zones on the basis of demographic and urban characteristics viz. upper zone (Z-I), middle zone (Z-II) and lower zone (Z-III). The two ambient water bodies were divided as follows (Table 1):

 ISBN : 978-81-923628-7-8

Table 1: Demarcation of zones in URE and TC

Sr. No.	Water body	Zone	Characteristics	Areas included
1	URE	UZ-I	Highly residential; influenced by industrial clusters of Dombivliand agricultural fields from the catchment; immersion practices frequent	Kalyan, Dombivli, Kharegaon, Balkumon south bank and Anjurdive, Anjur, Mankoli, Alimghar and Dive on north bank. (length:12.4 km)
		UZ-II	Sparse residential areas; impacted majorly by sand excavation activitie and Bhiwandi industrial areas; agricultural fields and solid waste disposal moderate; immersion practices rare	Balkum, Waghbil, Mograpada, Nagla and Gaimukh occurred on south bank while Bhiwandi, Kasheli, Kalher, Kevani-Dive, Kalwar, Dunge, Kharbao and Paigaon on north bank. (length:12.7 km)
		UZ-III	Highly residential; sand excavation activities; fishing activities; immersion practices frequent	Gaimukh jetty, Retibandar, Ghodbandar and Mira-Bhayandar areas (length:10.9 km)
2	TC	TZ-I	Highly residential; influenced by industrial clusters of Wagale estate and Vitawa-Airoli; salt pans; immersion practices frequent	Thane city. Vitawa, Airoli on east bank and Mulund, Bhandup, Vikhroli on west bank
		TZ-II	Highly residential; influenced by industrial clusters of Airoli-Ghansoli immersion practices frequent	Airoli, Ghansoli on east bank and Vikhroli, Ghatkopar on west bank
		TZ-III	Highly residential; influenced by industrial clusters of Ghansoli-Vashi; salt pans; immersion practices frequent	Koparkhairne, Vashi on east bank and Sion to Trombay on west bank

On site observation was carried out to study the anthropogenic activities imparting the threat due to plastic pollution along the entire stretches of URE and TC. The ambient water bodies contained number of point and non-point sources of plastic disposal. The hot-spots such as domestic clusters, solid waste disposal spots (point sources of plastic disposal), occasions of routine practices or some ritual activities viz. idol immersion (God Ganesh visarjan, Godess Gauri visarjanand Godess Durga visarjan), 'nirmalya'[1] disposal, 'naralipournima'[2] offerings and 'asthi-visarjan' (non-point sources of plastic disposal) were observed and recorded on field. URE was found with total 6 and TC was with total 9 plastic dumping grounds (point sources). Ranks were allotted to the dumping ground based on their size. The fisheries were recorded qualitatively and quantitatively, on site, at various landing

[1]'Nirmaya' is the process of disposing the remains of worship ('pooja') or rituals like idol immersion and funeral ('asthi-visarjan'). These activities cause large amount of plastic and polystyrene disposal in the ambient waters.

[2]'Naralipournima' is an important festival celebrated majorly by Hindus in the western coastal regions of India. Also known as 'Coconut Day' observed on the 'Pournima' (full moon day) in the month of 'Shravana' according to the Hindu calendar. Fishermen community along URE and TC celebrates this festival to ward off untoward incidents while sailing in the sea during which along with the offerings in worships huge amount of polythene bags are disposed.

ISBN : 978-81-923628-7-8

centers along URE and TC and also from the local fish markets such as Vashi, Ghansoli, Koparkhairne, Airoli, Thane, Kalwa, Vitava, Kharegaon, Anjur, Alimghar, Mankoli, Kalher, Kevani-Diva, Gaimukh and Mira-Bhainder. Specimens were collected from these landing centers or markets and identified using keys given in 'Fishes of India', (Day, 1883) and FAO sheets.

Result and Discussion

Massive plastic dumping spots and disposal were concurred along both URE and TC (Fig. 2 a & b). It was observed that in URE, UZ-II a huge solid waste dumping was allowed by Thane Municipal Corporation. The satellite images on google earth from 2004 to 2015 revealed tremendous impact on mangrove in the vicinity due to solid waste dumping. Moreover, in TC, TZ-I and TZ-II possessed higher amount of plastic. Several places the mangrove pneumatophores were tangled with plastic. The plastic debris were carried by tidal currents were formed into piles at certain places. At some instances the fishes, especially young ones of mudskippers were found smothering due to plastic (Fig. 2). It was observed that the TC hindered tidal-water flushing action which restricted the plastic material from escaping to ocean resulting in its accumulation (Kantharajan et *al*. 2018). The accumulated plastic could also velocity of tidal oscillations. Fish landings of 'Dol' net (a stationary bag net) catches from TZ-III contained huge amount of plastic. Fishers had to invest considerable amount of time for separating plastic from landings (Fig. 2, c-i).

Figure 2: Some solid waste dumping grounds spotted along URE and TC and their impact

Solid waste dumping at - (a) Huge plastic dumping and sorting near Kharegaon, UZ-I (b) Medium Solid waste dumping near Mahagiri, TZ-I

Plastic at Vashi in T-ZIII (ci); Young ones of mudskippers trapped in plastic (cii) in UZ-I and plastic clogging the roots of mangroves in TZ-I (ciii), near Mahagiri, Thane City

 ISBN : 978-81-923628-7-8

Solid waste dumping mostly comprised of non-degradable material principally, plastic: Huge Solid waste dumped near Kajupada in UZ-II; (di) Site image see the inset indicating size of bulldozer, (dii) Satellite images viz. in 2004 with intact mangroves and (diii) Site in 2006 with affected mangroves. Location on map: 19°17'28N and 72°55'32E

Total 5 out of 6 dumping grounds (point sources) on URE and 6 out of 9 on TC were large in size. Apart from these point sources there are several non-point sources of plastic disposal as stated earlier. URE scored 48 and TC 144 ranks according to their possible impact due to former point sources. Zonal impact of plastic was greater in TC as compared to that of URE. TZ-I and TZ-II were highest in ranks. TC scored higher in plastic pollution ranks (Table 2).

Table 2: Ranks allotted on the basis of number and size of plastic dumping along URE and TC

Plastic menace: Plastic was a great concern in the ambient waters, specifically in TC. There were several hotspots of plastic accumulation on URE and TC	URE	Number	Ranks	TC	umber	Ranks
	UZ-I	3	24	TZ-I	5	80
	UZ-II	1	8	TZ-II	3	48
	UZ-III	2	16	TZ-III	1	16
	Total→	**6**	**48**	**Total→**	**9**	**144**

The data of fish species abundance and fish catches in biomass were transformed to square root before obtaining resemblance matrix with Bray-Curtis Similarity. PCO was run with Permanova. Also the dendrograms were obtained with agglomerative cluster analysis of plastic pollution ranks in Primer version6 software. The dendrogram was then overlayed separately on PCOs for species abundance and biomass (Fig.3, a & b) respectively to reveal the similarity.

Figure 3: Zonal Fish Species Abundance (a) and Biomass (b) in URE and TC

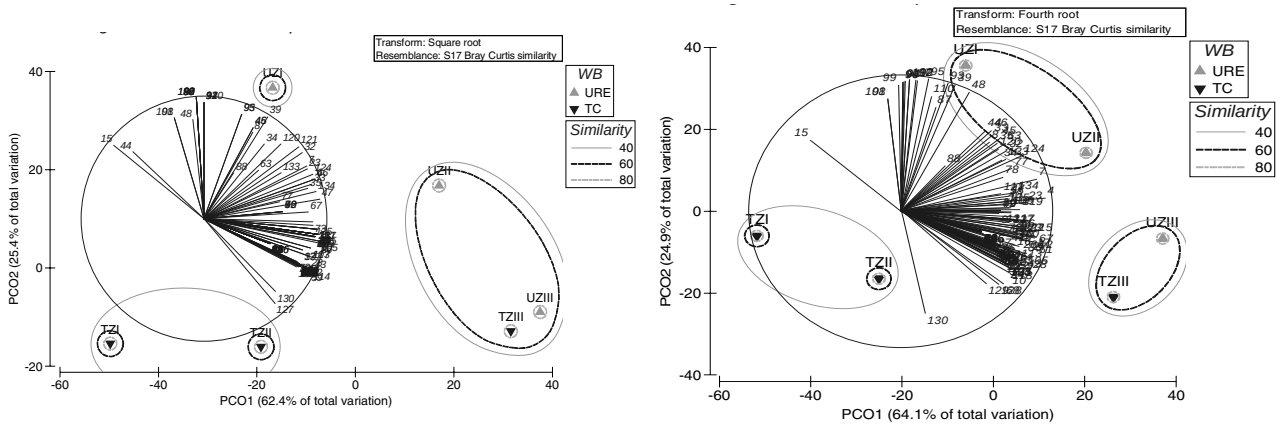

a **b**

The PCO ordination of zonal fish species abundance (a) and fish biomass (b) with overlay of the dendrogram of Bray-Curtis similarity agglomeration clusters of 40 to 80 percent of similarity of rankings on plastic pressure. The PCO varimax ordination of species abundance represented strongly at 87.8% while that of biomass represented strongly at 89% of variation. Highest species abundance was revealed in UZII, UZIII and TZIII; average in UZI whereas TZI and TZII showed lowest. The fish catches (biomass) ordination revealed that TZIII and UZIII were highest; UZI and UZIII were average; TZII lower while TZI was poorest.

It is evident that the fish catches depleted significantly in these zones in present study. TZ-I and TZ-II were lowest in fish abundance (Fig. 3a) and biomass (Fig. 3b). UZ-III, UZ-II and TZ-III were similar in abundance at 80% Bray-Curtis similarity resemblance (Fig. 3a). Whereas, catches (biomass) depicted highest in UZ-III and TZ-III whilst lowest in TZ-I and TZ-II in present study (Fig. 3b). This confirmed that TZ-I and TZ-II were highly disturbed due to plastic pollution. Although UZ-II, UZ-III and TZ-III revealed similarity in species abundance, UZ-II being average in fish catch as that of UZ-I. Overall Thane creek was highly disturb due to plastic peril. This might be due to the lack of complete flushing of creek water to ocean. The mass of plastic in the creek also impacting on the velocity of tidal oscillations which hindered the creek water. However it is evident that Ulhas River Estuary was benefited due to riverine flow and comparatively broader channel which allowed complete flushing of the tidal water and hence the condition remained better. This relieved the plastic pressure in URE intermittently and sustained better fisheries status.

Conclusion:

Plastic played important role to define the fish species abundance and biomass in the present study. Upper zones of TC viz. TZ-I and TZ-II were highly depleted with fisheries due to various anthropogenic activities causing plastic hazard. Oceanic segments of both URE and TC were high in fish abundance and catches. Whilst the upper regions which were disturbed due to profound anthropogenic activities causing plastic pollution were very low in fish species diversity as well as biomass discerning the direct relation with the levels of plastic peril in the ambient water bodies.

References:

1. Abou, El-Magd, E. Hermas, 2010, 'Human impact on the coastal landforms in the area between Gamasa and Kitchner Drains, Northern Nile Delta, Egypt', *J. Coastal Res*., 26: 3.

2. Day, F.J.B., 1883, '*The fauna of British India including Ceylon and Burma*, *Fishes'*, Willium Dawson and sons. London, Taylor and Francis, vol. I & II, 1:548pp; 2: 509.

3. FAO, 1984, 'Eastern Indian Ocean- Fishing Area 57; Western Central Pacific- Fishing Area 71 and Western Indian Ocean, Fishing Area 51', Species identification sheets for fishery purposes.

4. Joshi V.U. & Kale V.S., 2013. Environmental conflicts in coastal metropolitan cities in India: Case

 ISBN : 978-81-923628-7-8

studies of Mumbai and Chennai metropolitan regions. *SECOA* (4): 320-354.

5. Kantharajan, G., P.K. Pandey, P. Krishnan, V.S. Bharti & V. Deepak Samuel, 2018. Plastics: A menace to the mangrove ecosystems of megacity Mumbai, India. 16 (1): 1-5.

6. Mutsaddi, K.B., 1964, 'A Study of Gobioid, *Boleophthalmus dussumieri* (Cuv. & Val.).' Ph. D. Thesis, University Of Bombay.

7. Pejaver, M.K., 1984, '*Biology of Some Crustaceans from the Creek near Thane City'*, M. Sc. Thesis, University Of Bombay.

8. Qamrul, H. and Sawant, K.B., 1980, 'Studies on Fishes and Fisheries of the Ulhas River, District Thane', J. *of Univ. of Bombay*. 85: XLIX,; 25-38pp.

9. Rathod, S.D., 2005, 'Effect *of pollution on mudskipper fishery of Ulhas River Estuary with a special reference to the biology of Boleopthalmus dussumieri* (Cuv. & Val.)', Minor research project, University of Mumbai.

10. Rathod, S.D., 2016, 'Studies on Pollution Status, Fish Faunal Diversity and Biology of Some Important Fishery Species viz. *Mystus gulio* (Ham), *Boleophthalmus dussumieri* (Cuv. & Val.), *Scylla serrata* (Forsskal) and *Cardium asiaticum* (Brug.) from Ulhas River Estuary and Thane Creek. Ph. D. Thesis, University of Mumbai, Mumbai, Maharashtra, India, pp 377.

11. Rathod, S.D., Patil, N. N., Quadros G. and Athalye, R. P., 2002, 'Qualitative study of fin fish and shell fish fauna of Thane Creek and Ulhas River estuary'. Proc. *The National Seminar on Creek, Estuaries and Mangroves – Pollution and Conservation.*pp.135-141.

12. Sandilyan, S. & Kathiresan, K., 2012. Plastics – A formidable threat to unique biodiversity of Pichavaram mangroves. *Current Science* 103(11): 1262-1263.

13. Singare P.U., 2012, Study of Some Major Non-Biodegradable Solid Wastes along Thane Creek of Mumbai. World Environment, 2(3): pp. 24-30. DOI: 10.5923/j.env.20120203.01

14. Tandel, S.S., 1984, '*Biology of Some Fishes of the Creek near Thane'*, M*Sc.* Thesis, University of Bombay.

15. Zingde, M.D. and Govindan, K., 2001, '*Health status of coastal waters of Mumbai and regions around. In: Environmental Problems of Coastal Areas in India',* (ed.) Sharma, V. K., Bookwell Publ., New Delhi, 2001, pp. 119–132.

Synthesis and Characterization of CdSSe Thin Films Synthesized by Varying Deposition Temperatures

Cephas A. Vanderhyde[a] and Hemangi A. Raut[a]*

aViva College of Arts, Commerce and Science. Virar (W), Dist- Palghar.
Corresponding email: vanderhydec@gmail.com

Abstract : CdSSe thin films were prepared using cadmium acetate, thiourea and sodium selenosulphate in a chemical bath. The films were prepared at 293 K, 313 K, 333 K and 353 K. The crystallinity of the thin films were studied by using the XRD technique, the band gap was determined from the absorption spectra by applying tauc's relation and the morphology was studied using SEM.

Keywords: *CdSSe, XRD, SEM and UV-vis spectroscopy.*

Introduction: Cadmium sulphoselenide (CdSSe) is an important ternary semiconducting compound with a band gap that can vary from 1.72 (CdSe) to 2.42 (CdS) depending on relative compositional percentage of sulfur and selenide in the deposited thin films and exhibits high coefficient of an absorption and band-to-band type of transition [1-5]. Hence, emission of light from these ternary nanostructures covers more or less entire visible spectrum and thereby CdSSe could be very important particularly for light emitting device [5]. Also, interesting tunable optical emission and absorption from CdSSe nanocrystals is possible by controlling S/Se ratio. Few reports are available on the preparation of CdSxSe1-x nanostructures [5-8], using physical methods that are expensive and also require sophisticated instruments. Theoretical study based on stimulated emission from CdSxSe1"x nanobelts by optical excitation has been reported [9, 10]. Only few reports are available [11,12, 14] on the deposition and characterization of CdSSe thin films using chemical bath deposition method. Since in these reports XRD data were not compared with standard JCPDS rather than that depending on S/Se concentration shifting of 2˜ values of XRD pattern were described. Due to scarcity of reports on the deposition of CdSSe thin films, we planned to deposit CdSSe thin films at different temperatures.

Chemical bath deposition (CBD) of metal chalcogenide thin films has numerous advantages over other methods due to its easiness, simplicity and lack requirement of any sophisticated instruments. Also the preparative conditions were easily controlled and varied depending on the need and hence CBD method was used for the deposition of CdSSe thin films.

We are reporting on the preparation of CdSSe thin films by chemical bath deposition. In order to study the effect of temperature on the deposition of CdSSe thin films, the deposition was carried out at temperature 293, 313, 333 and 353 K. The deposited thin films were characterized using different techniques as mentioned in the abstract.

2. Experimental Procedure:

2.1Substrate Cleaning:

The procedure used to clean the glass substrates was by simply by dipping the glass substrates in Conc. H2SO4 and then rinsed with deionized water. The substrates were further cleaned in an ultrasonicating device at 50 Hz and 30 min at 333 K.

2.2Deposition:

Cadmium sulphoselenide thin films were deposited using analytical grade cadmium acetate Cd(CH3COO)2, thiourea NH2SNH2, Na2SeSO3 and ammonia (NH3) 25% solution. All chemicals were purchased from s. d. fine Ltd. and used without further purification. For the deposition of CdSSe thin films, 50 ml of 0.25M Cd(CH3COO)2 solution was added in a 150 ml capacity glass beaker. In this solution, ammonia 25% was slowly added with constant stirring, so as to make the solution clear and transparent. Further to this 25 ml of both NH2SNH2 and Na2SeSO3 (freshly prepared) of 0.25 M solution of each were added slowly with constant stirring. Then the cleaned glass substrates were immersed in this aqueous solution containing precursors at suitable angle with the normal from the base of the beaker. The deposition was carried out at 293, 313, 333 and 353 K (temperature) without mechanical stirring. The substrates coated with CdSSe thin film prepared at 293, 313, 333 and 353 K

 ISBN : 978-81-923628-7-8

(temperature) were removed after 96, 20, 10 and 5 hours respectively, then rinsed in flowing de-ionized water, and dried in atmospheric air.

2.3 Reaction Mechanism

The reaction mechanism for the growth of CdSSe thin films proceeds via numerous steps that are explained by C.A. Vanderhyde et al [13].

Formation of cadmium acetate complex:

$$Cd(CH_3COO)_2 + 4NH_3 \rightarrow Cd(NH_3)4^{2+} + (CH3COO)_2^{2-} \quad (1)$$

Dissociation of thiourea:

$$(NH_2)_2CS + OH^- \rightarrow CH_2N_2 + H_2O + HS^- \quad (2)$$

Dissociation of sodium selenosulphate:

$$Na_2SeSO_3 + OH^- \rightarrow Na_2SO_4 + HSe^- \quad (3)$$

Formation of CdSSe:

$$Cd(NH_3)_4^{2+} + HS^- + HSe^- \rightarrow CdSSe\downarrow + 4NH_3\uparrow \quad (4)$$

3. Characterization of CdSSe Thin Films

Thickness measurement of CdSSe material was carried out by gravimetric weight difference method assuming the density of CdS and CdSe as 4.826, 5.81 gm / cm3 respectively. The X-ray diffraction patterns of prepared nanostructures were recorded using a Rigaku miniflex tabletop X-ray Diffractometer. The XRD data were collected with a scan rate of 3o per minute using a CuKα radiation. The shape, size and distribution of nanostructures were observed with scanning electron microscope (SEM) JEOL JSM-6010, IT 300 and Tescon (depending on availability of the instrument), attached to an energy dispersive Spectroscopy (EDS) analyzer to quantitatively measure the sample stoichiometric ratio. To study the optical properties, optical absorption spectra were recorded using a UV-vis spectrophotometer (Shimadzu UV 1800).

3.1 X-ray Diffraction (XRD) Study:

Fig.1 depicts the XRD patterns of the CdSSe thin films deposited at various temperatures. Cadmium sulphoselenide grows with a hexagonal phase at 293, 313, 333 and 353 K (temperature). The comparison of observed data with standard data [15] revealed the hexagonal structure of deposited thin films. It is also worth to mention that the films deposited at a low temperature (293 K) crystallized with hexagonal structure with orientation along (002) and (101) planes, and commonly observed strong (100) orientated plane was absent in the XRD pattern. It may be due to lower temperature of deposition that alters the nucleation and growth mechanism and final grown structure of deposited thin films. The XRD patterns of the CdSSe thin films deposited at 313, 333 and 353 K (temperature) showed well resolved peaks that could be indexed as (100), (002), (101), (102), (110), (200) and (004) that correspond to hexagonal phase of CdSSe [15]. Also the intensity of observed diffracted peaks was found to be increased with increasing temperature of deposited thin films. It is worth to note that the CdSSe thin film prepared at 293 K (temperature) was crystallized with different orientation as compared to CdSSe thin films prepared at higher temperature and the crystallinity was found to be improved.

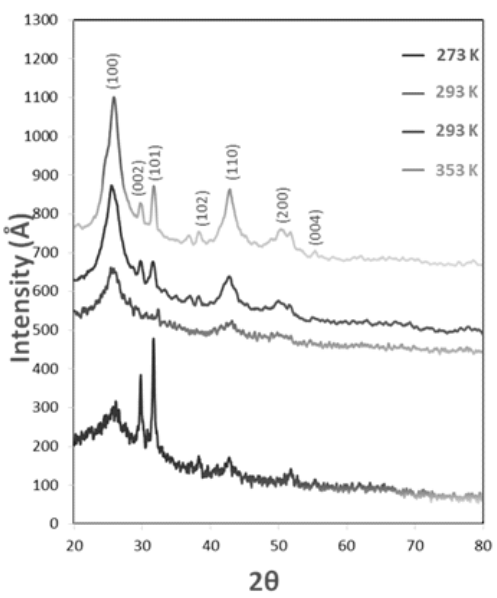

Fig.1 XRD patterns of CdSSe thin films deposited at different temperatures (293, 313, 333 and 353 K)

3.2 EDS Study

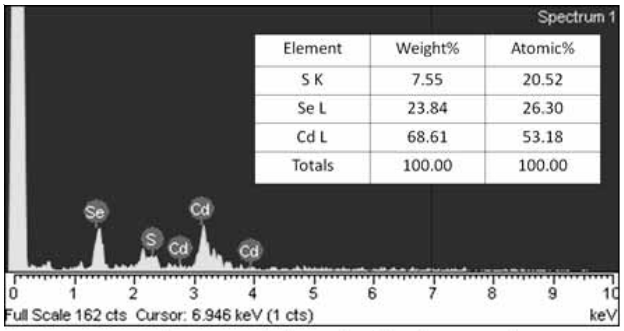

Fig.2 A typical pattern of CdSSe thin film deposited at 333 K

Fig.2 shows a representative EDS pattern and the information of the relevant elemental analysis for the CdSSe thin films deposited at 333 K. The pattern exhibits strong Cd, S and Se peaks. The elemental analysis does not reveal any impurity peaks, confirming the purity and uniformity of the deposited CdSSe thin films. The average atomic percentage of the Cd, S, and Se product is slightly rich in Cd for the sample deposited at 333 K.

3.3 Morphological Study:

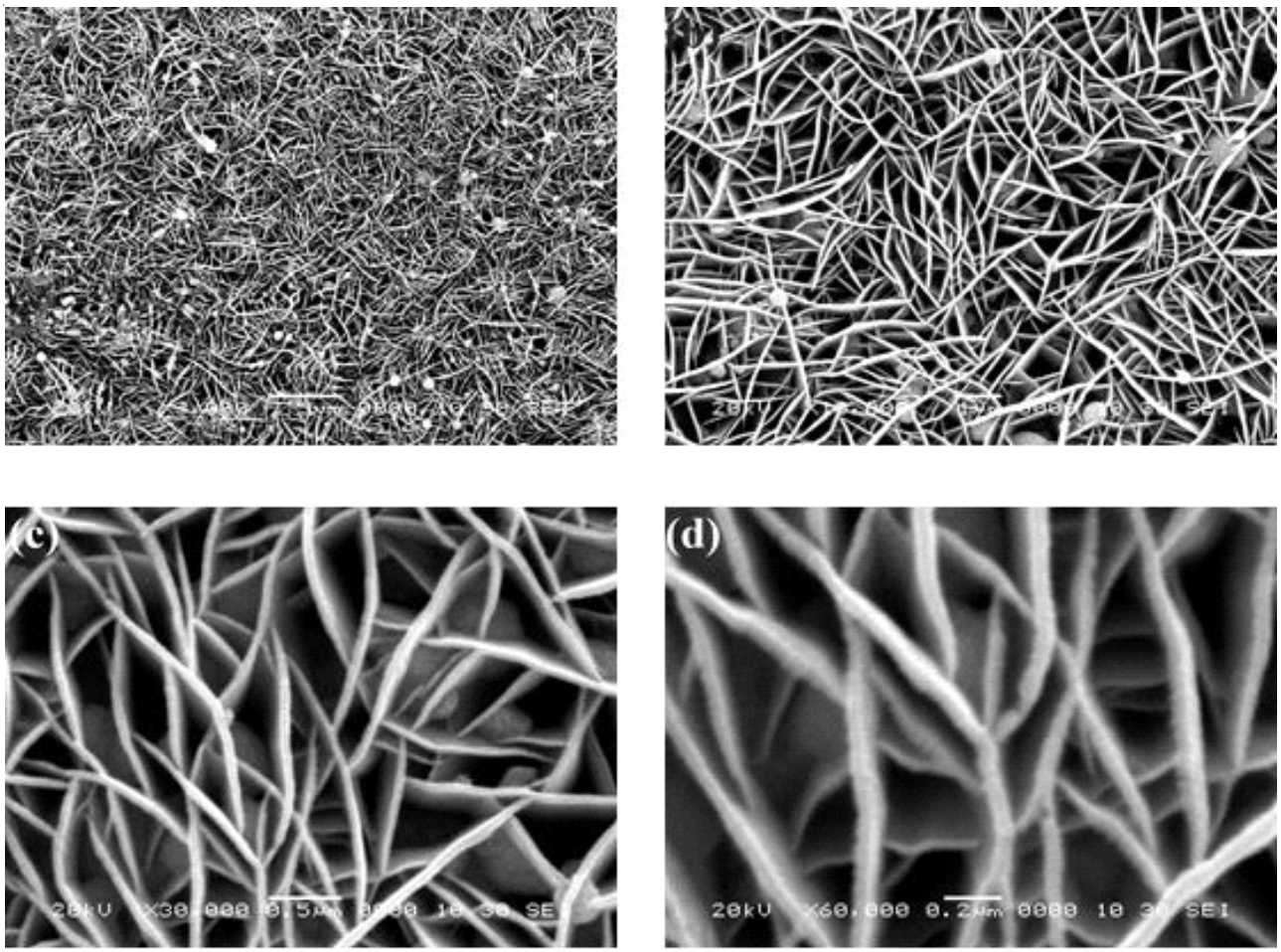

Fig.3 (a-d) SEM images of CdSSe thin film deposited at 293 K: (a) 3 kX, (b) 10 kX , (c) 30 kX, and (d) 60 kX

Scanning electron microscopic (SEM) technique was used to observe the morphologies of the deposited thin films. Fig.3 (a-d) shows the SEM micrographs of CdSSe thin film deposited at 293 K. The SEM images depicts that the CdSSe thin film deposited at 293 K is uniform and homogeneous, and well covered over the substrate surface. It also reveals a regular pattern sheet-like structures that are inter woven together without any cracks and voids. The thickness of these plates (sheet-like structures) is in the range 30-40 nm and length in the range of few micrometers. The thin sheets were grown perpendicular to the substrate surface and interconnected with each other to form interesting morphology. The SEM images of the film deposited at 293 K also depicts spherical type morphology which mingled at random sites among the sheets.

 ISBN : 978-81-923628-7-8

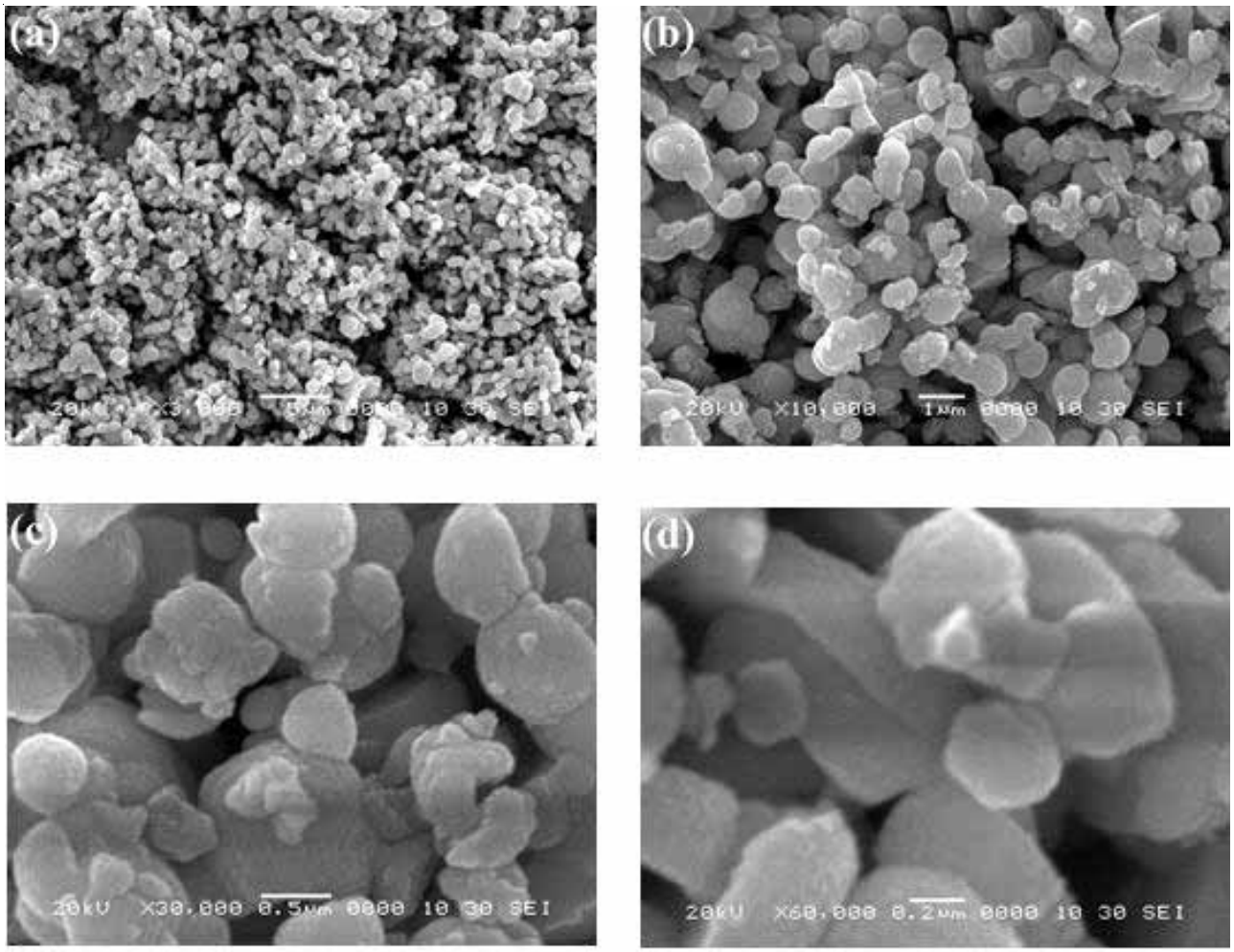

Fig.4 (a-d) SEM images of CdSSe thin film deposited at 313 K: (a) 3 kX, (b) 10 kX , (c) 30 kX, and (d) 60 kX

Fig.4 (a-d) shows the SEM micrographs of CdSSe thin film deposited at 313 K. A close look at lower magnification of SEM images revealed two layer growths that occur over the substrate surface. The smooth two dimensional (2D) CdSSe layer is uniformly deposited on the substrate surface so as to form an initial layer. Then initially formed layer was covered with three dimensional (3D) microsized CdSSe grains structure with irregular size and pattern. These micrograins are densely packed and closely connected with each other. Careful observation at higher magnifications shows that the 3D microstructures were composed of tiny CdSSe nanocrystallites. As a result, microstructural grains are bigger than the individual nanocrystallites. The observed morphology can be with a two stage growth mechanism. Initially, due to abundant availability of Cd2+, S2- and Se2- ions, first stage (2D lateral growth) is attributed to instantaneous rapid nucleation that covers the substrate surface. In the second stage, the ions are slightly depleted and the reaction takes place slowly to form explained 3D microstrucutres that grow at random sites on top of the first layer [16].

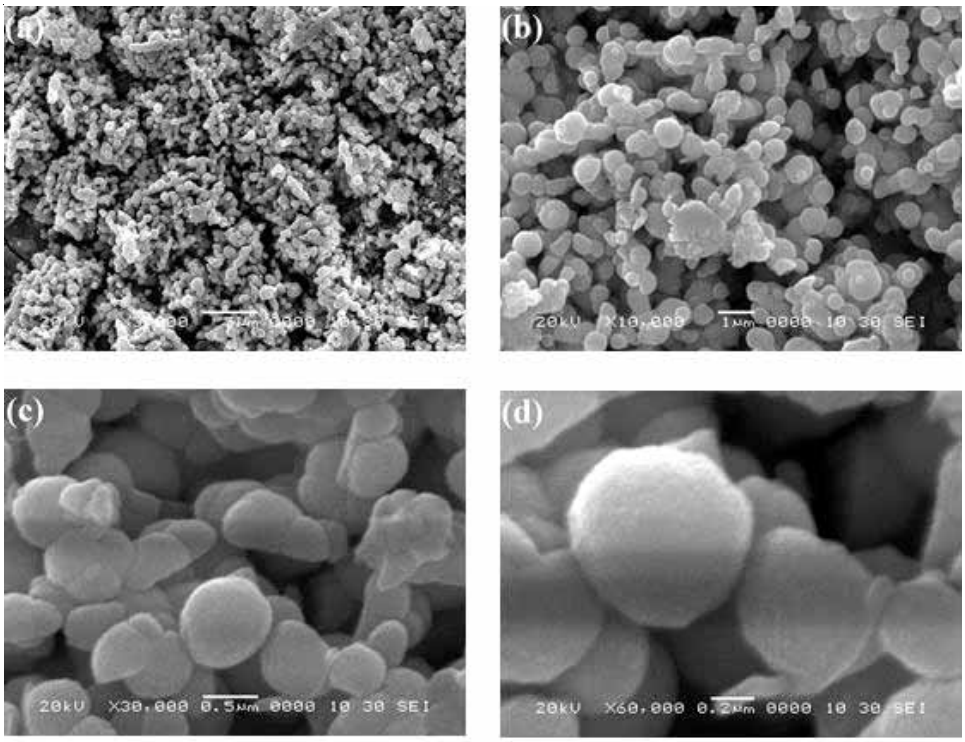

Fig.5 (a-d) SEM images of CdSSe thin film deposited at 333 K: (a) 3 kX, (b) 10 kX , (c) 30 kX, and (d) 60 kX

Fig.5 (a-d) shows the SEM micrographs of CdSSe at 333 K. The morphology of the deposited film is more or less similar to that of the film deposited at 313 K. Only the difference is that 3D microstructures deposited at 293 K are more irregular and that are deposited at 333 K shows somewhat regular spherical microspheres.

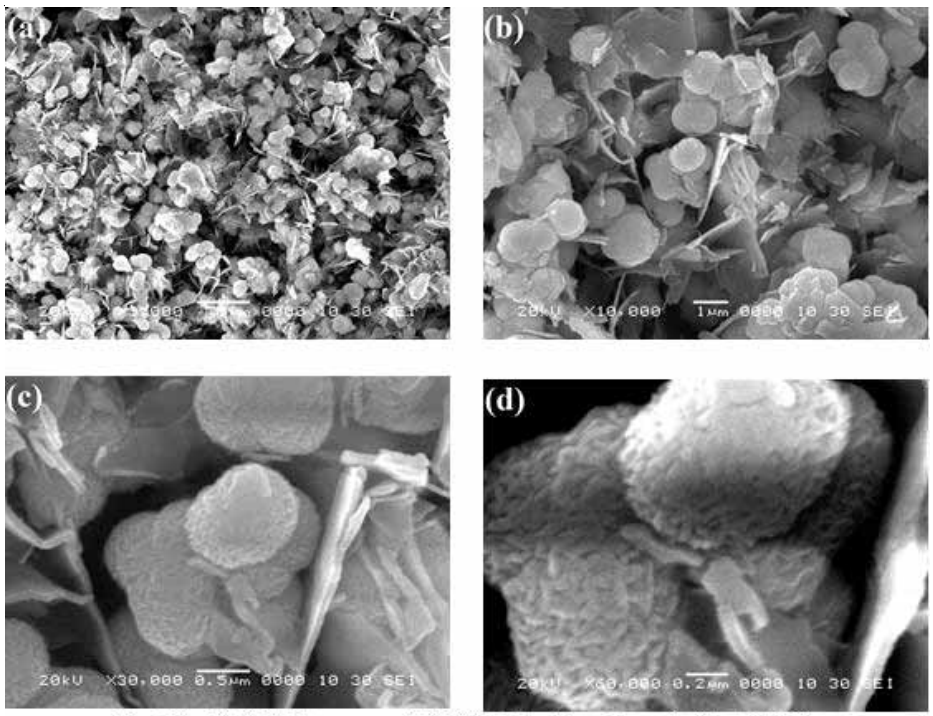

Fig.6 (a-d) SEM images of CdSSe thin film deposited at 353 K: (a) 3 kX, (b) 10 kX , (c) 30 kX, and (d) 60 kX

 ISBN : 978-81-923628-7-8

Fig.6 (a-d) shows the SEM micrographs of CdSSe at 353 K. The SEM images of 353 K showed a different morphology than that of the film deposited at 293 and 313 K. It consists of duplex type morphological pattern in which interconnected microspheres and sheetlike leaflets that are closely packed to form duplex pattern. At higher magnifications, it is clearly observed that the microspheres are consisted with tiny elongated peanut shape CdSSe nanocrystallites.

3.4 Optical properties (UV-Visible Spectrum): The data obtained of optical absorption (α) v/s the wavelength (λ) for CdSSe thin films were plotted. It showed an increase in optical absorbance with increasing temperature for the deposited thin films. It is clearly seen that the optical absorption onset shifted towards higher wavelengths for CdSSe thin films prepared at higher temperature. The absorption edge shifted to the higher wavelength reveals the decrease in band gap vales for CdSSe thin films in order of increasing temperature.

The band gap of CdSSe thin films deposited at different temperature was obtained by analyzing absorption data and using the Tauc's relation [13]:

$$\alpha = A (h\nu - Eg)^{n/2} / h\nu$$

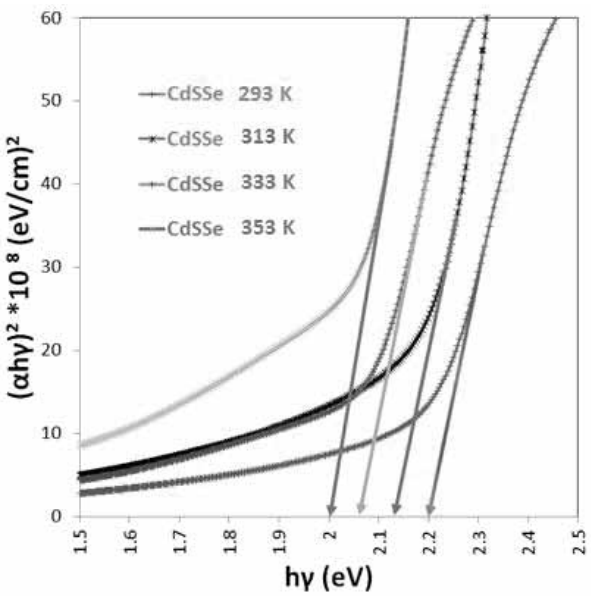

Fig.7 Band Gaps of the CdSSe Thin Films deposited at different temperatures (293, 313, 333 and 353 K)

where A is boltzmann constant, Eg is the band gap, α is the absorption coefficient of semiconductor, $h\nu$ is the photon energy and n is a constant equal to 1 for direct gap semiconductors and 4 for indirect gap semiconductor materials. The variation of $(\alpha h\nu)^2$ verses $h\nu$ (Fig.7) is linear at the absorption edge. Extrapolating the straight-line portions of the plot $(\alpha h\nu)^2$ verses $h\nu$ for zero absorption coefficient value give the 'Eg' and are listed in Table . The 'Eg' of CdSSe thin film prepared at 293 K is 2.2 eV, which is higher than the standard bulk 'Eg' value of CdSSe. The 'Eg' for thin films prepared at 313, 333, 353 K was 2.13, 2.06 and 2.0 eV respectively. The difference in the values of energy band gap is due to a size quantization effect commonly observed in CdSSe nano-crystallites [13-16]. The decrease in the band gap 'Eg' can be due to the influences of various factors such as improvement of crystallite size, change in structural parameters, increase / decrease in carrier concentrations, presence of impurities, deviation from stoichiometry of the film and lattice strain [13,14].

4. Conclusion

The CdSSe thin films were deposited at different temperatures ranging from 293-353 K using CBD technique. The film developed at 293 K was poorly crystallized, also depicted a minor quantity of impurities. The increase in deposition temperature made it possible to nullify the existence of impurities. In this research work, CdSSe thin films grew with a purely hexagonal phase. The polycrystalline CdSSe thin film deposited at 293, 313, 333 and 353 K showed quantum size effect and the band gaps were estimated at 2.2, 2.1, 2.06 and 2.0 eV respectively. The synthesizing temperatures played a significant role on the morphology as well of the thin films developing novel structures.

References

[1] W. Qingqing, X. Gang, H. Gaorong, (2005) J. Solid State Chem. 178 2680

[2] P. Dalvand, M. R. Mohammadi, D.J. Fray, (2011) Materials Letters 65, 1291

[3] Y. K. Liu, J. A. Zapien, Y. Y. Shan, H. Tang, C. S. Lee, S. T. Lee, (2007) Nanotech. 18, 365606

[4] A. Pan, H. Yang, R. Yu, B. Zou, (2006) Nanotech. 17, 10836

[5] Yu Lee Kim, Jae Hun Jung, Kyung Ho Kim, Hyun Sik Yoon, Man Suk Song, Se Hwan Bae and Yong Kim, (2009) Nanotech. 20, 095605

[6] S. K. Apte, B. B. Kale, R. S. Sonawane, S. D. Naik, S. S. Bodhale, B. K. Das, (2006) Mater. Lett. 60, 499

[7] A. Pan, H. Yang, R. Liu, R. Yu, B. Zou, Z. Wang, (2005) J. Am. Chem. Soc. 127, 15692

[8] Y. J. Choi, I. S. Hwang, J. H. Park, S. Nahm, J. G. Park, (2006) 17, 3775

[9] Y. K. Liu, J. A. Zapien, Y. Y. Shan, H. Tang, C. S. Lee, S. T. Lee, (2006) Nanotech. 17, 3775

[10] A. Pan, R. Liu, F. Wang, S. Xie, B. Zou, M. Zacharuas, (2006) J. Phys. Chem. B, 110, 22313

[11] F. I. Ezema, R.U. Osuji, (2007) Chalcogenide Lett. 4, 69

[12] R. S. Mane, C. D. Lokhande, (1997) Thin Solid Films, 304, 56

[13] C. A. VanderHyde, S. D. Sartale, J. M. Patil, K. P. Ghoderao, J. P. Sawant, R. B. Kale, (2015) Solid State Sci. 48, 186

[14] K. V. Khot, S. S. Mali, N. B. Pawar, R. R. Kharade, R. M. Mane, P. B. Patil, P. S. Patil, C. K. Hong, J.H. Kim, J. Heo and P. N. Bhosale, (2015) RSC Adv., 5 40283

[15] JCPDS data File No. 40-0838

[16] G. Hodes, Chemical Solution Deposition of Semiconductor Films, (2002) CRC Press, pp. 172

 ISBN : 978-81-923628-7-8

Dielectric, Magneto-dielectric and Magnetic Properties of $x[Co_{0.9}Ni_{0.1}Fe_2O_4]$-(1-x)$[0.5Ba_{0.7}Ca_{0.}3TiO_3$-$0.5BaZr0_{.2}Ti_{0.8}O_3]$ Multiferroic Composite

Abhishek Kakade[a] and Dr. S. B. Kulkarni[a*]

[a]Department of Physics, The Institute of Science, 15 Madam Cama Road, Mumbai, 400032, India
*E-mail address: sbk_physics@yahoo.com (Dr. S.B. Kulkarni)

In the present work, we have synthesized $x[Co_{0.9}Ni_{0.1}Fe_2O_4]$-(1-x)$[0.5Ba_{0.7}Ca_{0.}3TiO_3$-$0.5BaZr0_{.2}Ti_{0.8}O_3]$, x = 0.1, 0.2, 0.3, 0.4 & 0.5multiferroic composite by hydroxide co-precipitation method. The structural and morphological analysis of the composite $x[Co_{0.9}Ni_{0.1}Fe_2O_4]$-(1-x)[0.5Ba0.7Ca0.3TiO3-0.5BaZr0.2Ti0.8O3] was carried out by using X-ray diffraction and Scanning Electron Microscopy. The XRD spectra confirm the perovskite phase and spinel phase. Dielectric properties of the composite were studied using Impedance analyzer. The variation of dielectric constant and loss of tangent (Quality factor) with applied magnetic field between 0 T to 1 T in the frequency range of 500 Hz to 1 MHz were investigated. Magnetocapacitance were measured for magnetic field up to 1 Tesla, which increases with increase in magnetic field. Dielectric constant possesses contribution due to magnetic field dependent interfacial polarization and variation due to induced stress which can be explained on the observed MD effect. Saturation magnetization of composites increases with increase in CNFO content.

Keywords: *Multiferroic, Dielectric, Magnetocapacitance, Magnetization.*

Study of Dielectric and Magneto-dielectric Properties of $x[Co_{0.9}Ni_{0.1}Fe_2O_4]$-(1-x)$[Ba(Zr_{0.2}Ti_{0.8})O_3]$ Multiferroic Composite

Abhishek Yadav[a], Santosh Shinde[a], Sarthak Hajirnis[a], Kiran Gaikwad[a], Abhishek Kakade[a] and Dr. S. B. Kulkarni[a*]

[a]Department of Physics, The Institute of Science, 15 Madam Cama Road, Mumbai, 400032, India
*E-mail address: sbk_physics@yahoo.com (Dr. S.B. Kulkarni)

In the present work, we have synthesized $x[La_{0.7}Sr_{0.3}MnO_3]$-(1-x)$[Ba(Zr_{0.2}Ti_{0.8})O_3]$ Multiferroic composite by hydroxide co-precipitation method. The structural and morphological analysis of composite $x[La_{0.7}Sr_{0.3}MnO_3]$-(1-x)$[Ba(Zr_{0.2}Ti_{0.8})O_3]$ was carried by X-ray diffraction and SEM. The XRD spectra show perovskite cubic structure for ferroelectric and rhombohedral crystal structure with hexagonal axis of symmetry for magnetostrictive material. Dielectric properties of the composite were studied using Impedance analyzer. The variation of dielectric constant and loss of tangent (Quality factor) with applied magnetic field between 0 T to 1 T in the frequency range of 500 Hz to 1 MHz are investigated. Dielectric constant possesses contribution due to magnetic field dependent interfacial polarization and variation due to induced stress which can be explained on the observed MD effect.

Keywords: *Co-precipitation, Dielectric, Magneto-dielectric, Multiferroic.*

Sulphated Yttria-zirconia as a Catalyst System for the Synthesis of 1,3-dioxolanes- A [3+2] Cycloaddition Approach

Sandeep S. Kahandal*

Department of Chemistry, V.P.M's B. N. Bandodkar College of Science, Thane (W), Maharashtra, India.
E-mail address: sskahandal@vpmthane.org/ sandeepkahandal@gmail.com

Dioxolane compounds were proven to be the useful intermediates in various organic transformations. 1,3-Dioxolane unit is also used as a carbonyl protecting moiety in the case of aldehydes and ketones in carbohydrates and steroid chemistry. In addition, they are suitable derivatives of diols for GC, GLC and mass spectrometry. The catalytic activity of the sulphated yttria-zirconia was investigated for the synthesis of 1,3-Dioxolane from epoxides and ketones. Various metal oxides, mixed metal oxides and their sulphated counterparts were tested for the synthesis 1,3-dioxolanes. It was found that sulphated yttria-zirconia catalysts exhibited good catalytic activity under solvent free conditions. The catalyst system could also be used up to six catalytic cycles without any significant loss in catalytic activity.

Keywords: *Sulphated yttria-zirconia; 1, 3-Dioxolane; solvent free.*

Computational Study of Acetonitrile in Singlet, Triplet and Quintet State Using Density Functional Theory Method

Bhagwat Kharat[a*] and Ajay Chaudhari[b]

[a] Department of Physics, Swami Vivekanand Sr. College, Mantha, Jalna, India
[b]Department of Physics, The Institute of Science, Mumbai-400032, India
[*]Corresponding author's E-mail address: Bhagwat6776@gmail.com

This work reports optimized geometry of acetonitrile in singlet, triplet and quintet state using density functional theory method. The Finite-Field approach has been used to obtain the static first (β) and second (γ) hyperpolarizabilities of acetonitrile in different spin state. Acetonitrile shows the lowest energy at B3LYP/aug-cc-pvdz level among different levels used here. The geometrical parameters and vibrational frequencies of acetonitrile in ground state from this work are in excellent agreement with the experimental determinations .Almost all the vibrational modes in a triplet as well as quintet state are red shifted than the corresponding modes in singlet state except the CCN bending and C-C stretching modes in triplet and the C-C stretching mode in quintet. Theã value of acetonitrile in quintet state is increased by about 500 a.u. than the singlet state using electron correlation method. The HOMO-LUMO gap in a singlet state is larger than that for the triplet and quintet state.

Keywords: *Acetonitrile, spin state, vibrational spectra, hyperpolarizabilities, and DFT method.*

 ISBN : 978-81-923628-7-8

Microwave Assisted, Sonochemical Synthesis of $CoFe_2O_4$ as Potential Supercapacitor Electrode Material

Akash Kanojiya[a], Aliya Tisekar[a], Karan Kotalgi[b] and Paresh H. Salame[b]

[a]Department of Physics, B. N. Bandodkar College of Science, Thane-400601
[b]Department of Physics, Institute of Chemical Technology Mumbai, Matunga, Mumbai-400019

In this paper, we present a novel synthesis technique for fabricating single phase $CoFe_2O_4$ nano-powders as potential electrode materials for supercapacitor application by incorporating the power of sonochemical synthesis route, assisted by the microwave heating. Using this combination of technique, we have achieved accelerated synthesis mechanism for $CoFe_2O_4$.

The sonochemically synthesized, microwave heated compound was characterized by using powder X-ray diffraction (XRD), Fourier Transformed Infrared Spectroscopy (FTIR), Raman Spectroscopy and Scanning Electron Microscopy (SEM) techniques for their structural and surface morphological properties. A single phase formation with particle size 50-60 nm was observed for the sample synthesized using this novel route. Electrochemical properties were studied using Cyclic Voltammetry (CV) and Galvanostatic Charge-Discharge (GCD) method which revealed the maximum specific capacitance of 63.1 F/g within potential window of 0 to 0.5 V. Internal resistance of the cell was determined using electrochemical impedance spectroscopy (EIS) and was modelled using equivalent parallel RC circuit.

Keywords: *Cobalt Ferrite; sonochemical method; Microwave synthesis; supercapacitors.*

Effective CeO_2 Nanoparticles Catalysed for Synthesis of Heterocyclic Bis (Indolyl) Methanes Under Mildconditions

Dr. Vishvanath D. Patil* and Amruta Salve

Organic Chemistry Research Laboratory, Department of Chemistry,
C.K.Thakur A.C.S.College New Panvel, India

Heterocyclic Bis(indolyl)methanes derivatives have been synthesized using a catalytic amount of ceria nanoparticals in $CHCl_3$ at room temperature, .CeO_2 nanoparticles were found to be an efficient catalyst in the reaction of indoles with carbonyl compounds to afford the corresponding bis(indolyl)methanes. .The significances of this method are mild reaction condition, excellent yield and simple work up procedure.

Keywords: *Nanocattalyst,Ceria nanoparticle, Bis (indolyl) methanes.*

Relaxation Dynamics in Biomolecules Investigated by Dielectric Spectroscopy

Anil Sonkamble[a], Sidram Dongarge[b] M. Malathi[c] and Umakant Biradar[b]

[a]Department of Physics, Dayanand Science College, Latur-413512 (Maharashtra)India.
[b]Department of Physics, Mahatma Basweshwar College, Latur-413512 (Maharashtra) India.
[c]Condensed Matter Research Laboratory, School of Advanced Sciences, VIT University, Vellore-632 014, Tamilnadu, India.

Relaxation dynamics in biomolecules were studied here using dielectric spectroscopy. Dielectric properties of Zinda Tilismath and Eucalyptol in the frequency range from 10 MHz to 1 GHz have been obtained by time domain reflectometry (TDR) technique at 300 K. The frequency dependence of dielectric constant and dielectric loss factors were determined for Zinda Tilismath and Eucalyptol. The dielectric permittivity spectra for these biomolecules were analyzed by the Havriliak-Negami expression and fitted in Debye model. The static dielectric constant ($\hat{}_0$), high frequency limiting dielectric constant ($\hat{}\propto$), and relaxation time (τ_0) were also measured. From this study it has been observed that both biological molecules show a similar dielectric behavior at 300 K. The present investigation is an evidence of terpenes which found in Zinda Tilismath through a dielectric approach.

Keywords: *Biomolecules; Time domain reflectometry; Dielectric relaxation.*

Synthesis of Carbon Fiber form Sugarecane Bagasse for Supercapacitor

Arvind D. Kamkhedkar, Kailash R. Jagdeo* and Suyash S. Agnihotri

Department of Physics, DSPM'S K.V. Pendharkar College, Dombivli-421203.*
Email: kailashjagdeo@gmail.com

Carbon synthesized from sugarcane bagasse has been used as an electrode in Electrochemical Double Layer Capacitor (EDLC). In this study we synthesized the carbon fiber using sugarcane bagasse. In the synthesis process, the as obtained sugarcane bagasse is washed and dried then soaked in calcium carbonate ($CaCO_3$) for a week and NaOH for 15 days. The obtained fibers were pyrolyzed in the presence of Ar at 750^0C for three hours .The obtained carbon is anneal in CO_2 atmosphere at 750 ^{0}C for an hour. The SEM/EDAX shows the morphology of obtained sample is carbon fiber. Cyclic Voltammetry is used to measure the specific capacitance of obtained carbon fiber at different scan rate. The study shows the obtained carbon fiber are promising material in development of EDLC supercapacitor.

Keywords: *Carbon fibers; Electrochemical Double Layer Capacitor;Supercapacitor.*

 ISBN : 978-81-923628-7-8

Study of High Performance Plasma Polymerized Polythiophene Films and its Application as Sensor

Baliram Nadekar[a], Ajinkya Trimukhe[b], Rajendra Deshmukh[b] and Pravin More[a*]

[a]Department of Physics, The Institute of Science, Fort , Mumbai 400032, India.
[b]Department of Physics, Institute of Chemical Technology, Matunga, Mumbai 400019, India.
*Corresponding author: email – pravin.more@gov.in, pravin.more@iscm.ac.in

Thiophene monomer is polymerized using method of plasma polymerization. Pulsed plasma technique was used to deposit Polythiophene on glass substrate. Plasma polymerized polythiophene films were then modified with Iodine for enhancement of sensor performance. Material characterization studies were performed using different analytical instruments. Surface morphology of films was studies using SEM and Optical microscopes. Elemental analysis and particle size variation studies were performed by FTIR and XRD. Gas sensing performance for Methanol and Ethanol was seen to be very high at room temperature and at ppb level.

Keywords: *Plasma polymerization; Gas sensors; thin films; VOCs, Polythiophene.*

LED Lighting : A Promising Artificial Lighting Technology

Dr. Devayani Chikte (Awade) [1]* and Dr. S.K. Omanwar

[1]Department of Physics, G. N. Khalsa College, Matunga, Mumbai (MS), India.
[2]Department of Physics, Amravati University, Amravati (MS), India.
*Corresponding author Email:devi.awade@gmail.com

LED lighting is emerging as a promising option due to several advantages along with energy saving such as high luminous efficiency, environment-friendliness, small volume, and long persistence. In this type of lighting light-emitting diodes (LEDs) are used as sources of illumination rather than electrical filaments or gas. An Artificial lighting technology has gradually broadened the horizons of human civilization. It hasextended our daily working hours further past the boundaries of sunlit times. The incandescent lamp did this dramatically after its invention in the 1870s.Currently a large part of electricity is used for artificial lighting. The cost of this energy to the consumer is very high. The adverse impact of this energy to the environment is the millions of tons of carbon emitted into the atmosphere which is a keycontributorto theglobal warming.LED lighting is considered as green technology which converts directly electricity to visible white light using semiconductor materials and has the potential to be an energy-efficient, eco-friendly technology which reduces CO2 emission and is safe to human life.

Corrosion Behavior of Nano-Bilayer Coating of TiN and ZrN Produced by Cathodic Arc PVD Process on NiTi

Kailas B. More[1], Kailash R. Jagdeo[2] and Surface Modification Technology Pvt. Ltd[3]

1. Dept. of Physics, J.S.M College, Alibag (MS), India.
2. Dept. of Physics, DSPM's K. V. Pendharkar College, Dombivli (MS), India.
3. G No. 9 To 11, Emerald Premises, Behind Modi Hyundai Waliv Phata Sativali Road, Vasai East, Vasai-401208, Maharashtra, India.

Biomaterials like NiTi and stainless steel alloys are widely used as human body implants as a substitute for the living tissue for satisfying normal functionalities of the body.

However; Due to continuous shower of body fluid, harmful Ni ions leach out from the surface of these alloy, a protective passive layer and Nickel free surface on NiTi shape memory alloy should be produced by TiN and ZrN bilayer coating deposited by cathodic arc PVD process for biomedical application. The deposition was carried out at- 54V,-200V,-350V,-500V substrate bias voltage at 200^0C temperature for 30 min. The surface modification by the cathodic arc PVD process of NiTi and its biocompatibility properties were studied. The Corrosion resistance was investigated in simulated body fluid at 37^0C by an electrochemical test using Tafel extrapolation method. Bilayer TiN-ZrN coating on NiTi exhibited better corrosion resistance property than the barer NiTi and stainless steel 316L. Bilayer TiN-ZrN coating improves corrosion resistance. Crystallographic orientation, surface topography and bilayer coating composition were studied using X-ray diffraction, scanning electron microscope SEM, energy dispersive spectrum (EDS) respectively.

Keywords: *Nano- bilayer, Tafel extrapolation method, corrosion resistance.*

Synthesis of Coumarin Based Fluorescent Compounds

Kailas K. Sanap[a]

[a]Department of Chemistry, N.B. Mehta Science College, Bordi, Palghar-401701

Coumarins (2H-1-benzopyran-2-ones) and polycyclic compounds containing coumarin moiety occur in many plants and have important applications in biology. They form a group of more than 50 drugs, which are used in medicine and have diverse biological activities, viz. anticoagulant, antifungal, hypertensive, CNS depressant, antihelmintic, hypnotic, antitumor agents, and HIV protease inhibition. Coumarin compounds are used as additives in foods, perfumes, cosmetics, pharmaceuticals, cigarettes, and alcoholic beverages. They find application in fluorescent dyes, as they are effective fluorophores, characterized by high fluorescence quantum yields. Undeniably, they constitute the largest class of fluorescent dyes and are widely used as emission layers in organic light-emitting diodes (OLED), optical brighteners, and nonlinear optical chromophores.

Initially, different 7,8 substituted coumarin-4-acetic acids were prepared and simultaneously 7-diethylaminocoumarin-3-carbaldehyde was prepared from diethylaminosalicyldehyde. In the last step 7,8 substituted coumarin-4-acetic acids and 7-diethylaminocoumarin-3-carbaldehyde were reacted to give highly fluorescent 1,2-biscoumarinylethenes. These compounds are having good colors ranging from orange to reddish brown. They are subjected for further studies.

Keywords: *Coumarin, light emitting diodes, fluorescence, quantum yield.*

 ISBN : 978-81-923628-7-8

Microwave Assisted Sonochemical Synthesis of Nanostructured $FeCo_2O_4$ as Potential Cathode Materials for Supercapacitors

Karan Kotalgi and Paresh H. Salame

Department of Physics, Institute of Chemical Technology Mumbai, Matunga, Mumbai-400019

Iron Cobaltite ($FeCo_2O_4$) is successfully prepared *via* Wet chemical route using accelerated Sonochemical approach, the synthesis process was further hastened by using microwave furnace for solid state reaction in lieu of conventional furnace.For structural characterization is investigated using powder X-Ray Diffraction (XRD), Fourier Transform Infra-Red Spectroscopy (FTIR), Raman Spectroscopy etc. A single spinel phase was revealed by these techniques with very few impurities. The particle morphology over these phase formed powders was investigated using Scanning Electron Microscope (SEM). For elemental and compositional analysis X-ray Photoelectron Spectroscopy (XPS) and Energy dispersive x-ray analysis (EDS) was employed. A stoichiometric composition was revealed by using both these techniques.To evaluate its electrochemical performance the material was coated over stainless steel (SS) mesh and was tested in a three-electrode system. The $FeCo_2O_4$ compound showed an areal capacitance of 89.188 mF/cm^2 at 30mV/s. The areal capacitance showed by the material put its candidature as a potential supercapacitor.

Keywords: *Iron Cobaltite; SonochemicalSynthesis; Microwave Synthesis; supercapacitors.*

NO_2 Gas Sensing Properties of ZnO Thin Film Prepared by Sol-gel Method

K. V. Madhale[a, d], B. N. Jamadar[b], A. R. Nimbalkar[c*], N. B. Patil[d] and S. B. Kulkarni[e*]

aDepartment of Physics, Walchand college of Engineering, Sangli. Maharashtra, 416415, India.
bDepartment of Physics, Walchand college of Engineering, Sangli. Maharashtra, 416415, India.
cDepartment of Physics, Dattajirao Kadam Arts, Science and Commerce College, Ichalkaranji, Maharashtra, 416115, India.
dSharad Institute of Technology, Polytechnic, Yadrav, Ichalkaranji, Maharashtra, 416121, India.
eDepartment of Physics, The Institute of Science, Mumbai.
*Corresponding Author: amolakshay28@gmail.com

Nitrogen dioxide (NO_2) sensing properties of ZnO thin film synthesized by simple Sol-gel spin coating method are studied. The structural, optical and gas sensing properties of the thin film is studied byusing X-ray diffraction (XRD), field emission scanning electron microscopy (FESEM), UV-Visible spectroscopy (UV-VIS). X-ray diffraction and scanning electron microscopy showed that the ZnO thin films have hexagonal wurtzite crystal structure. The optical band gap of deposited film is found to be 3.18 eV. The ZnO thin film shows the highest gas response to NO_2 at 200 ^oC operating temperature. Maximum response up to 2.30 is achieved towards 10 ppm NO_2 at 200 ^oC operating temperature. ZnO films are highly selective towards NO_2 in comparison with other gases like H_2S, Cl_2 and LPG.

Keywords*: ZnO thin film, NO_2 gas, XRD, Gas sensor.*

Effect of Particle Size on Gas Sensitivity of CO_2 Gas Using Nano Sized Metal Oxides

[1]Mude K.M.,[2]Mude B.M.,[3]Zade R.N.,[4]Patange A.N. and [5]Yawale S.P.

[1]Department of Physics,Bhavan's College, Andheri (W) -400058, India.
[2]Department of Physics,Ramnarain Ruia College,Matunga (E) -400019, India
[3]Department of Chemistry,Siddharth College,Fort,Mumbai-400001, India
[4]Department of Chemistry,Bhavan's College, Andheri (W) -400058, India
[5]Department of Physics, Govt.Vidarbha Institute of Science and Humanities,Amravati-444604, India.

The function of gas sensing is very much vibrant in todays era as far as environmental aspects are concern.The nano particle sized structures illustrate excellent properties, particularly with lower grain sizes. This leads to various improvements in their performance. The sensitivity of the sensor largely increases with the reduction of the size. To study effect of particle size on gas sensitivity of CO_2 gas using nanosized metal oxides, we select the nanosized of CuO and ZnO. There is hardly any change in the sensitivity values observed for the particle size that is larger than 50nm for CuO and ZnO .We noticed after characterization and analysed that, the sensitivity shoots up to give a swift boost in the sensitivity values for particle size less between 50nm for ZnO and CuO.

Keywords: *CuO, ZnO, Sensitivity and Nano Particle Size.*

Study of Structural, Morphological and Optical Properties of $Cu_{1-x}Mn_xO$ Nanoparticles Prepared by Co-precipitation Technique

Nitin Gurude, Dipak Kadam, L. H. Kathwate, M. B. Awale and Vishwanath Mote*

Thin Films and Materials Research Laboratory, Department of Physics,
Dayanand Science College, Latur- 413 512, Maharashtra, India
Corresponding email id: vmote.physics@gmail.com

$Cu_{1-x}Mn_xO$ (x= 0, 0.01, 0.02 and 0.03) nanoparticles were prepared by a simple and cost effective co-precipitation technique at room temperature. The structural, morphological and optical properties of the films were studied by using X-ray diffraction (XRD), Field emission scanning electron microscope (FESEM) and UV spectrophotometer techniques. XRD analysis reveals that all prepared films has monoclinic structure without any extra impurities phases. The values of lattice parameters 'b'and 'c' decreased with increasing Mn content of CuO nanoparticles and Mn^{2+} ions were successfully incorporated into the lattice positions of Cu^{2+} ions. The average crystallite sizes were observed in the range of 16 to 21 nm. SEM studies showed polycrystalline appearance with clearly defined grains. UV-Visible measurement shows that all the nanoparticles of absorption edge are changes of Mn doped CuO nanoparticles.. The direct optical band gap energy for pure CuO thin film is found to be variation with Mn doping.

Keywords: *$Cu_{1-x}Mn_xO$ nanoparticles, Co-precipitation, XRD, SEM, Optical property.*

 ISBN : 978-81-923628-7-8

Synthesis and Characterization of Zinc Cobaltite Metal Oxide Electrode for Supercapacitor Application

Nidhi Tiwari[a], Snehal Kadam[a] and Shrinivas Kulkarni[a*]

[a]Materials Research Laboratory, Department of Physics, The Institute of Science,
Dr. Homi Bhabha State University, Madam Cama Road , Mumbai-400032.
*Corresponding author: *sbk_physics@yahoo.com*

In recent years energy storage devices are the prominent candidates for the upcoming generation of electrochemical applications. Among the various electrode materials for supercapacitors, ternary metal oxides (TMOs) represented by $A_xB_yO_z$ have attracted much attention because of their low cost, environmental friendliness, high theoretical specific capacitance, and multiple oxidation states. In the present work, $ZnCo_2O_4$ type of spinel transition metal oxide is synthesized via hydrothermal route on stainless steel substrate. The resulting electrodes were analyzed by using X-ray diffraction spectroscopy (XRD), scanning electron microscopy (SEM) and electrochemical characterization techniques like cyclic voltammetery(CV), galvanostatic charge discharge(GCD) & electrochemical impedance spectroscopy(EIS). The obtained results exhibit that hydrothermally synthesized $ZnCo_2O_4$ has a potential for supercapacitor application.

Keywords: *Zinc cobaltite; Hydrothermal; Supercapacitors.*

Formaldehyde and Fluroform Sensing by Metal Doped Ethylene : A First Principle Study

Nilesh Ingale[a] and Ajay Chaudhari[a*]

[a] Department of Physics, The Institute of Science, 15, Madam Cama Road, Mumbai 400032, India.
*Corresponding author: (E-mail:ajaychau5@yahoo.com)

HCHO and CHF_3 sensing properties of Li metal doped C_2H_4 complex are studied by first principles calculations. The HCHO and CHF_3 get adsorbed with 1.31 and 0.30 eV adsorption energy on C_2H_4Li complex. Adsorption of HCHO and CHF_3 results in charge transfer, 0.12 (e^-) charge get transferred from HCHO and CHF_3 to C_2H_4Li complex. Quantum mechanical stability of the complexes is confirmed with vibrational frequency analysis. Calculated values of binding energies of Li metal atom to the C_2H_4 substrate show that the metal atoms remain bound to the C_2H_4 substrate even after adsorption of HCHO and CHF_3.Temperature and pressure dependent Gibbs free energy corrected adsorption energies indicate that both molecule get adsorbed on C_2H_4Li at 300 K. This is also confirmed through ADMP-MD simulations.

Keywords: *VOCs; gas sensor; DOS;ab initio calculation; molecular dynamics.*

Synthesis and Characterization of Manganese Cobaltite as Electrode Material for Supercapacitor Application

Pavan V. Khadekar[a], Harshita D. Shenoy[a], Ganesh T. Nagarvani[a], Jayshri M. Patil[a], Snehal L.Kadam[a], Rahul S. Ingole[a,b] and Shrinivas B. Kulkarni[a*]

[a] Materials Research Laboratory, Department of Physics, The Institute of Science, Mumbai-400032, Maharashtra
[b] *Department of Physics, Shrimant Babasaheb Deshmukh Mahavidyalaya, Atapadi, Dist-Sangli-415301, Maharashtara*
*Corresponding Author: *sbk_physics@gmail.com*

In the present work, Manganese cobaltite ($MnCo_2O_4$) electrode material was successfully synthesized by simple, low cost hydrothermal method on Stainless steel substrate. The structural, morphological and surface area characterizations of synthesized electrode material were carried out using XRD and SEM techniques. The electrochemical properties of synthesized electrode were analyzed by using cyclic voltammetry, galvonostatic charge discharge and electrochemical impedance spectroscopy in 1M KOH aqueous electrolyte. The Manganese Cobaltite electrode shows excellent supercapacitive performance. The result shows that hydrothermally synthesized Manganese Cobaltite on stainless steel is the promising electrode material and would be most appropriate for supercapacitor application.

Keywords: *Manganese Cobaltite; Hydrothermal method; Stainless steel; Supercapacitor.*

Hydrogen Adsorption on Boron Substituted Metal Functionalized Benzene

Priyanka Tavhare and Ajay Chaudhari

Department of Physics, The Institute of Science, FORT, Mumbai 400 032, Maharashtra, India
Corresponding author: ajaychau5@yahoo.com

We have studied hydrogen adsorption properties of metal-doped benzene and boron substituted benzene complexes using second ordered Møller-Plesset method with 6-311++g(d,p) basis set. Hydrogen storage properties of metal-doped benzene vary with positions of boron atom in a benzene ring. Two boron atoms are substituted at 1-2, 1-3 and 1-4 positions of benzene ring and labeled as BB_{1-2}, BB_{1-3} and BB_{1-4} respectively. These pristine as well as modified benzene is functionalized with Li, Be and Ti atoms. The H_2 uptake capacity of C_6H_6Li, $BB_{1-2}Li$, $BB_{1-3}Li$ and $BB_{1-4}Li$ complexes is found to be 6.64, 6.82, 4.65 and 6.82 wt% respectively. All Be-doped complexes can adsorb one H_2 molecule each and having H_2 uptake capacity less than the target specified by US Department of Energy (4.5 wt% by 2020). The H_2 uptake capacity of Ti-doped benzene is enhanced by 1.52 wt% after boron substitution. The H_2 adsorption on all Li-doped complexes is found to be exothermic whereas it is endothermic on Be and Ti-doped complexes at room temperature. The H_2 uptake capacity of Li and Ti-doped complexes decreases while performing Atom centered density matrix propagation molecular dynamics simulations whereas it remains unaffected for Be-doped complexes at 300 K.

Keywords: *Hydrogen storage, boron substitution, NBO analysis, ab initio calculations.*

 ISBN : 978-81-923628-7-8

Hydrogen Uptake Capacity of B_6H_6(Be, Li and Ti) and its Ions: A First Principles Study

Ravinder Konda [a] and Ajay Chaudhari[a*]

[a] Department of Physics, The Institute of Science, 15, Madam Cama Road, Mumbai 400032, India.
*Corresponding author: ajaychau5@yahoo.com

The hydrogen storage capacity of Be, Li and Ti doped closo borane (B_6H_6) and their cations is obtained using second order Møller- Plesset (MP2) method. B_6H_6Be, B_6H_6Li and B_6H_6Ti complexes can interact with two, three and four hydrogen molecules respectively whereas one additional H_2 molecule gets adsorbed on their cations. Adsorption of H_2 molecules on B_6H_6Be and B_6H_6Li complexes is found to be thermodynamically unfavorable whereas it is favourable on B_6H_6Ti at room temperature. $B_6H_6Be^+$ can store H_2 molecules with positive H_2 adsorption on $B_6H_6Li^+$ and $B_6H_6Ti^+$ complexes it is negative. The effect of temperature and pressure on Gibbs free energy corrected adsorption energy is also studied. The desorption temperature for the B_6H_6Be, B_6H_6Li, B_6H_6Ti, $B_6H_6Be^+$, $B_6H_6Li^+$ and $B_6H_6Ti^+$ complexes is found to be 128, 51, 500, 346, 102 and 166 K respectively. The kinetic stability of the complexes is studied by means of HOMO-LUMO gap. Nature of interaction between the H_2 molecules and complexes is studied. The H_2 uptake capacity of all complexes obtained from electronic structure calculations is confirmed with Molecular dynamics (MD) simulations.

Keywords: *Hydrogen storage, Closo-borane, Molecular dynamics simulations.*

Solvothermally Synthesized TiO_2 Photocatalyst and their Photocatalytic Activity

Rekha B. Rajput and Rohidas. B. Kale*

Department of Physics, The Institute of Science, Madam Cama Road,
Mumbai-400032, India
E-mail address: rekha070@gmail.com, rb_kale@yahoo.co.in

TiO_2 photocatalyst was successfully prepared using the solvothermal method with titanium isopropoxide (TTIP) as a precursor. The reaction was carried out at 160 °C for 5 h. The prepared sample was characterized by using X-ray diffraction (XRD), UV–visible absorption spectroscopy, PL spectroscopy and scanning electron microscopy (SEM) along with energy dispersive X-ray spectroscopy (EDAX). The photocatalytic activity of TiO_2 catalysts showed the complete degradation of Methyl orange within 20 mins under visible light irradiation.

Keywords: *Titanium Isopropoxide, Photocatalyst, Solvothermal Method, Methyl Orange.*

Synthesis of Polypyrrole Using FeCl3 as an Oxidant with SLS as Dopant

V. Mayekar[a], R.S. Kajrolkar[a],O. Ramdasi[a], S. S. Karandikar[a], P.S. Prabhu[a] and V. Arava[a]

[a]Department of Physics, RamnarainRuia Autonomous College, Matunga, Mumbai – 19

Conductingpolymers have been of great use because of their compatibility and varied uses such as in gas sensors, solar cells etc. This experiment entitled 'Synthesis of Polypyrrole using $FeCl_3$ as an oxidant and doping it with SLS' at room temperature as well as 3^0C to 5^0C was conducted to check the conductivity of Polypyrrole (polymer) with some impurities. In the synthesis of polypyrrole, $FeCl_3$ was used as an oxidizing agent which formed an iron(III) complex. SLS, also called sodium lauryl sulphate, was used as a dopant which helps in controlling particle size. Then the black precipitate obtained in the end was studied and characterized to check electrical conductivity. It yields noticeable changes between room temperature and controlled temperature synthesis. The infrared spectra of absorption and emission were studied using FTIR spectroscopy. Then the XRD spectra of the samples werecompared to understand the nature of obtained polypyrrole samples. The I vs V characteristics were checked by using four probe method and the I vs V graph wereanalysed to check the conductivity of the polypyrrole sample.

Keywords : *Polypyrrole;XRD; UV; FTIR..*

Synthesis, Characterization and Study of Graphene Oxide for Environmental Nitrate Ion Sensing

Revati P. Potdar and Pravin S. More*

Department of Physics, The Institute of Science, Madam Cama Road, Mumbai-400032, India.
Email: revapotdar2008@gmail.com, p_smore@yahoo.co.in

Oxidation of nitrogen by microorganisms present in soil, water and plants produces nitrate ions in the environment. These nitrate ions are soluble and mobile in water and can migrate to water table. The presence of nitrates in water supplies leads to water pollution. Nitrate contamination in water leads to problems in humans and animals like damaging central nervous system, birth defects and blue baby syndrome. Nitrate ions are a threat to environmental water quality and thus need to be detected. In this study, we report a method for detection of nitrate ions using Graphene Oxide. Graphene Oxide was synthesized by exfoliating Graphite Oxide sheets by ultrasonication. Modified Hummer's method was used to synthesize Graphite Oxide sheets. The structural properties of the Graphite Oxide sample were studied using X-ray diffraction (XRD) pattern and FTIR spectra. XRD pattern revealed that the oxidation of Graphite took place successfully and FTIR exhibits C=O, C-H, COOH and C-O-C bonds indicative of Graphite Oxide. Lastly, to study the detection of nitrate ions by Graphene Oxide, fluorescence emission spectroscopy was carried out and its result was interpreted.

Keywords: *Graphene oxide, nitrate sensing, fluorescence spectroscopy, modified hummer's method.*

 ISBN : 978-81-923628-7-8

Molecular Interaction Studies In Binary Liquid Mixtures Of Allyl Amine (AA) and 2-Methoxy Ethanol (2ME) from Ultrasonic Studies and IR Spectroscopy

Sangita S. Meshram[a], Bhalchandra K. Mandlekar[b], Umakant B. Tumberphale[c] and Prashant G. Gawli[d]

a Dept of Physics, B.N.Bandodkar Science College, Thane-431605, Maharashtra. India.
b Dept of Physics, B.N.Bandodkar Science College, Thane-431605, Maharashtra. India.
c Dept of Physics, N.E.S. Science College, Nanded-431605, Maharashtra. India
d Head of Department of Physics, B.S. College, Basmath, Dist. Hingoli – 431512, Maharashtra. India.

Ultrasonic studies is a potential tool in evaluating intermolecular interactions and nonlinear properties in binary liquid mixtures. Ultrasonic Velocity for binary mixture Allyl amine (AA)and 2-Methoxy Ethanol (2ME) have been measured for 2MHz ultrasonic frequency at 303 K. Various theoretical approaches for sound Simple Mixing Rule (U_{SMR}),Rao (U_{Rao}) ,Impedance Relation (U_{IR}), Vandeel ($U_{Vandeel}$) and Nomatto ($U_{Nomatto}$) have been applied to obtain the theory of best fit for the system for the temperature taken for investigation. Conformational analysis of the formation of hydrogen bond between Allyl amine (AA)and 2-Methoxy Ethanol (2ME) is supported by the FT-IR .The present investigation is aimed at experimental determination of ultrasonic velocity and its comparison with different theories and molecular interactions.

Keywords: *Ultrasonic velocity; Molecular interactions ; Simple Mixing Rule; Impedance Relation.*

Study of Dielectric and Magneto-dielectric Properties of $x[Co_{0.9}Ni_{0.1}Fe_2O_4]$-(1-x)$[Ba(Zr_{0.2}Ti_{0.8})O_3]$ Multiferroic Composite

Sarthak Hajirnis[a], Kiran Gaikwad[a], Abhishek Yadav[a], Santosh Shinde[a], Abhishek Kakade[a] and Dr. S. B. Kulkarni[a*]

[a]Department of Physics, The Institute of Science, 15 Madam Cama Road, Mumbai, 400032, India
*E-mail address: sbk_physics@yahoo.com (Dr. S.B. Kulkarni).

In the present work, we have synthesized $x[Co_{0.9}Ni_{0.1}Fe_2O_4]$-(1-x)$[Ba(Zr_{0.2}Ti_{0.8})O_3]$ Multiferroic composite by hydroxide co-precipitation method. The structural and morphological analysis of composite $x[Co_{0.9}Ni_{0.1}Fe_2O_4]$-(1-x)$[Ba(Zr_{0.2}Ti_{0.8})O_3]$ was carried by X-ray diffraction and SEM. The XRD spectra showperovskite cubic structure for ferroelectric and spinel cubic structure for magnetostrictive material. Dielectric properties of the composite were studied using Impedance analyzer. The variation of dielectric constant and loss of tangent (Quality factor) with applied magnetic field between 0 T to 1 T in the frequency range of 500 Hz to 1 MHz are investigated. Dielectric constant possesses contribution due to magnetic field dependent interfacial polarization and variation due to induced stress which can be explained on the observed MD effect.

Keywords: *Co-precipitation, Dielectric, Magneto-dielectric, Multiferroic.*

Gas Sensing Response of Transition Metal Doped ZnO Thin Film

Savita S. Dange[a] and P. S. More[a]

[a]Department of Physics, The Institute of Science, M. G. Road, Mumbai-400 032.

*Corresponding author: savita.dange@gmail.com

H_2S is a colourless, flammable and highly toxic gas. It is released from coal mines, oil and natural gas industries.Also H_2S gas is used in many industrial processes. The short term and long term exposure limit of H_2S is 10 minutes and 8 hours respectively. Human exposure to higher concentration of H_2S gas results in neurobehavioral toxicity. Therefore it is essential to monitor and control the concentration level of H_2S gas. Doped ZnO is promising candidate for H_2S gas detection. In our work, gas sensing properties of nanostructured doped ZnO thin film have been investigated towards H_2S gas for different temperatures. The sensor film was prepared by chemical bath deposition method at room temperature. We report metal doped ZnOfilm shows enhancement in gas sensing response towards H_2S gas for 50 ppm concentration. The sensor film showed the highest percentage response at 300^o C. The structural and optical properties of the sensor film was characterized by X-ray diffraction (XRD), UV-Vis spectroscopy and Scanning electron microscopy (SEM).Particle size of doped ZnOseen from SEM is about 50 nm.

Keywords: *Nanosrystalline, ZnO, gas sensor.*

Synthesis and Characterization of Bismuth Sulfide Thin Film by SILAR Method

Rahilah S. Shaikh and Rohidas. B. Kale*

Department of Physics, The Institute of Science, Madam Cama Road, Mumbai-400032, India

E-mail address: rahi7fm1996@gmail.com, rb_kale@yahoo.co.in

Bi_2S_3 thin film was grown by simple and low cost successive ionic layer adsorption and reaction method (SILAR) onto the glass substrate at room temperature. The prepared thin film was characterized by X-ray diffraction (XRD), UV–Vis spectroscopy, scanning electron microscopy (SEM) and energy dispersive X-ray spectroscopy (EDX). The films is annealed at 200°C for 1h in air. It is found that deposited film turn from amorphous to polycrystalline after annealing. The structural, morphological, optical and electrical properties of annealed and without annealed film was studied.

Keywords: *Chemical synthesis, Bi_2S_3 nanomaterial, Thin film, Optical propertie.*

 ISBN : 978-81-923628-7-8

Synthesis and Characterization of PEG Embedded Fe-modified Graphene Composite Sensors for LPG Sensing Application

Shivani A. Singh[1] and Pravin. S. More[*]

[1*]Nano Material Application Lab., Department of Physics, Institute of Science,
Madam Kama Road, Fort, Mumbai-400032, India
E-mail:shivani285932gmail.com,pravin.more@gov.in

This paper deals with tile studies carried out on sensitivity, selectivity, response and recovery time of a sensor array comprising of PEG embeddedFe-modified graphene composite sensors. The molar concentration (M) level of Fe additive was varied systematically from 0.5 M to 3.0 M. Initially, the sensitivity of all the sensors of the array has been studied for LPG followed by detailed analysis of transient response of PEG embedded Fe-modified graphene composite sensors as it possesses better sensitivity for all the test gases.The response and recovery time of the PEG embedded Fe-modified graphene composite sensors has been found to depend on type of gas and its concentration (up to100 ppm). The highest value of % sensitivity is obtained for LPG at the considerably lower temperature of 310K for 2.0M PEG embedded Fe-modified graphene. The XRD, SEM, UV-vis, FTIR spectroscopy and four probe techniques were employed to establish the structural, morphological and study gas sensing characteristics of the materials, respectively. These analyses show that this modified material can be useful for LPG gas sensing applications and to be used in diverse areas.

Keywords: *LPG Gas Sensor; PEG; Fe- modified; four probe techniques; Hummer's method.*

PEG-Assisted Morphological Transformation of 3D Flower_Like ZnO to 1D Micro-/Nanorods and Nanoparticles for Enhanced Photocatalytic Activity

Shweta N. Jamble, Karuna P. Ghodero and Rohidas B. Kale

Department of Physics, The Institute of Science, Madam Cama Road, Mumbai-400032, India.
Email id: jamble.shweta@gmail.com, rb_kale@yahoo.co.in

A simple, non-toxic, cost-effective and environmentally benign hydrothermal method has been used to synthesize ZnO with different morphologies [1]. The importance of ZnO material is due to its wide band gap (3.37eV) and high exciton binding energy (60 meV) at room temperature [2]. The ZnO has a wide range of applications in laser diodes, solar cells gas sensors and photocatalytic activity [3]. The effects of polyethylene glycol (PEG) addition on the structural, morphological, optical properties and photocatalytic performance of the ZnO micro/-nano structures were studied. The synthesized ZnO products were of highly crystalline hexagonal phase. The reorientation of crystal planes took place without any alteration of the crystalline phase with the addition of PEG. The morphology of the ZnO products could be controlled using appropriate amounts of PEG in the reaction precursor. Compositional analysis revealed that the obtained products were a pure phase with a 1:1 atomic ratio of Zn versus O. The band gap of ZnO without PEG additive was determined to be 3.36 eV and changed slightly with the addition of PEG. The photoluminescence (PL) study revealed defect-related emissions and the enhancement or decreases in PL intensity depended significantly on the amount of the PEG addition. The photocatalytic activity of the ZnO catalyst was evaluated for methylene blue dye, which shows 98% degradation within 60 min.

Keywords: *Hydrothermal synthesis; electron microscopy; adsorption-photocatalysis; visible light irradiation.*

Synthesis and Study of Carbon Quntum Dots Using Facile Oven Assisted Carbonization METHOD

Samiksha Pandey[a], Soni Yadav[b] and V. Raikwar[c]

[a, b, c] R. J. College, Ghatkopar, Mumbai-400086

Carbon quantum dots which are generally small carbon nanoparticles (less than 10 nm in size) with various unique properties, have found wide use in many fields during the last few years. In this work, we describe the recent progress in the field of CQDs, focusing on their synthesis method, luminescent mechanism, and applications in biomedicine, optronics, and catalysis and sensor issue. We have used extracts of fruits like coconut, apple and papaya which are commonly found in markets as precursors. We have developed a fast, environmental friendly and low cost oven -assisted carbonization method for synthesis of highly fluorescent carbon dots. The properties of carbon dots were investigated by UV visible spectroscopy, photoluminescence spectroscopy and scanning electron microscopy. The CQDs have found application in different areas such as biomedicine, photocatalysis, photosensor, solar energy conversion, light emitting diodes etc.

Keywords: *Carbon quantum dots, fruit extracts, carbonization.*

Synthesis and Characterization of Manganese Oxide as Electrode Material for Supercapacitor Application

Snehal L. Kadam[a], Rahul S. Ingole[a,b] and Shrinivas B. Kulkarni[a*]

[a] Materials Research Laboratory, Department of Physics, The Institute of Science, Mumbai-400032, Maharashtra

[b] Department of Physics, Shrimant Babasaheb Deshmukh Mahavidyalaya, Atapadi, Dist-Sangli-415301, Maharashtara

*Corresponding Author: *sbk_physics@gmail.com*

In the present work, Manganese oxide (MnO_2) electrode material was successfully synthesized by simple, low cost hydrothermal method on carbon cloth substrate. The structural, morphological and surface area characterizations of synthesized electrode material were carried out using XRD, SEM and BET techniques. The electrochemical properties of synthesized electrode were analyzed by using cyclic voltammetry, galvonostatic charge discharge and electrochemical impedance spectroscopy in 1M Na_2SO_4 aqueous electrolyte. The Manganese Oxide electrode shows maximum specific capacitance which is 479 F/g at scan rate 5 mV/sec. Charge discharge studies gives 75% columbic efficiency. The stability studies shows 80% retention of specific capacitance after the 1000 cycles. These results show that hydrothermally synthesized Manganese Oxide on carbon cloth is the promising electrode material and would be most appropriate for supercapacitor application.

Keywords: *Manganese Oxide; Hydrothermal method; Carbon Cloth; Supercapacitor.*

 ISBN : 978-81-923628-7-8

Supercapacitive Behaviour of [Co:Mn:Ru] Oxide Thin Film

[1]Joshi P. S., [2]Jogade S. M. and [3]Sutrave D. S.

[1]Walchand Institute of Technology, Solapur University, Solapur, Maharashtra-413006
[2] Sangameshwar Mahavidyalaya, Solapur-413003
[2]D.B.F Dayanand College of Arts and Science, Solapur University, Solapur, Maharashtra-413006
E-mail address: preetij12@gmail.com, dattatraysutrave@gmail.com

The research in material science shows that it is difficult to satisfy the requirements of different applications by a single material. Nanocomposite films can achieve more than a single or doped thin film. This paper includes the synthesis and supercapacitive behaviour of [Co:Mn:Ru] Oxide nanocomposite thin films . The homogenous films were deposited on glass plate by sol-gel spin coating technique .As deposited thin film electrodes showed the highest specific capacitance of 440 F/g at a scan rate of 10 mV/Sec and good cycling stability with about 75% retention after 1000 cycles. It also showed the specific energy and specific power of 158.76Wh/kg and 83.04 KW/kg respectively demonstrating the good electrochemical performance for supercapacitor application.

Keywords: *Nanocomposite, Sol-gel, Electrochemical Behaviour.*

Synthesis and Characterization of Bimetal Decorated Carbon Nanomaterials from Cotton Fiber

Suyash S. Agnihotri[1], Vikaskumar P. Gupta[2], Kailash R. Jagdeo[1*] and B. T. Mukherjee[2]

[1]Department of Physics, DSPM's K.V. Pendharkar College, Dombivli-421203.
[2]Nano science research center, DSPM's K.V. Pendharkar College, Dombivli-421203.
*Email: kailash_jagdeo1@yahoo.co.in

Carbon nanomaterials (CNMs) have the remarkable physical, thermal, mechanical properties which built large interest in most areas of science and technology. In this study, CNMs are synthesized using cotton fiber by the pyrolysis method at temperature 750˚C in inert atmosphere of Argon. The as obtained CNMs are decorated with bimetal combination (Cu-Ni) by thermal rapid evaporation. The SEM image shows transparent carbon nano-sheets decorated with Copper and Nickel. The EDAX and SEM confirms decoration. Hydrogen storage capacity values for this sample indicates bimetal decorated CNMs can serve as suitable and efficient hydrogen storage medium.

Keywords: *Hydrogen Storage*; *Carbon nanomaterials; Cotton fiber; Bimetal.*

Herbal Formulation of Biomaterial

Jagdish B. Kudav, Pooja J. Singh, Anjali A. Yadav and Anita S. Goswami-Giri*

Department of Chemistry
B. N. Bandodkar College of Science, Thane (MS) - 400601.
Corresponding Author - anitagoswami@yahoo.com

Moringa oleifera (L.) leaves bioactive compounds showed higher antioxidant activities such as free radical scavenging effect on human body. Due to diversified applications, leaves were selected for preparation of herbal soap with natural dyes. The colourful flowers of lantana were used for the extraction of Dye which is acts as inhibitor of insignificant colour of soap and is used in making the soap attractive.

Keywords: *Phenolic content, phytomedicine, antibacterial*

Hydrothermally Grown WO_3 Thin Films as a NO_2 Gas Sensor

C. Rukhsaar, Sayali Gadre, K. Ayesha and A. V. Kadam

Institute of Science, Dr. Homi Bhabha University, 15, Madam Cama Road, Fort, Mumbai-400032, India

A novel hydrothermal process using Propylene Glycol as binder as well as process optimizer has been employed to synthesize WO_3 thin films for Gas sensing applications. The XRD spectra for As-Prepared WO_3 film revealed that the as-prepared film was of WO_3 hydrate, and all diffraction peaks can be indexed to the orthorhombic phase of WO_3. Although, when the film annealed at 400^0C, the XRD pattern of WO_3 film has diffraction peaks, well indexed with the hexagonal phase of WO_3. Scanning electron microscopy (SEM) findings reveal that the size of grain without annealing was seen to be in micrometers where after annealing these grains size was observed to be in nanometers. Fourier transform infrared (FTIR) spectroscopic data reveal the modes of coordination of water molecules and oxygens in the WO3 film. FTIR Analysis confirms, WO_3 is based on the WO_6 octahedron unit, and each oxygen forms a W–O–W connection. The developed sensor is highly sensitive to NO_2 traces in the ppm range. Highest temperature for film to desorb as well regeneration of film is 180^0 C. Sensitivity of film at 180^0 C is saturated above 60 ppm. The response of these films is quick within 50-60 sec.

Keywords: *Tungsten trioxide; gas sensor; NO2; XRD.*

Synthesis and Fluorescence Properties of Eu^{3+} to Eu^{2+} in $BaAl_2Si_2O_8$ Phosphor Under Charcoal Atmosphere

U. B. Gokhe[1*], K. A. Koparkar[2] and S. K. Omanwar[2]

[1]Department of Physics, B N Bandodkar college of science, Thane (MS) 400601, India
[2]Department of Physics, SGB Amravati University, Amravati (MS) 444101, India
Corresponding author email: ubgokhe@gmail.com,

The series of Eu^{3+}/Eu^{2+} doped $Ba_{(1-x)}Al_2Si_2O_8$(x=Eu=0.01, 0.02, 0.03, 0.04 and 0.05 mole) phosphors were prepared by traditional solid state reaction method. The crystalline phase of $BaAl_2Si_2O_8$ host was verified by X-ray diffraction (XRD) analysis. Moreover, scanning electron microscopy (SEM) and EDAX was investigated for morphological and for content present in the as-prepared sample. On the SEM analysis, the average particle size was in the range of 2-10 μm. The photoluminescence (PL) excitation (λem = 615 nm) and emission (λex = 395 nm) of $Ba_{(1-x)}Al_2Si_2O_8:_xEu^{3+}$ were investigated. The optimum PL intensity was observed at 615 nm ($^5D_0 \rightarrow {}^7F_2$). The concentration quenching was observed at 0.03 mole concentration of Eu^{3+} ions in $BaAl_2Si_2O_8$. However, The PL excitation (λem = 428 nm) and emission (λex = 325 nm) of $Ba_{(1-x)}Al_2Si_2O_8:_xEu^{2+}$ were investigated. The optimum PL intensity was observed at 428 nm ($4f^65d^1 \rightarrow 4f^7$). The CIE color coordinates (*x=0.648, y=0.343*) clearly indicated that the phosphor $Ba_{0.97}Al_2Si_2O_8:_{0.03}Eu^{3+}$can be used as a potential candidate for deep red light emitting diodes under near-UV (n-UV) excitation. Also the CIE color coordinates of $Ba_{0.95}Al_2Si_2O_8:_{0.05}Eu^{2+}$ phosphor (*x=0.159, y=0.107*) is in blue region.

Keywords: *$BaAl_2Si_2O_8$:Eu;solid state reaction; XRD; n-UV LEDs.*

 ISBN : 978-81-923628-7-8

Structural Characterization of Synthesized Zinc Oxide Nanoparticles

Varun Kate[1] and J. Mayekar[2]

[1,2]Jai hind college, Churchgate

In this paper, zinc oxide nanoparticles were synthesized using zinc chloride and sodium hydroxide as the starting materials by wet chemical method. The synthesized zinc oxide nanoparticles were then characterized by x ray diffraction. The miller indices, peak position, peak intensities were determined. In addition to this structural parameters such as lattice parameters, bond length ,crystallite size etc were determined. The crystallite size was also calculated using W-H plot and comparative study was done with that of the scherrer formula.

Keywords: *Zinc oxide nanoparticles, x ray diffraction, scherrer formula, crystallite size.*

Specimen Preparation Techniques for Transmission Electron Microscopy

Dr. Nigvendra Kumar Sharma

Department of Physics, Maharashtra College,
246 – A, J. B. B. Road, Mumbai – 400 008

The structural investigations of the materials at the atomic level has become an interesting and a very fascinating area in physics since the discovery of sophisticated characterization techniques such as Transmission Electron Microscopy (TEM) and Electron Diffraction Techniques, Scanning Electron Microscopy (SEM), Atomic Force Microscopy (AFM), Scanning Tunneling Microscopy (STM) etc. The renowned & the Nobel Prize winner physicist Richard Feynman envisioned, in 1959, the theoretical capability of maneuvering things atom by atom. The Transmission Electron Microscope is one of the most widely used equipment worldwide for studying the materials at the atomic level. The TEM is extremely helpful in the study of the crystalline nature, Structure Orientation, Dislocations, Stacking faults, Voids, Phase transformation from Amorphous to Crystalline, or vice versa, Lattice parameters, Particle size and Defects etc. in the materials. The specimens of the materials, to be investigated by TEM, need to be prepared by using specialized techniques. The specimens can be prepared from Powdered Materials, Bulk Materials, Metallic Sheets and Thin Films.

While preparing the specimen for TEM from metallic sheets, we have to keep in mind that the specimens need to be prepared in the form of circular discs having diameter 3.05 mm and also the thickness of the specimens should not exceed 1000 A°. So to prepare specimens for TEM investigations from metallic sheets, with such specifications, the only technique used is Ion Milling Technique. Hence in this present paper, the detailed process of preparing the specimens of metallic sheets, for TEM analysis by suing the Ion Milling Technique will be discussed.

Keywords: *TEM; Specimen; Nanoparticles; Phase transformation; Dislocations; Stacking faults; Voids; Lattice parameters; Defects*

Vidya Prasarak Mandal, Thane

Group of Institutions

- Dr. Bedekar Vidya Mandir (Marathi Medium School)
- Sou. A. K. Joshi English Medium School
- K. G. Joshi College of Arts
- N. G. Bedekar College of Commerce
- B. N. Bandodkar College of Science
- VPM's TMC Law College
- VPM's Dr. V. N. Bedekar Institute of Management Studies
- VPM's Polytechnic
- VPM's Advanced Study Centre
- VPM's Polytechnic IT Centre
- VPM's Centre for Foreign Language Studies
- VPM's Department of Defence and Strategic Studies
- VPM's London Academy for Education and Research
- VPM's Academy of International Education and Research
- VPM's Maharshi Parshuram College of Engineering
- VPM's Institute of Distance Education
- VPM's Centre for Career and Skill Development
- VPM's Council of Senior Scientist's
- VPM's Group of Institutions' Unified Placement Cell (UPC)
- VPM's Swarânjali (स्वरांजली) - A platform for academic study of Indian Classical Music